Green Synthesis of cadmium telluride type II multi shell quantum dots for biolabelling

BY

NCAPAYI VUYELWA

A thesis submitted in fulfilment of the requirements for the degree of

MASTERS OF TECHNOLOGY

(IN CHEMISTRY)

At

Cape Peninsula University of Technology

Supervisor: Prof Samuel O. Oluwafemi

Department of Applied Chemistry

University Of Johannesburg, Doornfontein Campus

Johannesburg, South Africa

Co supervisor: Prof Sandile .P. Songca

Deputy Vice-chancellor: Academic Affairs and Research

Walter Sisulu University

Mthatha, South Africa

MARCH 2016

DECLARATION

I, NCAPAYI VUYELWA (214309878), declare that the contents of this thesis represent my own unaided work, and that the thesis has not previously been submitted for academic examination towards any qualification. Furthermore, it represents my own opinions and not necessarily those of the Cape Peninsula University of Technology.

Signed **Date**

ABSTRACT

The synthesis of water soluble CdTe, CdTe/CdSe and CdTe/CdSe/ZnSe nanoparticles (NPs) and their optical, cytotoxicity as well as imaging properties are presented. The synthesis was carried out under ambient conditions in the absence of an inert environment and involved the use of potassium tellurite (K_2TeO_3) and sodium selenosulphate (Na_2SeSO_4) as a stable tellurium and selenium precursor respectively, while mercaptopropanoic acid (MPA) was used as capping agents. In this method, the CdTe NPs were prepared by the addition of tellurium source solution to MPA-cadmium complex solution at different pH while keeping other parameters constant. The formation of the shell (CdSe) and multi shell (CdSe/ZnSe) were achieved by adding desired precursors to the growing CdTe core NPs at one hour interval. The temporal evolution of the optical properties and stability of the growing nanocrystals was monitored in detail by varying the refluxing time, pH and storing the NPs under ambient condition for several days. The as-prepared NPs were characterised using UV-Vis absorption and photoluminescence (PL) spectroscopy, transmission electron microscopy (TEM) and high resolution transmission electron microscopy (HRTEM). The formation of the shells was indicated by an immediate change in the colour of the reaction solutions after the addition of the desired precursor and the shift in the absorption wavelength towards red-region. The optical analyses showed an enhancement in the fluorescent intensity after the addition of the shell solution accompanied by red-shifting of the absorption and emission maximum. The stability study revealed an increase in the emission intensity as the ageing days increased. The stability study of the NPs in air at room temperature show highly improved stability of the core-shell NPs than the core. The TEM analysis showed that

the materials are small, monodispersed, spherical and highly crystalline. The cytotoxicity of the NPs was investigated on LM 8 and KM-Luc/ GFP cell line using an MTT protocol at different concentrations. The cell viability show significant improvement after the shell formation with CdTe/CdSe/ZnSe core multi shell NPs having the highest cell viability at higher concentration (60 µg/mL). Furthermore a decrease in cytotoxicity is revealed with increase in reaction time, thus NPs prepared at longer (7 h) reaction time showed lower cytotoxicity compared with those prepared at shorter (0.5 h) reaction time. The confocal laser microscope image of the cells after the addition of the as-synthesised NPs confirmed the transfection of the NPs by KM-Luc/GFP cell line, indicating that the NPs have been endocytosis. This study demonstrates the great potential of the as-synthesised core-multi shell nanoparticles for biological and any applications that require efficiency, high fluorescence intensity and stability.

ACKNOWLEDGEMENTS

I wish to thank:

God Almighty for giving me strength, hope, courage, power and make me focussed all through the way. When the going gets tough people wouldn't understand how I went through because as the roots you are hidden from them, they can't see you, they only see the miracles you do in my life. You deserve all the glory. You've anchored my life all the praises be to you.

Prof. S.O. Oluwafemi, supervisor, father, brother and a friend, thank you for being there all those difficult times, for your support, advices, the knowledge that you've transferred to me and your undying patience. Thank you, I would have never done it without you, may God give you more grace so that you stay as fruitful as you are.

Special thanks to Professor S.P. Songca for his time, patience, advices, support and understanding. Prof, it has been a privilege to work with you, I am really honoured to work with you.

My brothers and sisters in the Nano group, you shared with me the hardest moments of this project. I highly appreciate your efforts to make sure that I stay focused all.

My colleagues especially in the Applied science department (Potsdam campus), I felt your support all through the way and I am thankful to you all.

CSIR for allowing me to do my analysis, I highly appreciate you've made my work look great. Cape Peninsular University of Technology at large for opening its doors for me to further my studies, you've actually made my future brighter.

My mom (Nomalinge) and aunt (Nosisi), I might not know where the life's road will take me, but you've natured me with God as the foundation of my life and prayer as the weapon to success, thank you for that.

My Sisters: (Lundi, Pam and Nhishy) I am always proud to be part of you because you protect me from blowing winds so that after the storm I can stand again. Thanks for being inspiration in my life.

My precious son love, understanding and encouragement that you provided through my studies is highly appreciated. Sizwe my boy you've been so supportive - even when being 'without Mum' was hard, thanks for your time. You have given me a reason to live and look forward to everyday.

I would like to thank NRF for the financial support without you I would be drowning in depths, thank you.

The financial assistance of the National Research Foundation towards this research is acknowledged. Opinions expressed in this thesis and the conclusions arrived at, are those of the author, and are not necessarily to be attributed to the National Research Foundation.

Difficult roads often lead to beautiful destination.

DEDICATION

To my late grandmother Noluzile Falangile Ncapayi (May her soul rest in peace)

For her undying love and courage

Abreviations

ARG	Arginine
$Cd(Ac)_3$	Cadmium acetate
Cd	Cadmium
CdS	Cadmium sulphide
CdSe	Cadmium Selenide
CdTe	Cadmium telluride
DCC	N, N'-Dicyclohexylcarbodiimide
HRTEM	High resolution transmission electron microscopy
K_2TeO_3	Potassium tellurite
MPA	Mercaptopropanoic acid
Na_2SeSO_3	Sodium seleno sulphate
$NaBH_4$	Sodium borohydride
NaOH	Sodium hydroxide
NPs	Nanoparticles
PbS	Lead sulphide
PL	Photoluminescence
PL	Photoluminescence spectrophotometer
QDs	Quantum dots
QE	Quantum efficiency
QY	Quantum yield

Se	Selenium
TEM	Transmission electron microscopy
UV-Vis	Ultra-violet visible spectrophotometer
XRD	X-Ray diffractometer
ZnCl	Zinc chloride:
ZnSe	Zinc Selenide

Glossary

Figures

TABLE OF CONTENTS

OUTPUT

PRESENTATION AT ACADEMIC CONFERENCES

International (Outside South Africa)

1. Ncapayi Vuyelwa, Oluwafemi Oluwatobi, Songca Sandile; Kodama Tetsuya (2014): Optical and cytotoxicity properties of water soluble type II CdTe/CdSe nanoparticles synthesised via a green method , 2014 Material Research Society Fall Meeting, Boston , Massachusetts , America from 30 – 5 December.

2. Ncapayi Vuyelwa, Oluwafemi Oluwatobi, Songca Sandile; Kodama Tetsuya (2015): Simple green synthesis of water soluble type II CdTe/CdSe nanoparticles and their use in cellular imaging 9th international Conference of Society of free Radical Research-Africa , 4th International conference of international Association of medical and Biomedical Researchers, Hennessy Park hotel Mauritius 27-29 July.

3. Samuel Oluwatobi Oluwafemi, Vuyelwa Ncapayi, Sandile Phindile Songca (2015): Green synthesis of anisotropic oleic acid-capped CdSe nanoparticles under ambient conditions. IUPAC 45th World Chemistry Congress, Bexco, Busan, Korea 9th-14th August.

4. Ncapayi Vuyelwa, Oluwafemi Oluwatobi, Songca Sandile; Kodama Tetsuya (2015): Simple green synthesis of CdTe/CdSe/ZnSe core-multi shell with reduced cytotoxicity for bio imaging, 4th Nano Today Conference; JW Marriot Marquis Hotel, Dubai; 6th-10th December.

5. Vuyelwa Ncapayi, Oluwafemi Oluwatobi, Sandile Songca (2016): Optical and imaging properties of highly luminescent water soluble type II CdTe/CdSe nanoparticles synthesised via a green method. TMS 144th Annual Meeting and Exhibition, Walt Disney World, Orlando, USA, 15th -19th March.

Local Conferences

1. Vuyelwa Ncapayi; Oluwatobi .S. Oluwafemi , and Sandile P Songca (2014) : Optical and imaging properties of water soluble type II CdTe/CdSe nanoparticles synthesised via a green method. 2nd U6 international conference , CPUT Cape town campus, Cape Town, South Africa, from 5-10 September.

2. Vuyelwa Ncapayi, Oluwatobi S Oluwafemi, Sandile P Songca and Tetsuyi Kodama (2014): Optical and biological properties of highly fluorescent CdTe/CdSe nanoparticles synthesized via a facile green method. International Symposium on Macro- and Supra-Molecular Architectures and Materials, Emperors Palace Hotel, Johannesburg, South Africa, from 23-27 November.

3. Vuyelwa Ncapayi, Oluwatobi S. Oluwafemi, Sandile P. Songca and Tetsuya Kodama (2015): Simple Green Synthesis of CdTe/CdSe/ZnSe Core-Multi Shell with Reduced Cytotoxicity for Bio Imaging. 1stUNIVEN-WSU International Research Conference, East London, 02-07 September.

PUBLICATIONS IN PEER REVIEW JOURNALS

1. Oluwafemi O.S., Olamide A. Daramola O.A. and Ncapayi V. (2014): A facile green synthesis of type II water soluble CdTe/CdS core shell nanoparticles. Materials Letters 133; 9–13.

2. Ncapayi V., Oluwafemi S.O., Songca S.P. and Kodama T. (2015): Optical and cytotoxicity properties of water soluble type II CdTe/CdSe nanoparticles synthesised via a green method. Mater. Res. Soc. Symp. Proc. Vol. 1748.

CHAPTER ONE

INTRODUCTION

1.1 BACKGROUND

Nanotechnology is the application of science to control matter at level of atoms, molecules and supramolecular structures. Since nanotechnology is still embryotic there doesn't seems to be enough definition that everybody agrees on. It has been understood that nanotechnology deals with matter on a very small nanometer scale. It's hard to imagine how small a nanometer is but it is one billionth of a meter, for example on a comparative scale, if a marble were a nanometer, then one meter would be the size of the Earth. In other words, nanotechnology is a field that focuses on the development of synthetic methods, surface analytical tools for building structures and materials, understanding the change in chemical and physical properties due to miniaturization, and the use of such properties in the development of novel and functional materials and devices (Allhoff *et al.,* 2010; Prasad, 2008; Kahn, 2006) . Although modern nanoscience and nanotechnology are quite new, nanoscale materials were used for centuries but something as small as an atom is impossible to see with the naked eye. In fact, nanoparticles have been in existence way back as 1831, when Michael Faraday investigated the rubby red colloids of gold and publicized that the colour was due to the small size of the metal particles. Since then gold and silver nanoparticles (NPs) have found their way as colorants into glasses that were used for windows in churches for over 100 years (Faraday, 1831; Jain *et al.,* 2009**)**. For centuries, scientists have been studying and working with nanoparticles, however, the effectiveness of their work has been hampered by their inability to see the structure of these materials. Thus, the use of this term, "nanotechnology" has been growing since development of high resolution

microscopes to designing new materials such as electronics in computer components, in biotechnology for diagnostics tools and new drug delivery systems (Binnig and Rohrer, 1986). Nanotechnology doesn't have single focus like other science disciplines such as medicine that pertains to health care only, astronomy lost in the stars, zoology focusing on animals and others. Nanotechnology is a diverse field which involves physics, chemistry, microbiology, biochemistry, engineering even molecular biology. It holds promises for studying the detailed operation of individual atoms, cells and neurons, which could help to re-engineer living systems and in electronics for development of electronic devices (Dowling, 2004; Rajiv, 2010). The incorporation of ancient wisdom and present understanding of nanoscience can impart more light on future developments. Due to the divers architecture of nanoparticles they are of great scientific interest and many fields of endeavour contribute to nanoscience, including molecular physics, materials science, chemistry, biology, computer science, electrical engineering, and mechanical engineering (Gillich *et al.,* 2013 Jain *et al* 2009). Nanoscience offers an exciting possibility to study the state of matter. It acts as an intermediate between bulk materials and isolated atoms or molecular structures, as well as the effect of spatial confinement on electron behaviour. It also provides an opportunity to explore the problems related to surface or interface because of their interfacial nature. It involves the ability to see and to control individual atoms and molecules. Everything on earth is made up of atoms, the food we eat, the clothes we wear, the buildings and houses we live in and our own bodies too. These nanomaterial's are often referred to in literature as semiconductor nanoparticles, nanocrystals, quantum dots (QDs), nanoclusters, and typically have at least one dimension in the range of 1-100 nm (Jain *et al.,* 2009). They exhibit both physical and chemical properties within an intermediate state of

matter, between molecular and bulk. Their unique properties are attributed to two main factors; the large surface-to-volume ratio of atoms and their reduced dimensions in relation to the excitonic radius of the bulk material (Pitkethly , 2004, Gonsalves, *et al*, 2000, Bangal, *et al.,* 2005)

Due to these unique properties, they show different properties from bulk material such as large surface area, higher strength and lighter weight, heat resistant, chemical resistant and increased control of light spectrum once they reach the nano scale. Today scientists and engineers are discovering a wide variety of ways to deliberately construct nanoparticles (NPs) and take advantage of their enhanced properties. The ultimate scientific and technological impact of these nanoparticles (NPs) mainly depends on their novel electronic, optical, catalytic, physical and chemical properties. Hence, studies concerning quantum and electronic confinement observed in these materials are of exceptional importance in order to understand the science around nanomaterials.

1.2 Properties of semiconductor nanoparticles

Properties of nanoparticles arise from the interaction between the electrons, holes and their local environment. These particles are highly affected by sizes which decreased in respect to their bulk material and the process is referred to in literature as quantum confinement (Chan *et al.,* 2002). The optical as well as electronic properties are linked together by the following equation:

$E = hv = hc/\lambda$ ……..1

E = band gap energy difference, h = Planck's constant, c = the speed of light,

v = the frequency of the incident light, and λ = the wavelength of incident light.

The energy difference of the band gap is inversely proportional to the wave length of incident light thus nanoparticles absorb in the shorter wavelength than bulk material.

When a photon is absorbed, the excitation energy exceeds the band gap. During this process electrons are promoted from the valence band to the conduction band and the first lowest excited energy state is shown by the quantum confinement peak. Quantum confinement doesn't only affect the absorption but affect the emission properties of these materials resulting in the material that behaves differently from the bulk material (Chan *et al.,* 1998 and Mattoussi *et al.,* 2000). The reduction in the size of the nanoparticle in relation to the absorption wavelength makes NPs behave differently from their parental material and show discrete energy levels usually accompanied by fluorescence emission (Dabbousi *et al.,* 1997). The fluorescence properties can be characterised using many parameters such as emission colour and stability, colour purity, fluorescence brightness etc. (Lim *et al.,* 2003). In photoluminescence two types of emissions are considered which are band gap and deep trap emissions.

Band gap emission is fairly narrow and very close to the absorption and is characterized by a continuous surface, with most surface atoms exhibiting the coordination and oxidation state of the bulk. On the other hand, deep trap PL is

broad and is substantially red-shifted from the absorption. It has been associated with non- radiative recombination of localized surface trapped charge carriers (Jaiswal *et al.,* 2003 and Ballou *et al.,* 2004)**.**

The emission spectra of the QDs can be tuned across wide range from green to red by changing the size while their surface properties remain identical (Cutler *et al* 2013; Kobashayi *et al* 2007; Zrazhevskiy and Gao *et al.,* 2013). Their excitation spectra is very broad while their emission spectra is fairly narrow in contrast with organic fluorophores. In addition, they are resistant to photo oxidation and metabolic degradation. The inorganic nature of the nanoparticles make them resistant to metabolic degradation as they have shown to remain fluorescent and retained their emission in live cells and organisms for several weeks. Therefore they stand as excellent material for biological applications over organic dyes. The changes in optical properties governed by the reduction of particle size inspired the researchers to develop advanced synthetic routes for nanoparticles of different semiconductor materials.

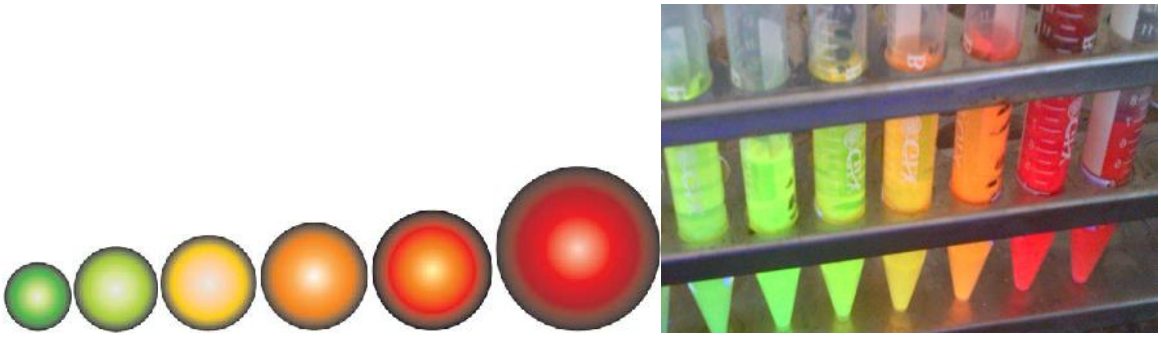

Figure 1.1 Images indicating increase in particles size of NPs as fluorescence shift from green to red region.

1.3 Synthesis of semiconductor nanoparticles

1.3.1 Synthesis of core nanoparticles

Nanoparticles are being viewed as fundamental building blocks of nanotechnology. They are the starting point for preparing many nanostructured materials and devices. Their synthesis is an important component of rapidly growing research efforts in nanoscale science and engineering. The nanoparticles of a wide range of materials can be prepared by a number of methods which involves both chemical and physical approaches. These approaches depends on either chemical reactivity or physical impact in order to adjust nanostructure building blocks and can be categorise as either ‘bottom-up’ or ‘top-down’ approach.

The bottom-up approach refers to the build-up of a material atom-by-atom, molecule by-molecule or cluster by cluster (Wong *et al.,* 2009 Wu *et al.,* 1993). Top-down approach involves starting with a bulk material and designing or crushing it down to desire shape (Koch *et al.,* 1989). Top down technique is similar to the approach used by the semiconductor industry in forming devices, utilizing pattern formation (such as electron beam lithography) (Koch, 2003). Both approaches play very important roles in industry and most likely in nanotechnology as well. There are advantages and disadvantages in both approaches. The main challenge for ‘top-down’ approach is the creation of increasingly small structure with sufficient accuracy whereas in bottom-up approach, the main challenge is to make structure large enough and of sufficient quality to be useful as materials (Seeman and Belcher, 2002). Bottom-up approach promises a better chance to obtain nanostructures with less defects and more homogeneous chemical composition. On the hand, top-down approach most

likely introduces internal stress, in addition to surface defects. The different methods for the synthesis of nanoparticles will be discussed under these categories.

The chemical approach depends on the pyrolysis of precursors by rapid nucleation followed by controlled steady growth. Using the chemical approach, different high-quality semiconductor nanocrystals with desired particle sizes over the largest possible range, narrow size distributions, good crystallinity, controllable surface functionalization, high luminescent quantum yields can be obtained on a gram scale.

The colloidal method is the first reported for the synthesis of such small materials under chemical approach. La Mer, *et al.,* 1940, proved that by controlling the nucleation and the growth, highly monodispersed nanomaterial can be synthesised. This takes place through Ostwald ripening, where small crystals which are less stable dissolve and then re-crystallise to form more stable large crystals (La Mer *et al.,* 1940). This reaction involves separation of the nucleation and the growth process which can be achieved by correct choice of reaction conditions such as solvent, temperature and pH as well as passivating agent. Henglein made a significant contribution in this field of studies by altering the nucleation kinetics, thereby controlling the size of CdS (Henglein *et al.,* 1989). Methanolic solution without organic ligands as stabilizer has also been report for the synthesis of CdS and ZnS NPs. Colloidal synthesis is said to be successful for the synthesis of nanosized semiconductor, but certain important semiconductors such as CdSe, GaAs, InAs, cannot be easily synthesised by this route.

Organometallic route was employed to overcome problems associated with the synthesis of nanoparticles via the colloidal route. Organometallic route uses volatile

metal organic compounds. Murray in 1993 reported the first significant development using single and dual source organometallic precursors. This hot injection method make use of amphiphilic co-ordinating solvent that produced fine cadmium base NPs. Dimethyl cadmium was chosen as the cadmium source and trioctylphosphine selenide (TOPSe) as selenium source due to ease of preparation and good stability in an airless technique. This significant contribution on accessibility of NPs with narrow size distribution and increased quantum yield was of great importance. However the toxicity of the precursors and high cost of the method were undesirable (Murray *et al.,* 1993).

Based on this method, developments have accrued to improve the method as well as optical properties of the final product, such as particle size, solubility, quantum yield and many more. In 1998, Peng *et al.,* used this method to study the kinetics of the nanocrystals growth and, demonstrated how the nanocrystals size can be 'focused' through the addition of a monomer reagent during the course of the reaction. The strategy was designed to overcome Ostwald ripening or 'defocusing' of the size distribution (Peng *et al.,* 1998). Although these modifications have led to synthesis of high quality NPs and understanding of its optical and structural properties, however these reactions involves the use of expensive compounds which are air and moisture sensitive. In addition, the whole process involves harsh conditions such as hot injection of precursors which are toxic, volatile with low boiling points material and explosive at elevated temperature. Thus, the standard airless technique is vital.

Peng *et al.,* in 2001 reported the use of CdO as a cadmium precursor for the synthesis of CdSe NPS using a greener method in mild and simple condition (Peng *et al.,* 2001). Peng and co-worker proved that the synthesis of NPs is not that difficult

by using different cadmium precursors and series of solvents which includes TOPO, amine and fatty acids for the synthesis of CdSe NPs. Cadmium acetate and fatty acids were found to be more versatile as precursor and solvent respectively. The use of the phosphine based solvent and solubility of the precursors were the draw backs of this synthesis (Peng *et al.,* 2002). Bullen and Mulvaney (2004) reported the effect of oleic acid concentration on the growth of CdSe NPs with octadecene as the co-ordinating solvent in place of TOPO (Bullen and Mulvaney, 2004). The oleic acid and paraffin which are both natural products were also used for the synthesis of PbS NPs by Chen group in 2005. The oleic acid–capped PbS NPs produced were highly dispersible in a lot of organic solvent (Chen *et al.,* 2005). Deng *et al.,* 2005, follow the suit by using oleic acid and paraffin as both co-ordinating solvent and capping agent and put forward the first mechanism for the synthesis of CdSe NPs while Sapra in 2006 proposed the use of olive oil as co-ordinating solvent for the synthesis of CdSe NPs (Deng *et al.,* 2005; Sapra *et al.,* 2006). Extensive study based on these modifications has been reported to improve the method as well as the optical properties of the as-synthesised NPs. Wang and colleagues (2008) reported the synthesis of CdSe NPs using N, N-dimethyl-oleoyl amide as solvent and obtained particles with zinc blended structure while Manna *et al.,* 2009 uses ethylenediamine as a solvent and $CdCl_2$ as cadmium precursor for the synthesis of CdSe NPs (Wang *et al.,* 2008; Manna *et al.,* 2009). Microwave assisted synthesis of cadmium based NPs with oleic acid as a capping agent was reported by Ayele group (Ayele *et al.,* 2011). Akthtar (2012) used olive oil and oleic acid as capping agent for the synthesis of PbS NPs while octadecene was used as the stabilizing agent (Akthtar *et al.,* 2012). Although this was said to be a productive method, the hydrophobicity of these materials hinders them for some biological applications.

Recently, Mansur *et al.,* 2015 reported the synthesis of carboxymethylchitosan and chitosan passivated ZnS NPs. These ZnS-Nano conjugates were cytocompatible with intense fluorescence activity and were effective for specific targeting thus; they may be used in numerous applications in diagnosis and nanomedicine (Mansur *et al.,* 2015). Disadvantages associated with organically synthesised NPs such as insolubility in water and toxicity of the material can be overcome by synthesis of hydrophilic nanoparticles either by ligand exchange or direct synthesis but these materials tends to be unstable.

1.3.2 Core/Shell Nanoparticles

Another major concern associated with the biological application of quantum dots is the instability of the nanoparticles in biological fluids. This is the main source of the inherent cytotoxicity of quantum dots. The cytotoxicity has been attributed to the release of highly toxic metal ions and reactive oxygen in solution because the as-synthesised quantum dots sometimes does not possess distinct thick shell which has been found to reduce the toxic character. Hence they contaminate the intracellular compartment of cells (Biju *et al.,* 2010a; Jiang *et al.,* 2006; Cho *et al.,* 2007; Green *et al.,* 2007). This poses a huge drawback to their biological applications therefore, the search for QDs with high photo stability and biocompatibility is inevitable. Organically passivated core semiconductor nanoparticles tend to have relatively low quantum efficiencies. The low quantum efficiency is due to surface defects and dangling bonds situated on the nanoparticle surface which can lead to non-radiative electron-hole recombination. One method to overcome the challenges associated with passivated core semiconductor nanoparticles is to grow another material with a

wider band-gap on the surface of the core particle to produce a “core-shell” nanoparticle. Core-shell particles separate any carriers confined in the core from surface states that would otherwise act as non-radiative recombination centres. They are nanostructures composed of at least two materials in an onion-like structure where by a material with lower band gap is covered by a material with a wider band gap. The core-shell nanoparticles can be categorised as either type I or type II.

In type I core/shell NPs, the electron and the hole are confined in the core. This is due to the fact that, the conduction band of the shell is of higher energy than the core and the valence band is of lower energy than that of the core. Thus the charge carrier is localised in the core resulting in the material with narrow excitation wavelength and low excitation life time.

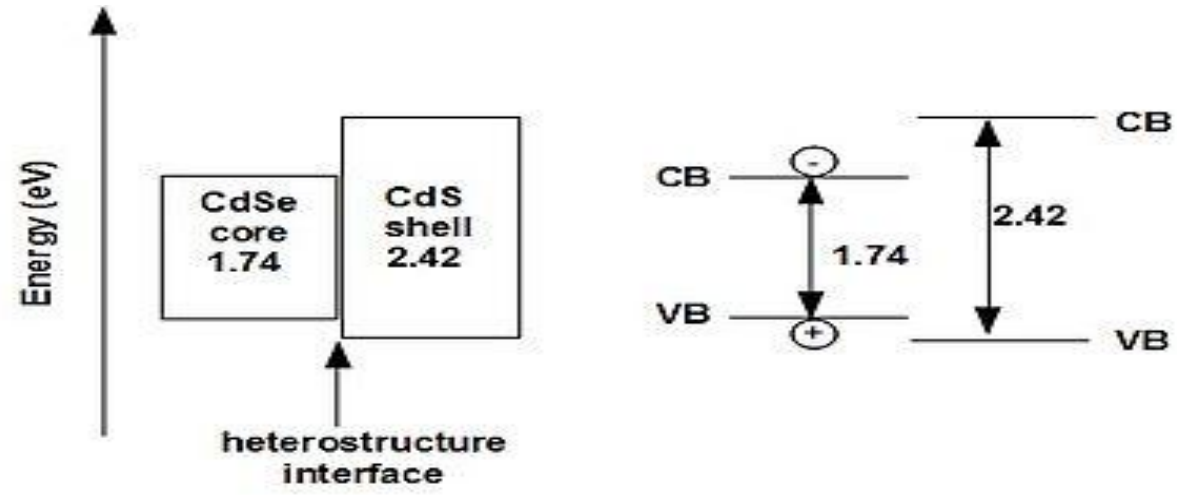

Figure 1.2 band gap of type I core-shell (CdSe/CdS) nanoparticles showing the electron localisation.

Type II have many novel properties that are different from type I such as broad excitation and high excitation life time because the charge carrier is localised in separate material. This is due to the fact that, the valence and conduction bands in

the core are either lower or higher than the shell therefore one carrier is confined in the core while the other is confined in the shell.

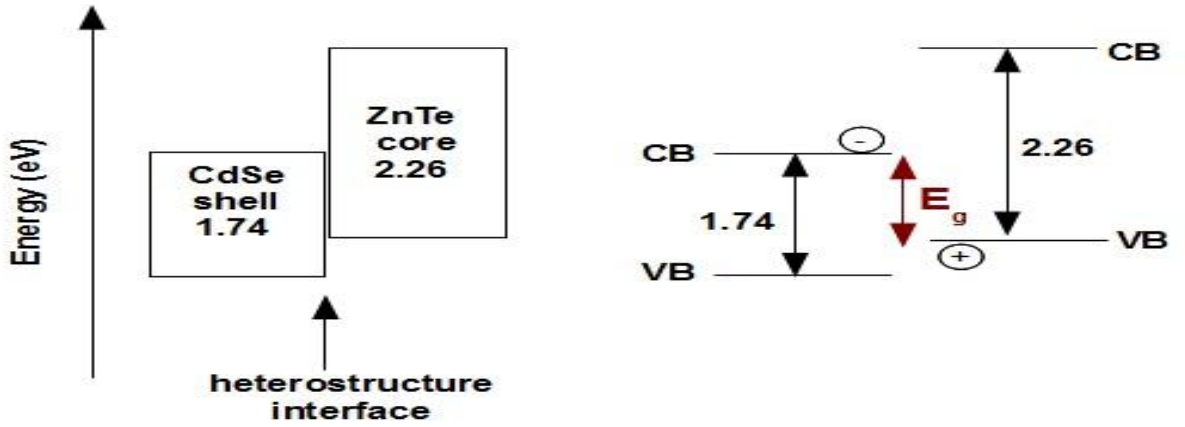

Figure 1.3 band gaps of type II core-shell (CdSe / ZnTe) nanoparticles showing the electron localisation.

This type of materials does not only effectively reduce surface defects and non-radioactive decay, but the emission wavelengths of NPs could also be tuned by their sizes and compositions (Kim *et al.,* 2003; Xie *et al.,* 2005; Chen *et al.,* 2004; Seo *et al.,* 2007). Advantages of type II is that the effective band gap is controlled both by the core and the shell and thus the emission can be controlled by varying the two variables i.e the size of the core and the thickness of the shell. The refinement of the core-shell nanoparticles over several years has made type II core-shell NPs more significant than type-I core/shell NPs. Type-II core/shell NPs have many novel properties such as the red-shift of the emission and a longer decay lifetime due to the formation of an indirect excitation while still maintaining their small particle size (Nemchinov *et al.,* 2008; Liu *et al.,* 2006; Wang *et al.,* 2011; Biju *et al.,* 2010a). Such emission is not possible with type I without drastic change in their particle size. Thus far, many type II core/shell NPs have been reported, including ZnTe/CdSe,

ZnTe/CdS, CdSe/ZnTe and ZnSe/CdS and most of these NPs are prepared through organometallic routes.

Though the method of synthesis via organometallic route and surface modification is very efficient, it is tedious and time-consuming. In addition, the optical properties of the parent NPs are often sacrificed when they are transferred into aqueous phase resulting in material with lower optical properties. These further processing often lead to the increment of NPs size and difficulty in functionalizing their surface with biomolecules when their size is about 100 nm (Medintz *et al.,* 2011). The oxide shell on bare core provide inert protective surface barrier and protect semiconductor cores from photo oxidation when exposed to air (Lin *et al.,* 2006; Simone *et al.,* 2013). Core shell NPs coated by an oxide shell are very interesting especially for biological and industrial applications (Xu *et al.,* 2010; Choe *et al.,* 2015; Wang *et al.,* 2015). Oxides like SiO, FeO, and ZnO have been used to protect cadmium base core NPs (Liu *et al.,* 2013, Xu *et al.,* 2010). Among these, zinc oxide is one of the important shell-forming materials because of its wider band gap; it is known to be nontoxic, bio-safe, and biocompatible. Rakgalakane *et al.,* prepared CdSe/ZnO core/shell based on the modification of Oluwafemi *et al.,* method for the preparation of the hexagonal CdSe NPs core. The core was produced using cadmium chloride and NaHSe as cadmium and selenium precursor respectively. The study showed that mixture of spherical and star core/shell NPs were produced as the concentration of the ZnO increases (Oluwafemi *et al*., 2009, Rakgalakane and Moloto, *2011)*. The use of passivating agent has also been used to increase the stability and decrease the toxicity of the cadmium based core/shell nanoparticles. Oluwafemi *et al.,* (2014) reported the synthesis of high fluorescence glutathione capped CdTe/CdS using, glutathione as the stabilizing agent as well as sulphur precursor source (Oluwafemi

et al., 2014). Zare *et al*., also reported the synthesis of CdTe/CdS NCs using photo induced colloidal synthesis of the shell at room temperature. The S species resulted from photo induction of the thiosulphate ion ($S_2O_3^{2-}$) and a substantial increase in quantum yield of up to 64% was obtained in water (Zare *et al.,* 2015). Recently modification of Oluwafemi *et al.,* method has been reported for the synthesis of CdTe/CdSe NPs by replacing the CdS with CdSe a wider band gap material (Oluwafemi *et al.,* 2014, Ncapayi *et a*l., 2015). Although toxicity of nanoparticles seems to be a barrier for biological application current researches are focusing on how to address this problem and further decrease the toxicity of the NPs. Microwave synthesis of near infrared (NIR) glutathione capped CdTe/CdSe NPs with the cell viability of about 90 % after 12 hours which was further decrease by functionalization of the material with arginine-glycine-aspartic acid has been reported by Chen *et al* (2015). Short reaction time with the aid of microwave, good capping abilities of glutathione and wider band gap of CdSe compared to CdS make the method more environmentally friendly (Chen *et al.,* 2015). The increase demands on NPs for biological applications made aqueous synthesis of NIR type-II core/shell NPs an area of interest.

1.4 Surface Passivation

Surfaces play an increasing role in determining quantum dots structural and optical properties as particle size become reduced. For example, due to an increasing surface to volume ratio with diminishing particle size, surface trap states exert an enhanced influence over photoluminescence properties, including emission efficiency, spectral shape and position. Furthermore, it is often through their surfaces

that semiconductor nanocrystals interact with ‘‘their world,’’ as soluble species in an organic solution, reactants in common organic reactions, polymerization centres, biological tags, electron-hole donors/acceptors, and so on. Controlling inorganic and organic surface chemistry plays a major role in controlling the physical and chemical properties of quantum dots. Over coating highly monodispersed CdSe with epitaxial layers of ZnS has become a routine and typically provides almost an order-of-magnitude enhancement in PL efficiency compared to the exclusively organic capped starting nanocrystals (Dabbousi *et al.,* 1997; El-Khair *et al.,* 2001, Luan *et al.,* 2008, Mathew *et al.,* 2015). The enhanced quantum efficiencies result from enhanced coordination of surface unsaturated, or dangling bonds, as well as from improved confinement of electrons and holes of the core. The latter effect occurs when the band gap of the shell material is larger than that of the core material, as is the case for CdSe/ZnSe and CdSe/CdS core shell particles. The passivation of the NIR core-shell and core multi-shell with hydrophilic or polymeric agents seem to be a right direction to overcome the issue of toxicity especially as the biological promising fluorophores. However, there is still on-going work in tuning the NPs composition as well as understanding their behaviour.

1.5 Application of Semiconductor nanoparticles

The unique properties of NPs have led to material which are potentially useful in many areas, these includes but not limited to catalysis, optical recording material, solar cells, sensors , lasers and bio-labelling and bio-imaging .

1.5.1 Electronics

Exceptional optical properties make NPs attractive components for integration into electronic devices. A significant advantage of NPs over traditional optoelectronic material is that they exist in solid state which makes them to be more compact, easily cooled and allow direct charge injection. In addition, NPs can interconvert light and electricity in a tunable manner depending on the size of the crystal. This act as improvement over silicon based which require modification of their chemical composition to alter the optical properties. All these have led to imperative applications of quantum dots in lasers. The advantage of QDs laser is that they possess fewer energy states than bulk material. This tends to reduce the spread of electrons thus making it easier to create lasing. Advantages of using NPs as starting material in electronics have led to development of numerous types of quantum dots such as ZnSe blue diode lasers materials (Wang *et al.,* 2014). Saunders and Turner reported that CdSe blended polymer facilitates charge separation and the generation of photocurrents under visible light irradiation while Alivisatos and co-workers have revealed that combination of CdSe nanorods and poly (3-hexylthiophene), create charge transfer junctions with high interfacial (Saunders and Turner, 2008; Alivisatos *et al.,* 1999). These researchers succeeded in optimizing the overlap between the cell absorption and solar spectrum and revealed that by improving the polymer-semiconductor interface, it should be possible to increase the carrier mobilities and hence the overall photo conversion efficiency of NPs.

1.5.2 Biotechnology

Nanoparticles also find application in medicine such as bio-attachment due to their several advantages over organic dyes. Nanoparticles exist in the same size as proteins and therefore do not suffer any steric hindrance problem; this makes them useful for medical application such as diagnosis. In cancer treatment, they are used to encapsulate dyes that destroys cancer cells as these dyes tends to roam around the body affecting skin and the eyes (Gao *et al.,* 2003; Bagalkot 2007; Cho *et al.,* 2007). NPs also exhibit broad absorption, high fluorescence and long term stability over traditional fluorophores which make them useful for bio-imaging. Many studies have been done to prove bio-imaging capabilities of quantum dots. Silica-coated CdSe QDs as labelling and imaging agents for cancer cellular imaging and cell tracking applications for the study of cancer and other diseases have been recently reported by Vibin (Vibin *et al.,* 2014). The ability of QDs for cancer imaging has also been investigated on perfluorocarbon/quantum dots (PFC/QDs) nanoemulsions conjugated with antibodies and has been proven to have greater capacity as an efficient nanoprobe for targeting breast cancer cells (Bae *et al.,* 2014 and Gorelikov *et al*., 2011). Recently, Herman just demonstrated the use of small chitosan-antibody stabilized conjugates ZnS nanocrystals as cancer biomarker for non-Hodgkin lymphoma (Mansur *et al.,* 2015). Metal nanoparticles like gold and silver have antibacterial activities thus, they can kill bacteria in water and therefore they are used for purification purposes (Medintz *et al.,* 2008; Zhou *et al.,* 2012).

1.6 Aim and objectives

1.6.1 Aim

The aim of this project is to provide a green, facile, cost effective and environmentally benign route for the direct synthesis of biocompatible CdTe/CdSe/ZnSe core-shell NIR emitting QDs and their application for biolabelling.

1.6.2 Objectives

- Direct synthesis of type II CdTe/CdSe core-shell QDs via a stable, facile and environmentally benign aqueous solution method.
- Direct synthesis of type II CdTe/CdSe/ZnSe core-multi shell QDs via a stable, facile and environmentally benign aqueous solution method.
- Detailed investigation of the pH and reaction time effects on the size, optical and structural properties of the as-synthesised QDs.
- Functionalisation of the as-synthesised type II QDs with amino –acid
- Optical and structural characterisation of the as-synthesised nanomaterials.
- Biological analyses of the as-synthesised nanomaterials.

CHAPTER : TWO

LITERATURE REVIEW

2.1 SYNTHESIS OF CdTe NANOPARTICLES

Cadmium telluride (CdTe) is a black zinc blend crystalline compound with a molecular weight of 240 g/mole and melting point of 1040^0C. It is a binary compound made of cadmium and tellurium with a band gap of 1.44 eV corresponding to the wavelength of 860 nm. It does not occur naturally and mainly used as a semiconductor material.

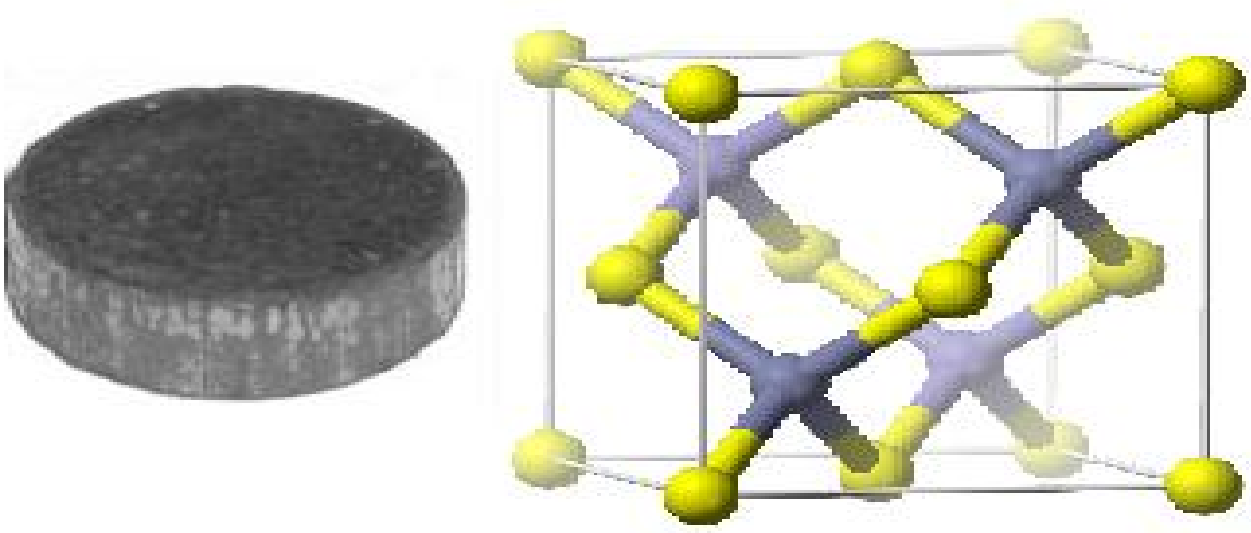

Figure 2.1 Images of the bulk CdTe indicated by grey ring and the 3d network structure.

Bulk CdTe is transparent in the infrared region with a fluorescence peak at a wavelength of 790 nm but once it is reduced to nanoparticles (CdTe NPs) it fluoresces in the visible to infra-red region. CdTe have low solubility in water at low temperature and unstable in air at high temperature. It produces toxic telluride gas and cadmium salt when etched with strong acid (Handbook of chemistry, 1979). Cadmium telluride nanoparticles are among the II-IV semiconductor materials that have been widely studied due to its properties such as high fluorescence quantum

yields, short radiative lifetimes, low thresholds for optical gain and linearly polarized emission. Because of its size dependent properties it has been useful in wide area of applications such as light-emitting diodes, photovoltaic and biological and chemical sensor (Moskowitz *et al.,* 1990; Fonthalan *et al.,* 2000, Zhang *et al.,* 2003; Mohammed 2013).

Several methods have been reported for the synthesis of CdTe NPs and these can be broadly categorised as organic approach, two phase approach and aqueous approach. Organic approach involves synthesis in organic solvents, this make the material soluble only in organic solvent and therefore undesirable for biological applications. The two phase approach involves the synthesis of the nanocrystals in either organic or aqueous phase followed by surface modification to render them hydrophobic or hydrophilic (Bai *et al.,* 2010). This approach solves some problems associated with the synthesis of hydrophilic nanomaterials, however it is tedious, time consuming and the resultant nanocrystals are usually of low quality compared to the parent nanocrystals before surface modification. For example, the resultant nanocrystals after surface modification are usually associated with lower fluorescence intensity and quantum yield. On the other hand, the aqueous phase approach is simple, cost effective, it uses mild reaction conditions and less toxic material however, it also has its own disadvantages such as instability of the material towards oxidation. These synthetic approaches for CdTe NPs have been extensively studied in order to understand the dynamics of the synthetic route as well as fundamental properties of CdTe NPs.

2.1.1 Organic Synthesis

This usually involves the synthesis of CdTe NPs in the presence of organic co-ordinating solvent at high temperatures. The first successful synthetic approach for CdTe QDs was an through organometallic route developed by Murray *et al.,* in 1993. This is indeed the most popular route for semiconductor nanoparticles. It is a hot injection technique that involves the use of metal-alkyl precursors (dimethyl cadmium), trioctylphosphine teluride (TOPTe), trioctylphosphine (TOP) and trioctylphosphine oxide (TOPO) as co-ordinating solvent at a temperature of 300 ^{0}C. Through this route high quality TOPO-capped CdTe and CdSe NPs were obtained (Murray *et al.,* 1993). Although the kinetics of this route produces the fundamental concept for the synthesis of cadmium based NPs, the toxicity and the high cost of the precursors is indeed undesirable. In addition, the method requires harsh conditions, standard airless techniques and it uses material with low boiling points that are explosive at high temperatures. It is therefore detrimental to health of living organisms and environment.

As a modification to Murray's method, Peng and Alivisatos make use of a mixture of trioctylphosphine oxide (TOPO) and hexylphosphonic acid (HPA) as co-ordinating solvent, TOPTe as tellurium precursor and dimethyl cadmium as cadmium precursor to synthesise CdTe NPs (Peng and Alivisatos, 2000). Talapin *et al.,* (2001) also reported the mixing of tri-n-octylphosphine with dodecyl amine (DDA) to obtain high luminescent CdTe nanoparticles (Talapin *et al.,* 2001). As the interest in the use of CdTe for different applications increased, more investigations were carried out to optimise the reaction conditions and improve the properties of the as –synthesised CdTe NPs. Peng and Peng reported the synthesis of CdTe NPs using CdO or Cd-fatty acid as precursors to replace the toxic dimethyl cadmium. The so called 'green

route' proved to be reproducible involving mild and simple reaction conditions, and could have potential for scale up and industrial applications. However, this process still involves the presence of additional stabilisers such as hexylphosphonic acid (HPA) which increases cost of production and the initial temperature of the reaction is still very high (Peng and Peng, 2001). Modifications of this route resulted in CdTe NPs with anisotropic shapes such as rods and tetrapod's (Dunge *et al.,* 2002 and Sheih *et al.,* 2005). Dagtepe *et al.,* also observed the formation of small magic-sized CdTe quantum dots (QDs) in the presence of Hexadecylamine (HDA) and TOPO as the coordinating solvent mixture at 240 ^{o}C while CdO was used as the cadmium-precursor (Dagtepe *et al.,* 2007). Highly luminescent CdTe nanocrystals have been synthesized using cluster compound and elemental tellurium with dodecylamine as capping agent at 147 ^{o}C (Chin *et al.,* 2008). This is a safer, reproducible route for the formation of rod-shaped and branched particles with PL QY as high as 37 % which increases to 52 % by addition of CdS shell. Mntungwa *et al.,* also reported the synthesis of HDA- capped CdTe using Oluwafemi *et al.,* adopted method. By varying the cadmium precursor and reaction time, spherical nanomaterials were obtained except for cadmium carbonate that produced nanorods. (Mntungwa *et al.,* 2011; Oluwafemi *et al.*,2008). McElroy *et al.,* reported the synthesis of CdTe QDs using a mixture of oleic acid and octadecene as the solvent for cadmium precursor while TOP was used to form TOP-Te solution at high temperature of 190^{0}C using a previously reported method by Wang and co-workers in 2009 (McElroy *et al.,* 2014, Wang *et al.,* 2009).

2.1.2 Two phase approach

This is the approach design to solve problems associated with both organic and aqueous synthesis. The CdTe NPs can be synthesised in either organic or aqueous phase and undergo surface modification to render them hydrophilic or hydrophobic in order to suite the desired application. The transfer of hydrophobic to hydrophilic can occur easily, while the transfer of nanoparticles from the hydrophilic to hydrophobic is often more difficult (Kanaras *et al.,* 2002; Algar & Krull 2007; Ananthakumar *et al.,* 2013). This is due to the fact that ligands used in organic phase are mostly very poorly soluble in water while those used in aqueous phase are often readily soluble in organic solvents (Simard *et al.,* 2000). In organic phase synthesis, this strategy involves substitution of a hydrophobic ligand with hydrophilic functional ligands. The ligands have anchoring groups at one end for binding to the nanocrystals via coordination onto the inorganic surface and hydrophilic functions at the other end that promote attraction to aqueous solutions (Pan *et al.,* 2001; Pradhan *et al.,* 2007). Substitution of organic capping with polar surface layers renders CdTe water soluble and bio compatible for several biological applications. The use of thiol ligands to render hydrophobic QDs water soluble is simple to implement, and it has been widely proven by literature. However, the long term use of the resulting QDs is strongly dependent on the affinity of the anchoring groups on the nanocrystals surfaces (Yang *et al.,* 2012). Furthermore, the ligand exchange results in the sacrifice of the parental properties such as increase in particle size, decrease fluorescence intensity and stability of the nanoparticles. Due to the limitation associated with surface modification of organically capped CdTe, aqueous synthesis of QDs has been an alternative way to tackle problem associated with phase transfer (Wang *et al.,* 2007; Aldana *et al.,* 2001and Zhang *et al.,* 2011). Ananthakumar and

co-workers reported the synthesis of organically CdTe QDs for photovoltaic applications via ligand exchange of aqueous soluble CdTe QDs. The CdTe QDs were previously synthesised in aqueous phase using thioglycolic acid as a capping agent followed by ligand exchange with 1-dodecathione as the capping agent to make material organically soluble. Organically capped CdTe QDs were then blended with P_3HT polymers for use as an active layer in hybrid solar cell structures (Ananthakumar *et al.,* 2013).

2.1.3 Aqueous synthesis

Water soluble NPs have been used in many biological applications such as *in-vivo* and *in-vitro* imaging, DNA hybridization and photodynamic therapy. Aqueous synthesis of CdTe NPs widens the application of CdTe NPs to other areas that were not possible with organically synthesised CdTe NPs. In this route, CdTe QDs are synthesis directly in water thus, the material are hydrophilic and therefore can be applied in any field of biology and biomedicine without any further alterations (Jin *et al* 2011; Jong *et al*., 2008). Aqueous synthesis of CdTe NPs is always associated with use of inert atmosphere to avoid oxidation of precursors and stabilising agents used during the synthesis. It also prevents the as-synthesised CdTe NPs from photo oxidation which usually lower the optical properties of the material compared to the ones synthesised via organic approach and increases its cytotoxicity (Chan et al., 2002; Kim *et al.,* 2004; Li *et al.,* 2011)

The early approach for the aqueous phase synthesis of CdTe QDs involves the use of stabilising agents, $CdCl_2$ as cadmium precursors and NaHTe as tellurium precursor under argon flow. Rogach *et al.,* reported the first synthesis of high quality

CdTe NPs using thioglycerol and mercaptoethanol as surface stabilizing agent for the synthesis of stable fluorescence CdTe NPs (Rogach *et al.,* 1996). This was a breakthrough in obtaining CdTe nanoparticles with stable fluorescence for a longer time. The co-ordination of cadmium ion and thiols by Cd-SR prevented uncontrollable growth of the nuclei however the fluorescence quantum yield was less than 3 %. After this report, the use of thiols became active in the field as they tend to stick firmly to the surface of the NPs. In 2000, the same group reported the use of mercaptoalcohols, mercaptoacids, and dithiols. The PL quantum yield increased to 18 % after 14 days of controlled heat treatment in an acidic condition (Andrey and Rogach, 2000). The enhancement of the fluorescence intensity is associated with formation of cadmium-thiols complex on the surface of the CdTe NPs when the pH of the solution is in the acidic range. The use of thiols has been extensively studied for the synthesis of CdTe NPs. Dodecanethiol was used to substitute MPA through phase transfer by Gaponik to obtain PL quantum yield of 40-50 % (Gaponik *et al.,* 2002). Liu *et a*l in (2006) reported the synthesis of MPA-capped CdTe NPs under air and nitrogen. Their results showed that NPs synthesised in air are more vulnerable to oxidation and this resulted in the release of cadmium ions (Liu *et al.,* 2006). This is in line with Zhang *et al.,*; earlier report that singlet oxygen is responsible for photo bleaching of thiol capped CdTe QDs in leaving cells. Water soluble CdTe QDs has also been reported through hydrothermal and microwave irradiation method resulting in material with reduced surface defect and increased quantum yield (Zhang *et al.,* 2006; Zhang *et al.,* 2003; Li *et al.,* 2005; Qian *et al.,* 2006; He *et al.,* 2006; He *et al.,* 2007; Li and Murase 2005). The use of inert atmosphere to avoid oxidation of tellurium precursors and high pressure in case of microwave made the synthesis not desirable for industrial scale due to high cost associated with these syntheses. In

trying to improve the reaction conditions for the synthesis as well as the optical properties of CdTe NPs there is still a lot of on-going research based on thiols stabilised CdTe NPs. It has been reported that the emission intensity can be enhanced by regulating the amount of surfactant used as they tend to create some surface defects when used in larger quantities. Thus, for hydrothermal synthesis, the formation of Cd-SH complex depends on the amount of thiol (Gao *et al.,* 2005; Shavel *et al.,* 2006; Murase *et al.,* 2007). After these reports, the enhancement of the CdTe NPs florescence intensity has been intensively studied. Murase *et al.,* 2007 investigated the effect of Cd^{2+} to TGA ratio. In this study five mole ratio ranging from 1.25 to 2.40 were used. Their analyses revealed that the TGA decompose to S-H and the use of different mole ratio of TGA resulted in CdTe NPs with different composition. Murase *et.al*., further highlighted that about half of the tellurium site on the surface were replaced by sulphur from TGA which started decomposing from the early stage of the synthesis and increased with increase in storage time (Murase *et al.,* 2007). Mercaptosuccinic acid (MSA) capped CdTe NPs have also been synthesised at lower temperatures (35 ^{0}C) in the presence of yeast solution by Bao *et al*. The protein capped CdTe NPs emitting at wavelength of 556 nm with PL QY of 33 % was achieved by one step synthesis after incubation for several days. The protein used in this synthesis made the as-synthesised CdTe NPs biocompatible and for bio-labelling applications (Bao *et al.,* 2010). Apart from MPA, MSA and TGA, glutathione as mercapto acid derivative has also been reported as effective thiol for CdTe NPs (Bu *et al.,* 2013). This produces NPs with higher fluorescence intensity than other thiols. The higher luminescence intensity has been attributed to its decomposition to produce sulphur that replace Te on the surface which act as passivating agent and reduces the dangling bonds/ vacancies(Xue *et al.,* 2011; Zeng

et al., 2007. Bu *et al.,* (2013) reported the synthesis of CdTe NPs with QYs as high as 57 % by using N-acetyl-L-cysteine as capping agent under hydrothermal synthesis in an autoclave. The reaction temperature was varied from 120 ^{o}C to 200 ^{o}C and the pH from 5 to 11. The highest QYs of 57 % was obtained at 200 ^{0}C and pH 5 (Bu *et al.,* 2013). Similar synthesis was reported by Yang *et al.,* for the detection of mercury in aqueous solution (Yang *et al.,* 2014). Recently, Oluwafemi *et al.,* also reported the synthesis of glutathione capped CdTe/CdS NPs with glutathione acting as both stabilizing agent and sulphur source. The formation of the CdS shell on CdTe core was facilitated by the decomposition of the gluthathione (Oluwafemi *et al.,* 2014). In another development, Masoud *et al* reported the synthesis of CdTe NPs via a sonochemical method based on the reaction between cadmium acetate (Cd (OAC) $_{2}$), $TeCl_4$, and potassium borohydride (KBH_4) in water, in the presence of various capping agents. The effects of several parameters such as capping agents, ultrasonic power, reducing agent, reaction time, and cadmium precursors were investigated. It was found that morphology, particle size, and phase of the products could be greatly affected by these parameters (Masoud *et al.,* 2015). The use of Mercaptosuccinic acid as stabilizing agent had also been reported for synthesising high fluorescence CdTe NPs using hydrazine as the growth promoter in the absence of an inert atmosphere. By varying hydrazine concentration, the results showed that red emitting CdTe NPs with QYs as high as 50 % within short period of time can be obtained at lower hydrazine concentrations (Tan *et al.,* 2015).

2.2 Synthesis of core-shell nanoparticles

Core/shell nanoparticles are quantum dots that contain at least two semiconductor materials such as CdTe/CdSe, CdSe/ZnS, etc. Epitaxial growth of a semiconductor material (shell) on another (core) enhances the possibility of tuning the basic optical properties of the core nanocrystals such as their fluorescence wavelength, quantum yield, and lifetime. In core/shell nanocrystals, the shell provides a physical barrier between the optically active core and the surrounding medium, thus, the nanocrystals are less sensitive to the environmental changes and photo-oxidation. The shell further provides an efficient passivation of the surface trap states, giving rise to a strongly enhanced fluorescence quantum yield which is the fundamental prerequisite for the use of nanocrystals in applications such as biological labelling and light-emitting devices (Seo et al 2007; Kim *et al.,* 2003; Xie *et al.,* 2005; Chen *et al.,* 2004). Core-shell nanoparticles overcome major concern associated with the biological application of nanoparticles i.e. their instability in biological fluid. This is also the main source of the inherent cytotoxicity of quantum dots. Cytotoxicity has been attributed to the release of highly toxic cadmium ions and reactive oxygen in solution. This is because the as-synthesised QDs materials sometimes do not possess distinct thick shell which has been found to reduce the toxic character. Hence they contaminate the intracellular compartment of cells which is a huge drawback for their biological applications (Biju *et al.,* 2010; Jiang *et al.,* 2006; Cho *et., al* 2007; Green *et al.,* 2007 and Liu *et al.,* 2014).

Core-shell NPs can be broadly classified into type I and type II. In Type I core-shell NPs the band gap of the shell material is larger than that of the core and both

electrons and holes are confined in the core. The shell is used to passivate the surface of the core, as it physically separates the core from its surroundings, decreasing the dangling bonds and therefore improves its optical properties. The formation of the shell is usually indicated by a small red shift in the emission position. In type II core shell NPs, either the valence-band edge or the conduction band edge of the shell material is located in the band gap of the core. Type-II NPs are aimed particularly for infra-red region emission. The interest of these systems is the possibility to manipulate the shell thickness and thereby tune the emission colour towards spectral ranges, which are difficult to obtain with other materials. There are a lot of issues to be considered before the designing of type-II QDs. Thus far, many type-II systems have been reported, including ZnTe/CdTe (CdSe, CdS), CdSe/ZnTe and ZnSe/CdS and CdTe/CdSe (Chen *et al.,* 2004; Liu *et al.,* 2006; Green *et al.,* 2007, Wang *et al.,* 2011). McElroy *et al.,* (2014) in 2014 conducted a study on CdTe/CdSe and CdSe/CdTe QDs for the fabrication of quantum dot sensitised solar cells. Additional layer of CdS was also introduced to reduce the overlap acting as the potential surface barrier (McElroy *et al.,* 2014). Their results showed that the wave function overlap is less in CdTe core quantum dots than those with CdSe core. Similar observation has been reported by Tyrell *et al* (Tyrell *et al.,* 2012). These syntheses are based on an organometallic route which is undesirable for biological applications. Therefore, the search for hydrothermal QDs with high photo stability and biocompatibility is inevitable. The NIR-emitting CdTe/CdSe QDs have been synthesised by Xia and Zhu, (2008) in aqueous solution for ultrasensitive Cu^{2+} sensing (Xia and Zhu, 2008). Yan and his co-workers also reported the successive ion-layer adsorption and reaction (SILAR) for synthesizing water-soluble L-cysteine-capped CdTe/CdSe QDs with NIR fluorescence for bio imaging applications.

Although these methods are feasible, they are time-consuming and result in material with lower PL QYs than those synthesize in organic phase. Therefore, it is desirable to develop a facile method for the preparation of high quality type-II core/shell NIR emitting QDs in aqueous solution. In another development, Zhang *et al.,* (2010) reported the synthesis of L-cysteine capped CdTe/CdS NPs and conjugate them with rabbit antibody for direct immuno-labelling and imaging of HeLa cells (Zhang *et al.,* 2010). CdTe/CdS NPs with amino acid and carboxylic acid functional groups surfaces have been prepared by Shan *et al.,* using L-cysteine as the capping agent. The nanowire L-cysteine capped CdTe/CdS NPs were of low quantum yield due to nature of the material as well as the capping agent (Shan *et al.,* 2014). Oluwafemi *et al., (2014)* reported the synthesis of glutathione capped CdTe/CdS NPs with improved stability and high quantum yield (Oluwafemi *et al.,* 2014). As an improvement to Oluwafemi *et al.,* (2014), Ncapayi *et al.,* (2015) reported the synthesis of MPA capped CdTe/CdSe NPs with reduced cytotoxicity (Oluwafemi *et al.,* 2014; Ncapayi *et al.,* 2015). The improved cell viability is attributed to the use of CdSe NPs, a wider band gap material compared to CdS. In a latest development, Chen *et al*., reported the synthesis of biocompatibility CdTe/CdSe NPs. The prepared GSH-CdTe/CdSe QDs demonstrated good water-solubility and dispensability, low cytotoxicity and strong NIR fluorescence, making them suitable for use as NIR imaging agent for molecular imaging in future studies (Chen *et al*, 2015).

2.3 Functionalization.

Inorganic colloidal nanoparticles are very small objects with inorganic cores that are dispersed in solvents. Depending on the material they possess a number of different properties such as high electron density and strong optical properties. Prerequisite for every possible application is the proper surface functionalization of nanoparticles, which determines their interaction with the environment. These interactions ultimately affect the colloidal stability of the particles, and may lead to a controlled assembly or delivery of nanoparticles to a target. Surface modification and functionalization of inorganic colloidal nanoparticles with a special focus on semiconductor nanoparticles, such as CdTe are of great importance. However, strategies used are often of general nature and apply in the same way to all types of nanoparticles. The functionalisation of nanoparticles with amino acid has been reported to further reduce toxicity. Generally, amino acids exist as zwitterions (internal salts) and exhibit spectra characteristics of both the carboxylate and primary amine salt. These two functional groups could make QDs responsive to bio-conjugation establishing the possibility of using them as fluorescent biomarkers (David *et al.,* 2011; Ethirajan, 2011 and Firczuk, 2011). Studies have shown that functionalisation of QDs surface using amino acid molecules reduce their toxicity significantly and enhance their water dispersibility without affecting their quantum yield (QY) and particle size. However, these reports are based on the ligand exchange of organically soluble QDs (Zhang *et al.,* 2011). Therefore, the functionalisation of aqueous synthesised QDs with amino acid as a highly luminescent probe for imaging and drug delivery is an area that needs to be adequately explored. Due to the enormous advantages of QDs over organic fluorophores, conjugation of antibodies to functionalised QDs for real time lymphatic

imaging and trafficking in replace of the organic fluorophores is an area that needs to be explored to improve the efficiency of this new technology (Chen *et al.,* 2015). Shi *et al.,* (2014) reported the functionalisation of MPA capped CdTe NPs with dopamine. The dopamine capped-CdTe NPs showed a slight blue shift in both absorption and emission position. The positively charged dopamine capped-CdTe NPs were successfully used as fluorescence probe for the detection of L-histidine in human serum (Shi *et al.,* 2014). Cyclodextrin is another material that is ideal for functionalisation of NPs. Cyclodextrins (CD) have attracted great interest in molecular chemistry due to the nature of their surface. The fact that cyclodextrin has a hydrophobic inner surface and hydrophilic outer surface makes them appropriate for improving biocompatibility, stability and solubility of QDs. Cyclodextrins have been used for functionalisation NPs such as CdSe/ZnS, CdSe/CdS, CdTe N (Ai *et al.,* 2012, Palaniappan *et al.,* 2012 and Chen *et al.,* 2012). Ai *et al., (2012)* and Chen *et al., (2012)* in 2012 reported the functionalisation of CdTe QDs with beta-Cyclodextrin. Ai and co-workers used the β-cyclodextrin functionalised CdTe QDs to construct sensitive biosensors for Amantadine (Ai *et al.,* 2012). Recently Yang and his colleagues used cyclodextrin functionalised CdTe QDs for detection of benzo[a]pyrene (BaP). They highlighted that functionalisation of the MPA capped CdTe QDs with cyclodextrin does not only improves the efficiency and intensity but also exhibit selective response when used for detection of BaP.

2.4 Cytotoxicity and Cell Labelling

The applications of QDs in cell imaging require the assessment of cytotoxicity and their penetration through the membranes. Mostly the cytotoxicity assessment and

cell imaging potential of QDs is carried on animal cells (Bar-Ilan *et al.,* 2009; Hsieh *et al.,* 2006; Yu *et al.,* 2014). The toxicity of the quantum dots in cells is associated with the instability of the NPs in biological fluids acting as the main source of the cytotoxicity inherent against cells. Thus, toxicity of QDs is mainly associated with their physicochemical properties (Hoshino *et al.,* 2004; Kirchner *et al.,* 2005). The diversity of nanoparticles as well as their capping materials made it is very difficult to elucidate all the toxicity mechanisms. The factors such as particle size, dosage, capping material often have different response on the toxicity of quantum dots (Lovric *et al.,* 2009; Su *et al.,*2009) . Several studies have shown that the cytotoxic of the quantum dots depends both on Cd^{2+} ions and the surface chemistry of the QDs (Su *et al.,* 2009; Chen *et al.,* 2012; Bradburne *et al.,* 2013). In a recent development Xu and co-workers investigated the effect of capping material on the toxicity CdTe NPs. In this study, three thiols were used MPA, GSH, and Cys and it was found that the toxicity of MPA-CdTe QDs was more than that of GSH-CdTe QDs and Cys-CdTe QDs on the GST protein growth at higher concentration of 50 nM (Xu *et al.,* 2015). This poses a huge drawback to their biological applications therefore, the search for QDs with high photostability and biocompatibility is inevitable. Su *et a*l in his sequentially cytotoxicity studies of water-dispersed CdTe QDs, CdTe/CdS core–shell QDs, and CdTe/CdS/ZnS core–shell–shell QDs and found that CdTe and CdTe/CdS are highly toxic which they associate with the leaching of cadmium ions to the surface while CdTe/CdS/ZnS QDs were non-toxic even at very high concentration thus due to ZnS shell which effectively passivate and protects the release of cadmium ions. Thus cytotoxicity can be modulated by production of multi-shell nanoparticles (Su *et al*., 2009). Green *et al.,* also reported that QDs with distinct thick shell posses reduced toxic character than bare core by reducing the level of

cadmium leached into the biological system (Green *et al*, 2007; Zhao *et al*, 2010). Chen *et al* results for biocompatible NIR GSH capped-CdTe/CdSe QDs showed low cytotoxicity against three normal cell lines (Chen *et al.,* 2015). Thus addition of shell and the use of polymeric capping agent make the QDs stable in biological fluid and therefore suitable for long term labelling studies.

CHAPTER 3

EXPERIMENTAL

3.1 Material

Cadmium acetate, potassium tellurite, 3-mercaptopropanoic acid, sodium borohydride, sodium hydroxide, zinc chloride, selenium powder, dimethyl sulphoxide, N, N'-Dicyclohexylcarbodiimide DCC, and L-arginine were purchased from Sigma Aldrich. All the chemicals were of analytical grade and used as purchased.

3.2 Method

3.2.1 Synthesis of CdTe core NPs

In a typical synthesis, 0.051 g (0.2 mmole) of dihydrated cadmium acetate was dissolved in 50 mL of HPLC water in a 100 mL three necked flask. 17 µL (0.2 mmole) of 3-mercaptopropanoic acid was added under stirring. The pH of the solution was adjusted from 3.67 to 9 using 1 M NaOH. The reaction mixture was stirred for 5 mins. In another flask, solution of potassium tellurite was prepared by dissolving 0.0103g (0.04 mmole) of K_2O_3Te in 50 mL of HPLC water. This solution was added to the above cadmium solution and allowed to react for 5 mins under continuous stirring followed by addition of 0.08 g $NaBH_4$ (2 mmole). The molar ratio of Cd/Te/MPA/$NaBH_4$ was fixed at 1:0.2:1:10. The solution was allowed to react for 5 mins and refluxed (in an oil bath at 98 ^{0}C) for seven hours. Aliquots were taken at different intervals to monitor the growth and luminescence of the as-synthesised CdTe QDs. The CdTe NPs were also synthesised at pH 11 and pH 12.

3.2.2 Synthesis of CdTe/CdSe core-shell NPs

The synthesis of the CdTe/CdSe core shell nanoparticles require a freshly prepared sodium selenosulphate as the selenium source, which was obtained by the reduction

of selenium using sodium sulphite. In a typical reaction, 0.5 g (4 mmole) of sodium sulphite and 0.1574g (0.2 mmole) selenium powder were dissolved in 50 mL of deionised water in a 100 mL three necked flask and refluxed at 70 ^{o}C for 6 h. In another flask, 0.051g (0.2 mmole) of dihydrated cadmium acetate was dissolved in 50 mL of deionised water in a 100 mL three necked flask. 17µL (0.2 mmole) of 3-mercaptopropanoic acid was added under stirring followed by the adjustment of the pH to 12 using 1 M NaOH. The reaction mixture was stirred for 5 mins to produce solution A. In another beaker, solution of potassium tellurite was prepared by dissolving 0.0103 g (0.04 mmole) of K_2TeO_3 in 50 mL HPLC water. This solution was added to solution A and allowed to react for 5 mins under continuous stirring followed by the addition of 0.08g $NaBH_4$ (2 mmole). The molar ratio of Cd/Te/MPA/$NaBH_4$ was fixed at 1:0.2:1:10. The entire solution was allowed to stir for another 5 mins and refluxed at 98 ^{0}C for 1 h. After an hour of refluxing, 0.5 mL (0.04 mmole) of freshly prepared Na_2SeSO_3 was swiftly injected into the solution. The Cd: Te:Se molar ratio was 1:0.2:0.2. The solution was then refluxed for 7 h to produce highly fluorescent CdTe/CdSe NPs. Aliquots were taken at different refluxing intervals to monitor the growth and optical properties of the as-synthesised CdTe/CdSe NPs. The same experiment was repeated for the synthesis at pH 11 and 12.

3.2.3. Synthesis of CdTe/CdSe/ZnSe core multi-shell

In a typical reaction, 0.051g (0.2 mmole) of dihydrated cadmium acetate was dissolved in 50 mL of distilled water in a 100 mL three necked flask. 17 µL (0.2 mmole) of 3-mercaptopropanoic acid was added to this solution under continuous

stirring. The pH of the solution was adjusted to the desired pH using 1 M NaOH, followed by stirring for 5 mins. 50 ml (0.0008 M) of potassium tellurite solution prepared as reported in section 3.3.1 was added to the above cadmium solution. The mixture was allowed to react for 5 mins under continuous stirring followed by addition of 0.08 g $NaBH_4$. The molar ratio of Cd/Te/MPA/$NaBH_4$ was fixed at 1:0.2:1:10. After another 5 mins of reaction, the solution was refluxed at 98 ^{0}C for one hour. After an hour under refluxing, 0.5 mL (0.02 mmole) of Na_2SeSO_3 was swiftly injected using a graduated pipette. Aliquots were taking at different intervals to monitor the growth and luminescence of the CdTe/CdSe core –shell. In a different reaction vessel, MPA –Zn precursor was prepared by dissolving the 0.04 mmole of zinc acetate in 50 mL of water followed by addition of 17 µL of MPA and the pH was adjusted to 9 using 1 M NaOH. The MPA-Zn solution was added to CdTe/CdSe solution after an hour under vigorous stirring and refluxed for 7 hours at 98 ^{0}C to produce CdTe/CdSe/ZnSe NPs. Aliquots were taken at different intervals to monitor the growth of NPs. The same experiment was reported for the synthesis at pH 11 and 12.

3.2.4 Optical and structural characterization.

The absorption spectra of as-synthesised CdTe, CdTe/CdSe, and CdTe/CdSe/ZnSe nanoparticles were taken using a Perkin Elmer Lambda 25 UV-Vis spectrophotometer and the emission spectra were recorded on a LS 45 Perkin-Elmer spectrophotometer with a Xenon lamp at room temperature using water as a solvent in a 10 mm path length quartz cuvette. Fluorescence analyses were carried out at excitation wavelength of 400-450 nm. In preparation for the analyses 50 µL of the

sample was diluted with 2950 µL of HPLC water (ratio 1:59) due to the high fluorescence intensity of the undiluted sample. The surface chemistry of all the as-synthesised nanoparticles was investigated using Lambda one FT-IR Perkin Elmer spectrometer with an ATR sample holder. Measurements were performed by placing the sample on a glassy part of the sample holder. The transmission electron microscopy (TEM) and high resolution TEM were used to obtain the shape and the size of the as-synthesised NPs using a JEM-2100 JEOL electron microscope. The samples were prepared by placing a drop of a dilute solution of sample on a copper grid and allowed to dry completely at room temperature before being loaded into the microscope.

3.2.5 Cell viability study

3.2.5.1 Cell culture

The Dulbecco's modified Eagle medium (DMEM) (Sigma-Aldrich, St. Louis, MO, USA) supplemented with 10 % fetal bovine serum (Thermo Fisher Scientific, Waltham, MA, USA), 1 % L-glutamine-penicillin-streptomycin (Sigma-Aldrich) and geneticin (0.5 mg/mL, G418 sulfate, Sigma-Aldrich) was prepared and then warmed to 37 ^{0}C using warming stones in preparation for the cell culture .

The cells were removed from the liquid nitrogen (-20 ^{0}C), and there after defrosted using the water bath at 37 ^{0}C. The defrosted cells solution (1.5mL) was added in 3.5 mL of DMEM in a 10 mL centrifuge tube. The cell was concentrated by centrifuge at 1360 rpm for 5 min followed by decantation of the supernant. The adhesive cells were removed from the centrifuge tube by tapping and addition of 10 mL of the

medium. The cell solution was transferred to 10 mm cultural dish with the aid of serological pipette. The cultural dish was examined through the microscope to check the cell confluence and thereafter incubated at a 5 % carbon water jacketed incubator for 24 h. After 24 h, the cultural dish was removed from the incubator and was observed under the microscope to check if the cells are adhesive. The old medium was removed and the cell was washed with 10 mL PBS. After decantation, 10 mL of the new medium was added and cell was incubated for 48 h.

3.2.5.2 MTT Assay Protocol

The colorimetric MTT (3-(4,5-cimethylthiazol-2-yl)-2,5-diphenyl tetrazolium Bromide) assay is based on the ability of the mitochondrial succinate-tetrazolium reductase system to convert the yellow dye (MTT) to a blue formazan product. KM-Luc/GFP cells were suspended at a concentration of 1.0×10^5 cells/mL in Dulbecco's modified Eagle medium (DMD). Subsequently, 100 μL of the cell solution was added in each well of a 98-well plate (BD Biosciences) and incubated at 37 in a water jacket incubator (5 % carbon dioxide and 95 % air mixture). 24 h later, 20 μL of QDs were added to each well, while 20 μL of phosphate-buffered saline (PBS) was added as the control group. Then, samples were incubated at 37 . 24 hours later, cell viability was determined using 3-(4,5-dimethylthiazol-2-yl)-2, 5-diphenyltetrazolium bromide (MTT) assay. MTT (5 mg/mL) solutions were added to each well and samples were incubated at 37 . After 1 hour incubation, the supernatant medium was gently aspirated and 100 μL of DMSO was added to lyse the cells and dissolve the MTT solution to give deep-blue formazan in preparation for absorbance measurements. The plates were gently shaken to complete the dissolution of any

formazan crystals immediately. The absorbance reading was carried out using an automated plate reader (Sunrise Rainbow Thermo; Wako Pure Chemical Industries, Ltd., Osaka, Japan) at 590 nm. The absorbance values were converted to cell viability using control.

3.2.6 Fluorescence Imaging

The transfection was performed according to manufacturer's instructions using lipofectamine which is a cationic liposome as a transfecting agent. The cells were plated in a 12 well plate at a density of 2.5 x 10^5 cells/mL. The medium was changed every day, until 85 % cell confluence was achieved.

The QD-lipofectamine complex was prepared at room temperature 30 mins before being administered to the KM-Luc/ GFP cells. Briefly, different concentration of quantum dots were prepared by dilution using medium as a solvent, followed by addition of 3.5 uL of liposome to form 100 µL complex solution. The complex solution was incubated at room temperature for 30 mins and later administered to the cell. The well plates were then incubated for 6 h to render cells adhesive, after 6 h the old medium was replaced by a new medium. The transfected cells were then incubated for 18 h to make 24 h of incubation period. The transfected cells were viewed under the confocal fluorescence microscope with an argon laser excited at the wavelength of 580 nm.

CHAPTER FOUR

RESULTS AND DISCUSSION

4.1 Optical analysis

4.1.1 CdTe Nanoparticles.

The synthesis involves the use of low cost, environmental benign reagents and was carried out in aqueous medium using cadmium acetate and potassium telluride as cadmium and tellurium precursors respectively while mercaptopropanoic acid was used as the capping agent. After the addition of $NaBH_4$, the solution turned yellow and the colour become intense as the temperature of the reaction approached 90 ^oC indicating the formation of CdTe NPs. The reaction progress as well as increase in particle size was shown by the change in the colour of the reaction solution from yellow to orange and finally to red with bright fluorescence under the UV light. Figure 4.1 shows the absorption and emission spectra of as-synthesised CdTe NPs at pH 9. The absorption maxima ranges from 494 nm to 556 nm as the reaction time increased from 0.25 h to 7 h (Fig. 4.1 A) indicating increase in particle size. The absorption spectra showed sharp excitonic peaks with sharp absorption band edge indicative of monodispersed particles with narrow size distribution. The decrease in the sharpness of the excitonic peak as the reaction progressed is attributed to increase in particle size distribution. The diameter of the as-synthesised CdTe NPs as calculated using Yu *et al.,* method varies between 2.3 nm and 3.1 nm as the reaction time increases from 0.25 h to 7 h (Yu *et al.,* 2003). Figure 4.1B is typical evolution of the photoluminescence spectra of the as-synthesised MPA-capped CdTe NPs as a function of time at an excitation wavelength of 400 nm. The sample used for the analyses was diluted at ratio 1:60 sample: distilled water (50 µL of a

sample into 2950 µL of water) due to their high fluorescence intensity. Similar to the absorption spectra, the emission spectrum is red shifted from 521 nm to 565 nm as the reaction progressed from 0.25 h to 7 h All the emission maxima for the as-synthesised CdTe NPs are blue shifted with respect to the corresponding band gap exhibiting band edge luminescence with a stoke shift of less than 22 nm. The as-synthesised NPs emit from green (at the beginning of the reaction) to orange region (toward the end of the reaction) as indicated by a bright fluorescence under the UV light. The overlaid emission spectra show broad emission spectra at the beginning of the reaction (0.25 h) attributed to broad size distribution or defocusing of the spectra. However, as the reaction progressed, focusing of the spectra occurred (0.5-7 h) (Donega *et al.,* 2003; Ncapayi *et al.,* 2015). The broadness of the emission peak at the beginning of the reaction might be due to fast nucleation resulting in material with different particle size. This later undergoes Ostwald ripening process to form uniform bigger particles. The broadness can also be attributed to the presence of the unreacted monomers at the beginning of the reaction which act as the surface defects and results in luminescence quenching (Mntungwa *et al.,* 2011). The high fluorescence intensity of about 89 arbitrary unit (a.u) was obtained at 0.25 h and increased as the reaction continued, reaching a maximum of 502 a.u at 1.5 h . After 1.5 h the emission intensity decreased to 471 a.u at 7 h reaction time. This might be attributed to the insufficient passivation due to the formation of bigger particle size as the reaction progressed. The full width at half maximum (FWHM) of all the as-synthesised CdTe NPs at pH 9 were below 60 nm throughout the reaction. This indicates that the as-synthesised CdTe NPs are of good optical characteristics, desirable dispersibility and uniformity (Yang *et al.,* 2007).

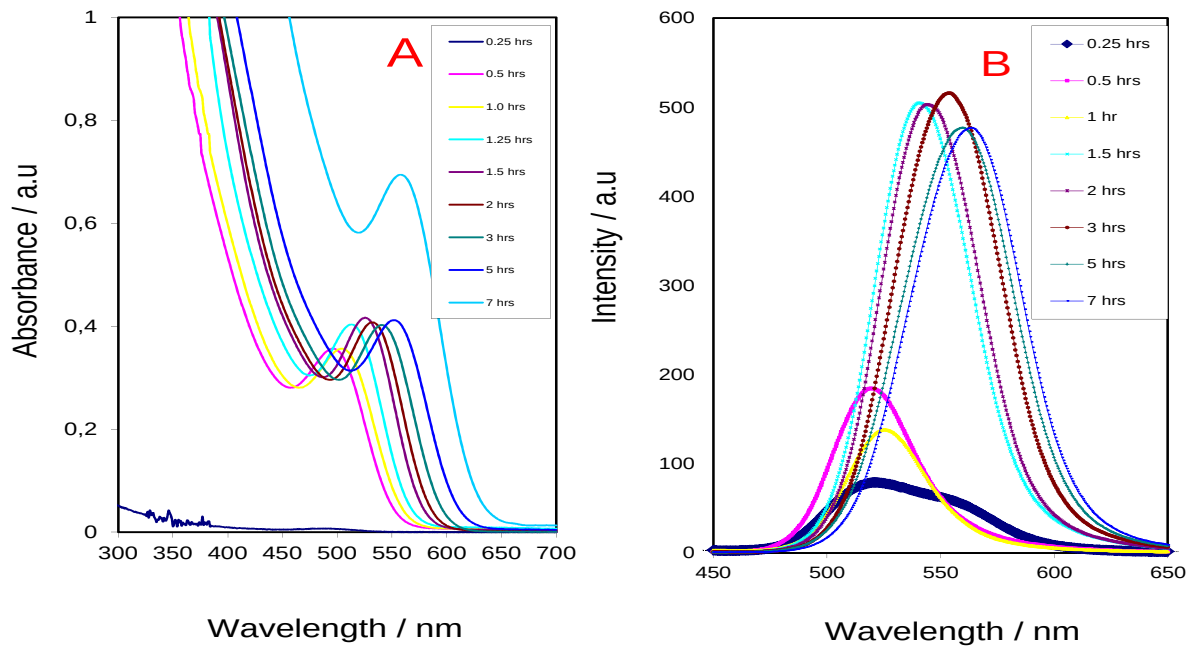

Figure 4.1: (A) absorption and (B) emission spectra of as-synthesised CdTe NPs at pH 9 at different reaction times.

Table 1: optical properties of MPA capped CdTe NPs at pH 9

Reaction time (h)	Absorption Maximum (nm)	Emission Maximum (nm)	Emission intensity (a.u)	FWHM (nm)	Particle Size (nm)	Stoke Shift (nm)
0.25	495	517	89	40	2.29	22
0.5	509	520	184	41	2.44	11
1	513	527	134	42	2.48	14
1.5	521	542	502	46	2.57	21
2	530	545	500	50	2.70	15
3	540	546	509	54	2.85	6
5	551	554	476	56	3.06	3
7	556	559	471	56	3.10	3

Figure 4.2 A shows the absorption spectra of the as-synthesised MPA-capped CdTe NPs at pH 11. The CdTe NPs shows absorption maximum peak ranging from 503 nm to 548 nm as the reaction time increased from 15 mins to 7 h. The absorption spectra showed sharp absorption band edge indicating monodispersed particles. The absorption band edge varies between 565 nm and 620 nm. The average particle size diameter as calculated using Yu *et al., equation* was found to vary between 2.4 nm and 3.15 nm. The absorption spectrum indicates that the growth of nanoparticles at this pH is very slow with a shift of 43 nm in the absorbance maximum position as the reaction progressed from 0.25 h to 7 h. The emission maxima for all the as-synthesised CdTe NPs from 0.25 h to 7 h at pH 11 as indicated in Figure 4.2B are

red shifted with respect to their corresponding excitonic peak and exhibit band edge luminescence for excitation at 400 nm. All the particles emit from green to orange region under the UV light with emission position ranging from 528 to 568 nm within 7 h. The sharp narrow emission width accompanied by high fluorescence intensities indicates the growth of NPs with few electronic defects. The increase in the fluorescence intensity as the reaction time increased from 1 h to 5 h might be due to depletion of the precursors (unreacted Cd^{2+} ion) which usually act as surface defect and then lower the luminescence intensity. As the reaction time increased the amount of the unreacted Cd^{2+} ion present in the solution decreased hence, increase in the surface passivation and subsequent increased in the luminescence intensity. The decrease in the emission intensity without any significant changed in the emission position after 5 h could be attributed to the presence of excess CdS layer (capping agent) on the surface of the CdTe NPs. The excess CdS layer could act as a new source of non-radiative recombination site and thus, cause decrease in luminescence intensity. Similar observation had been reported by Oluwafemi *et al.,* (2014); therefore, the optimum reaction time under this reaction condition is 5.

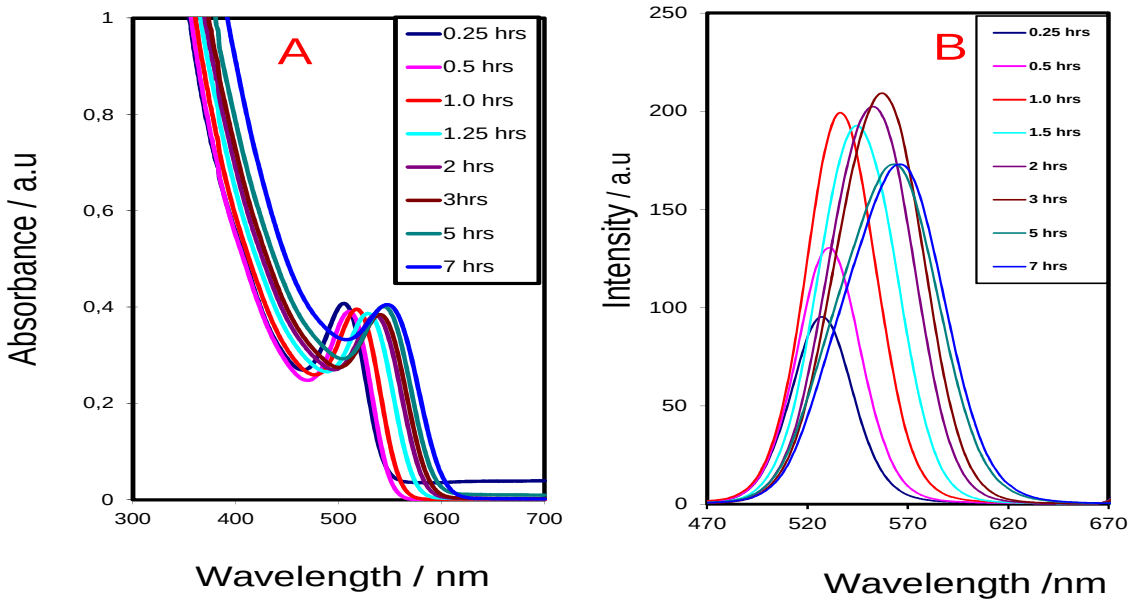

Figure 4.2 A) absorption and B) emission spectra of MPA capped CdTe NPs at pH 11

Table 2 : optical properties of MPA capped CdTe NPs at pH 11.

Reaction time (h)	Absorption maximum (nm)	Emission maximum (nm)	Emission intensity (a.u)	FWHM (nm)	Particle Size (nm)	Stoke shift (nm)
0.25	502	529	98	37	2.40	27
0.5	510	534	134	35	2.45	24
1	512	539	198	41	2.49	27
1.5	526	548	190	46	2.64	22
2	536	552	203	50	2.79	16
3	540	559	207	58	2.85	19
5	544	565	171	58	2.93	21
7	545	568	171	58	2.95	23

The absorption and emission spectra of CdTe NPs at pH 12 are shown in Fig 4.3 A and B. Due to high fluorescence intensity of CdTe NPs synthesised at pH 12 and the limitations of the PL spectrometer, the sample was diluted to ratio 1:375 (Sample to water) which is six time more than sample used at pH 9 and 11. The absorption spectra (Fig 4.3A) show sharp absorption peak at the beginning of the reaction (0.25 - 0.5 h). As the reaction time increased the absorption shoulder becomes broad (1.0 h) which may be attributed to the production of particles with different sizes (broad size distribution). At 1.25 h the absorption shoulder is very sharp and this continues for the rest of the reaction as indicative of monodispersed particles with narrow or focussed size distribution. The absorption band gap at different reaction time is blue shifted in relation to the excitonic radius of the bulk CdTe due to quantum confinement. The excitonic peak varies from 497 (0.25 h) to 547 nm (7 h). This red-shift in the excitonic peak as the reaction time increased corresponds to increase in particle size. The absorption band edge varies between 553 nm (0.25 h) and 617 nm (7 h) with particle size between 2.3 nm to 2.9 nm. The corresponding photoluminescence spectra (Fig 4.3B) exhibit defects free band-edge luminescence at the excitation wavelength of 400 nm. In a similar pattern with the absorption spectra, the emission maxima are red shifted as the reaction time increased. The PL spectra are narrow and symmetrical indicating focussed size distribution. The narrow band width and small stoke shift (27 to 16 nm) of the CdTe NPs indicate that the emission is dominated by band edge luminescence without any significant trap state emission. The high fluorescence intensity as the reaction time increase is attributed to decrease in the amount of unreacted Cd^{2+} and Te^{2-} ions present in the solution which usually act as surface defects and quench the fluorescence.

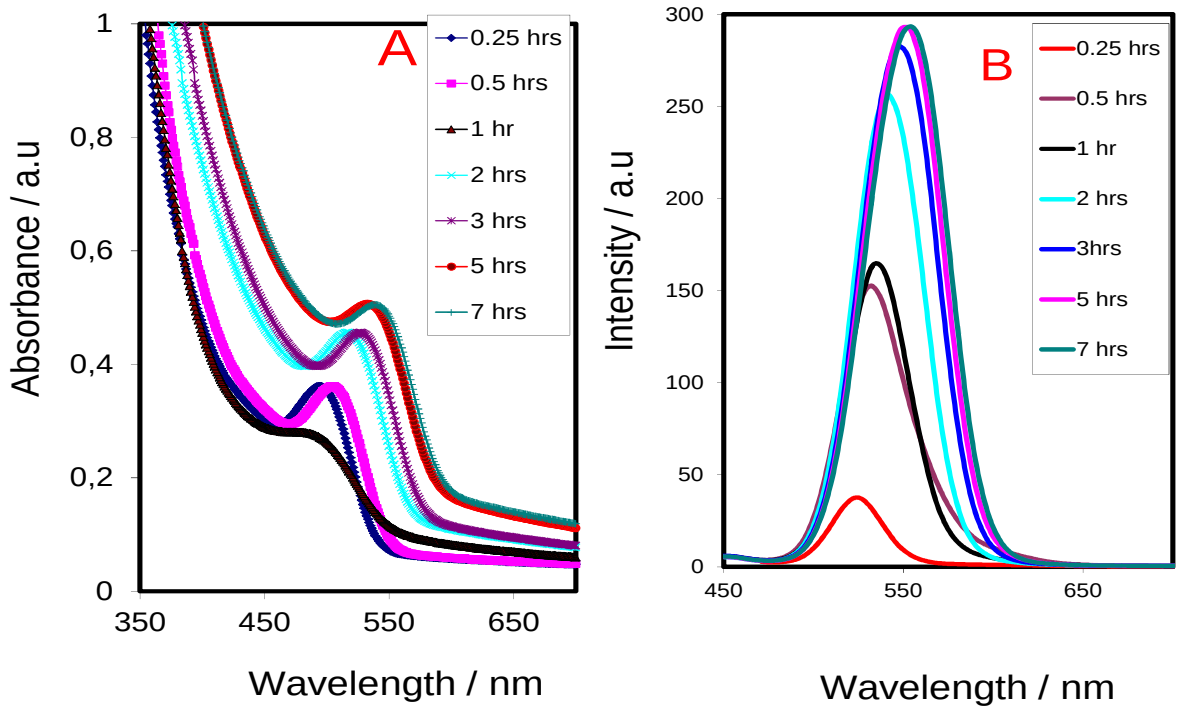

Figure 4.3 (A) Absorption spectra and (B) Emission spectra (λ400 nm) of MPA capped CdTe NPs at pH 12.

Table 3 : optical properties of MPA capped CdTe NPs at pH 12

Reaction time (h)	Absorption Maximum (nm)	Emission Maximum (nm)	Emission intensity (a.u)	FWHM (nm)	Particle Size (nm)	Stoke shift (nm)
0.25	497	529	38	38	2.3	32
0.5	503	530	152	44	2.4	27
1	509	539	164	42	2.4	30
1.5	515	540	256	44	2.5	25
2	528	541	265	49	2.7	13
3	536	548	282	52	2.8	12
5	540	552	291	52	2.9	12
7	547	558	293	52	3.0	11

4.1.1.1 pH effect

Studies have shown that the pH value influences the optical properties of NPs (Rogach *et al.,* 2000; Bu *et al.,* 2013). Figure 4.4 reveal the effect of pH on the optical properties of as-synthesised CdTe NPs at different pH. At all the pH, the absorption and emission maxima increased as the reaction time increased. In addition, the optical spectra indicate that the growth of the nanoparticles decreases as the pH increased. The lowest growth rate was obtained at pH 12. During the entire reaction time, the increase in the absorption maximum position as the reaction time increased from 0.15 h to 7h are 63, 49 and 43 at pH 9,11 and 12 respectively. The higher growth rate at pH 9 is attributed to the slower decomposition of MPA. At pH 9, the release of sulphide ion needed for the

formation of CdS layer (capping agent) on the surface of NPs was very slow. This caused Ostwald ripening process/ aggregation of the as-synthesised NPs due to delayed passivation of the NPs surface which resulted in particle size increased and hence, increased in the absorption maximum position. The slower growth at pH 12 is responsible for the narrow size distribution, high intensity, (Fig 4.4C) and narrow FWHM (Fig 4.4D) obtained at this pH compared to the results from other pH. The higher pH 12 has higher intensity than the lower pH which is in line with Donega *et al., that* slower particle growth usually leads to decrease in surface roughness and defect and thereby increasing the luminescence intensity (Donega *et al., 2003*)

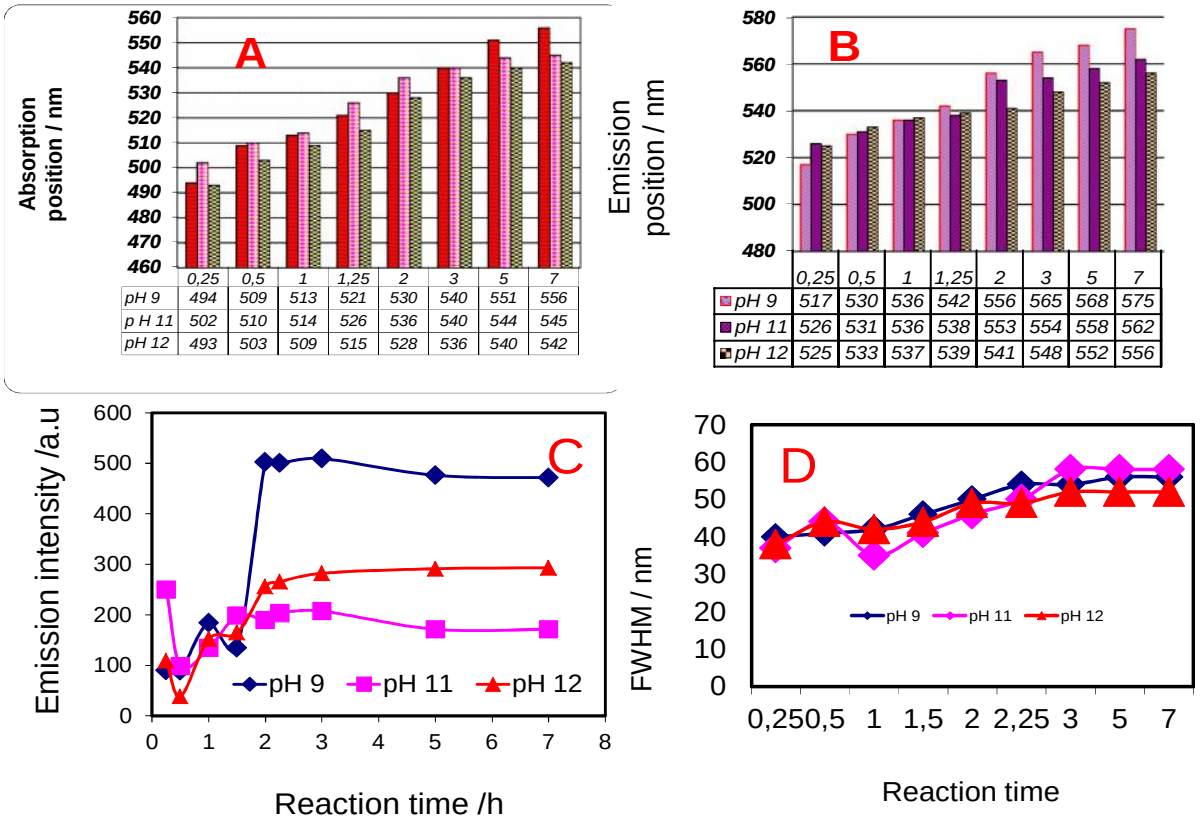

Figure 4.4: Effect of pH on (A) Absorption maximum and (B) Emission maximum ($\lambda_{400\ nm}$) (C) normalised emission intensity and (D) FWHM of MPA capped CdTe NPs at different reaction time.

4.1.2 CdTe/CdSe Nanoparticles

The as-synthesised CdTe/CdSe NPs were formed by the addition of the selenium precursor to the CdTe NPs solution after 1 h. The formation of the CdSe shell was instantaneous by immediate change in the colour of the solution from yellow to orange after the addition of sodium selenosulphate. This also gave bright orange fluorescence under the UV light which is different from that of the original CdTe NPs (yellow) under the UV light. Figure 4.5 (A) and (B) present the absorption and fluorescence spectra of the as-synthesised CdTe/CdSe NPs at pH 9 at different reaction time. The absorption spectra (Fig.4.5 A) revealed a red shift in absorption

maxima from 471 nm to 570 nm as reaction time increased from 0.25 h to 7 h indicating increase in particle size and quantum confinement effect. A significant shift of about 21 nm towards red-region was observed in the absorption spectra immediately after the addition of the selenium precursor indicating the formation of CdSe shell on top of the core. The sharp absorption maxima as well as the band edges might be attributed to narrow or focused size distribution due to effective passivation of the CdTe surface by the inorganic CdSe shell. The NPs exhibit orange to red fluorescence under the UV light. The PL spectra in Fig 4.5 B shows increase in emission maxima from 519 nm at 0.25 h to 592 nm at 7 h and exhibit band edge luminescence throughout the reaction. The emission spectra are narrow and become broader with prolonged heating with a full width at half maximum ranging from 40 nm (0.25 h) to 60 nm (7 h). The broadness of the emission spectra at prolonged reaction might be due to larger size distribution. The significant red shift in the absorption position accompanied by the increase in fluorescence intensity thus confirmed the formation of CdTe/CdSe NPs. The fluorescence intensity of the as-synthesised CdTe/CdSe NPs increase from 135 a.u (0.25 h) to 349 a.u within 2 h reaction time after 60 times dilution. The emission intensity starts to decrease after 2 h and reach 143 a.u at 7 h. The decrease in intensity after 2 h might be attributed to the formation of bigger particles and the formation of excess CdSe shell as the reaction time increased. As the number of CdSe layer on the CdTe core increased, these defects may become a new source of non- radiative recombination sites causing a decrease in PL intensity (Lim *et al.,* 2015).

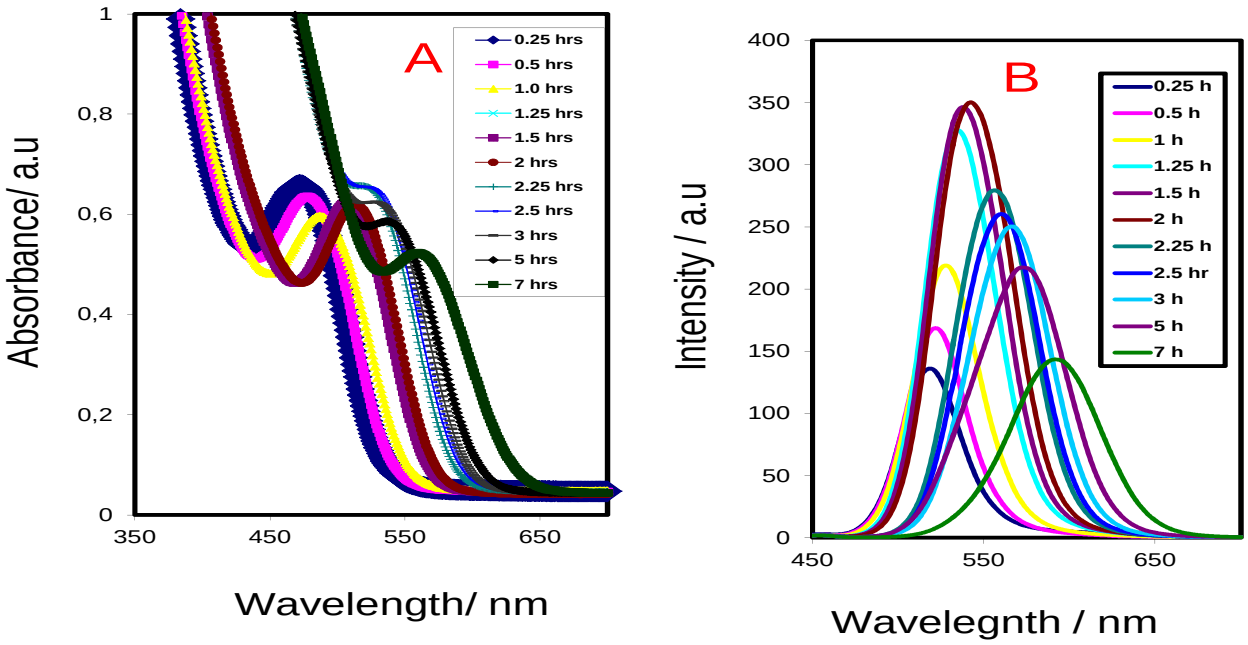

Figure 4.5: (A) Absorption and (B) emission spectra of as-synthesised CdTe/CdSe NPs at pH 9 as function of time.

Table 4: optical properties of MPA capped CdTe/CdSe NPs at pH 12

Reaction time (h)	Absorption Max (nm)	Emission Max (nm)	Emission intensity(a.u)	FWHM (nm)	Particle Size(nm)	Stoke shift (nm)
0.25	495	520	135	40	2.1	45
0.5	498	524	168	36	2.1	44
1	502	529	217	42	2.3	37
1.5	514	539	346	50	2.5	25
2	518	545	349	53	2.5	23
2.5	527	562	260	53	2.7	35
3	540	576	250	54	2.9	36
5	543	575	217	60	2.9	32
7	570	593	143	60	3.5	23

Figure 4.6 (A) and (B) shows the absorption and emission spectra of the as-synthesised CdTe/CdSe NPs at pH 12 respectively. The absorption as well as the emission maxima positions is blue shifted in relation to the bulk band gap of the core indicating quantum confinement. The absorption spectra (Fig. 4.6 A) show sharp excitonic peak indicating materials with focussed size distribution. The absorption maxima are red shifted as the reaction time increased indicating increase in particle size. A significant shift of about 36 nm was observed in the absorption spectrum after the addition of selenium precursor signifying the formation of the shell on the surface of the CdTe NPs core. The emission spectra (Fig. 4.6 B) followed the same

trend like the absorption spectra as the reaction time increased with significant red shift in the emission maximum position after the addition of selenium precursor. This is also accompanied by substantial enhancement of the fluorescence intensity. This enhancement has been attributed to the passivation of the surface vacancies of the core by the shell. The emission spectra show that sample produced 1.5 h after the addition of selenium produced the highest fluorescence intensity. The slight decrease in emission intensity after 1.5 h has been attributed to the insufficient passivation due to the increase in particle size of the material as the reaction progresses. The as-synthesised CdTe/CdSe NPs emit in the broad spectrum range from yellow to red region and exhibit band edge luminescence for excitation at 400 nm with a stoke shift ranging between 19 - 32 nm as indicated in table 4.The similar stoke shift for the rest of the reaction time after 3 h indicate constant growth rate. The full width at half maximum (FWHM) for all the as-synthesised CdTe/CdSe NPs was less than 50 nm indicating material with good optical properties.

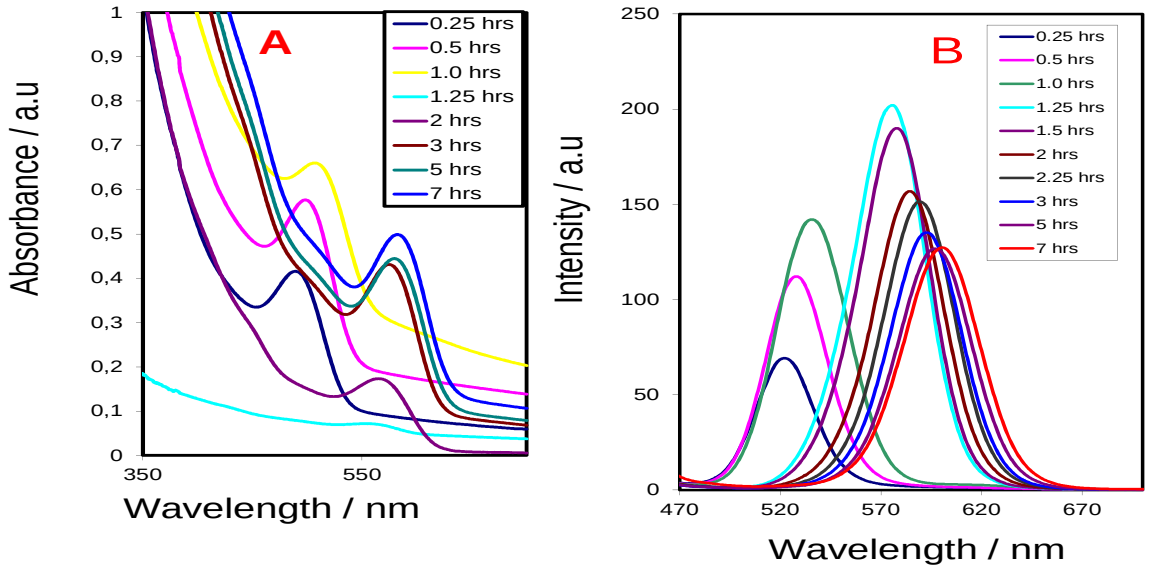

Figure 4.6 Absorption spectra (A), emission spectra (B) for the as-synthesised CdTe/CdSe NPs at pH 12 as a function of time.

Table 4: optical properties of MPA capped CdTe/CdSe NPs at pH 12

Reaction time (h)	Absorption Maximum (nm)	Emission Maximum (nm)	Emission intensity (a.u)	FWHM (nm)	Particle Size (nm)	Stoke shift (nm)
0.25	491	522	69	31	2.3	31
0.5	497	529	111	35	2.3	31
1	509	536	142	40	2.4	27
1.5	578	576	202	41	2.9	31
2	579	578	190	41	3.1	26
2.5	579	590	151	42	3.5	21
3	584	593	135	42	3.6	19
5	588	597	127	43	3.8	19
7	592	601	127	47	3.9	19

4.1.2.1 Effect of pH

The effect of pH in the optical properties of CdTe/CdSe is indicated in Fig 4.7 by the graphical representation of (A) absorption maxima, (B) Emission position, (C) Emission intensity and (D) FWHM of as-synthesised NPs at pH 9 and 12. The absorption and emission position indicate uniform growth at the beginning of the reaction (0.25-1h) for both pH 9 and 12. However after the formation of CdSe shell a significant redshift at pH 12 is observed. This resulted in pH 12 emitting at higher wavelength than pH 9. The increase in absorption emission maximum wavelength after the formation of CdSe shell was accompanied by enhancement of the

fluorescence intensity for both pH 9 and pH 12, with pH 12 having the highest fluorescence intensity. The fluorescence intensity decreased at 1.5 h and for the rest of the reaction. This might be attributed to the increase in particle size resulting in improper passivation of the CdTe/CdSe NPs surface by MPA. It can be observed from Fig. 4.7 (D) that all the NPs have narrow size distribution with FWHM ranging from 35 to 60 for pH 9 and 31 to 45 for pH 12 nm. This narrow size distribution was accompanied with high photoluminescence intensity for all the materials at different pH respectively. This ultimately verifies that the material obtained through this route is highly monodispersed with similar size distribution with pH 12 having the best results.

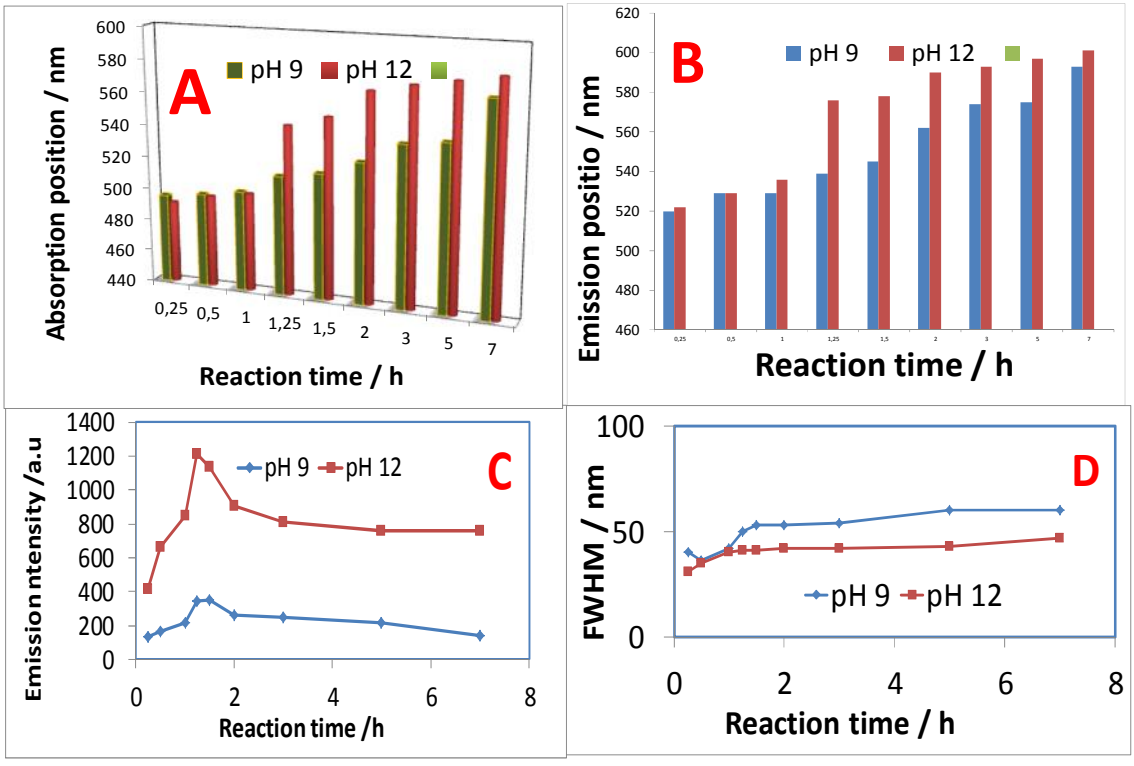

Figure 4.7 Effect of pH on (A) Absorption maximum and (B) Emission maximum ($\lambda_{400\ nm}$) (C) normalised emission intensity and (D) FWHM of MPA capped CdTe NPs at different reaction time.

4.1.3 CdTe/CdSe/ZnSe Nanoparticles

The CdTe/CdSe/ZnSe core multi shell NPs were synthesised using ZnSe as the second shell in order to further reduce the toxicity of the NPs and obtain near infrared emitting NPs. The absorption and emission spectra of CdTe/CdSe/ZnSe core multi shell NPs at pH 9 is shown in Fig 4.8 A and B. In a similar trend with CdTe NPs and CdTe/CdSe NPs synthesis, the absorption maxima are red shifted with prolonged heating. The absorption spectra (Fig. 4.8 A) show three stages of growth indicating the formation of three layers: CdTe, CdTe/CdSe and CdTe/CdSe/ZnSe NPs. The absorption spectra show absorption band edge at 538 to 548 nm (0- 1h) for the CdTe NPs core, 598 to 603 nm (0.25–1 h) after the addition of the CdSe shell) for CdTe/CdSe NPs and 614 to 661 nm (0.25–5h) after the addition of ZnSe shell for CdTe/CdSe/ZnSe NPs. The significant red shift of 50 and 11 nm after the addition of selenium and zinc precursor to the CdTe NPs solution and CdTe/ CdSe NPs solution respectively after 1 h reaction time confirm the formation of both CdTe/CdSe and CdTe/CdSe/ZnSe. This is different from the shift of about 2-5 nm observed when the CdTe NPs solution was allowed to go completion (7 h) without the addition of the inorganic shell. Similar shift (2-5 nm) was also observed when the CdTe/CdSe NPs solution was allowed to go to completion. The emission spectra in Fig 4.8 B exhibit band edge luminescence at excitation wavelength of 400 nm. The narrow emission spectrum as shown in figure 4.8 B is indicative of particles with focussed size distribution owing to proper passivation of the surface vacancies by the shell.

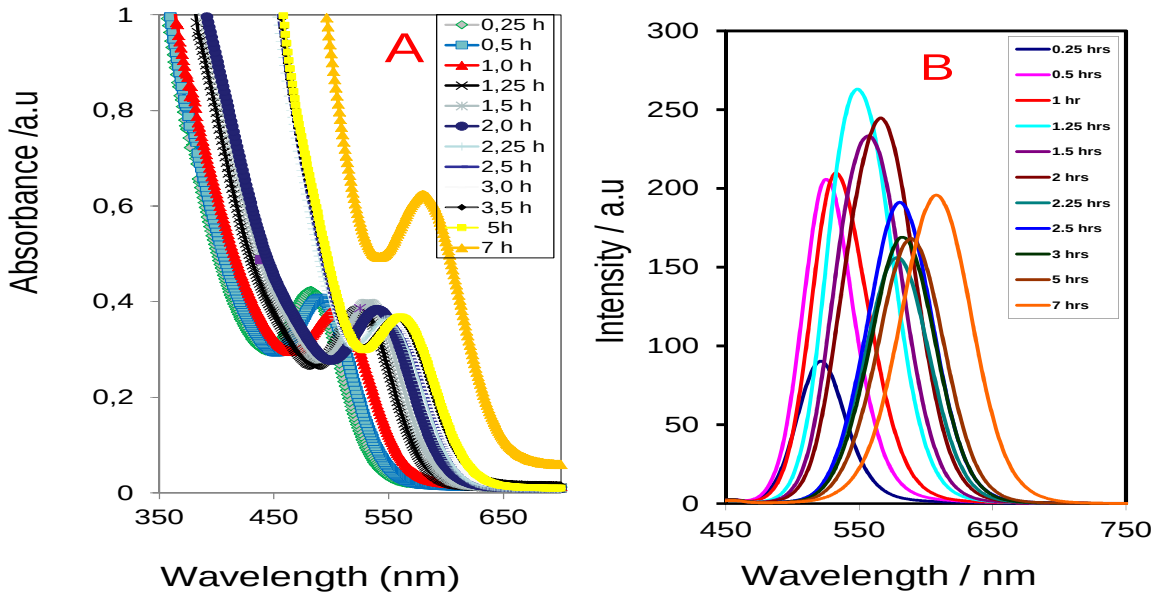

Figure 4.8 A) Absorption and B) Emission spectra of as-synthesised MPA capped CdTe/CdSe/ZnSe NPS at pH 9 as a function of time.

Table 5: optical properties of MPA capped CdTe/CdSe/ZnSe NPs at pH 9

Reaction time (h)	Absorption Maximum (nm)	Emission Maximum (nm)	Emission intensity (a.u)	FWHM (nm)	Particle Size (nm)	Stoke shift (nm)
0.25	490	521	90	41	2.2	31
0.5	498	526	204	38	2.3	28
1	501	533	211	26	2.4	32
1.5	538	557	233	29	2.8	19
2	548	568	244	40	3.0	20
2.5	562	574	190	22	3.3	12
3	564	582	168	28	3.4	18
5	571	590	167	29	3.5	19
7	589	609	194	30	4.1	20

Figure 4.9 A show the absorption spectra of as-synthesised MPA capped CdTe/CdSe/ZnSe NPs at pH 11. The absorption maximum ranges from 503 nm to 595 nm as the reaction time increased from 0.25 h to 7 h with an absorption band edge between 565 nm and 650 nm. The absorption spectra showed sharp absorption band edge indicating the presence of monodispersed particle size. The average particle size diameter as calculated using Yu *et al.,* varies between 2.22 nm to 4.4 nm. The absorption spectra showed a very slow growth as the reaction time progress with a red shift of 43 nm from 0.25 hours to 7 hours. The emission maxima for all the as-synthesised CdTe/CdSe/ZnSe NPs from 0.25 h to 7 h at pH 11 as indicated in Fig. 4.9 B are red shifted with respect to their corresponding exitonic peak and exhibit band edge luminescence for excitation at 400 nm. All the particles emit from green to red region under the UV light with emission position ranging from 522 to 602 nm within 7 hours. The sharp narrow emission width accompanied by high fluorescence intensities indicates the growth of NPs with few electronic defects. The fluorescence intensity ranges between 250 a.u at 15 min increased to 408 a.u at 1.5 h and thereafter decrease again, with 7 h having the fluorescence intensity of 293 a.u. The increase in the fluorescence intensity as the reaction time increase to 1.5 h is due to the proper passivation of the CdTe core by the CdSe and the decrease after 1.50 h might be attributed to increase in particle size as ZnSe shell grow on the CdTe/CdSe core-shell NPs .

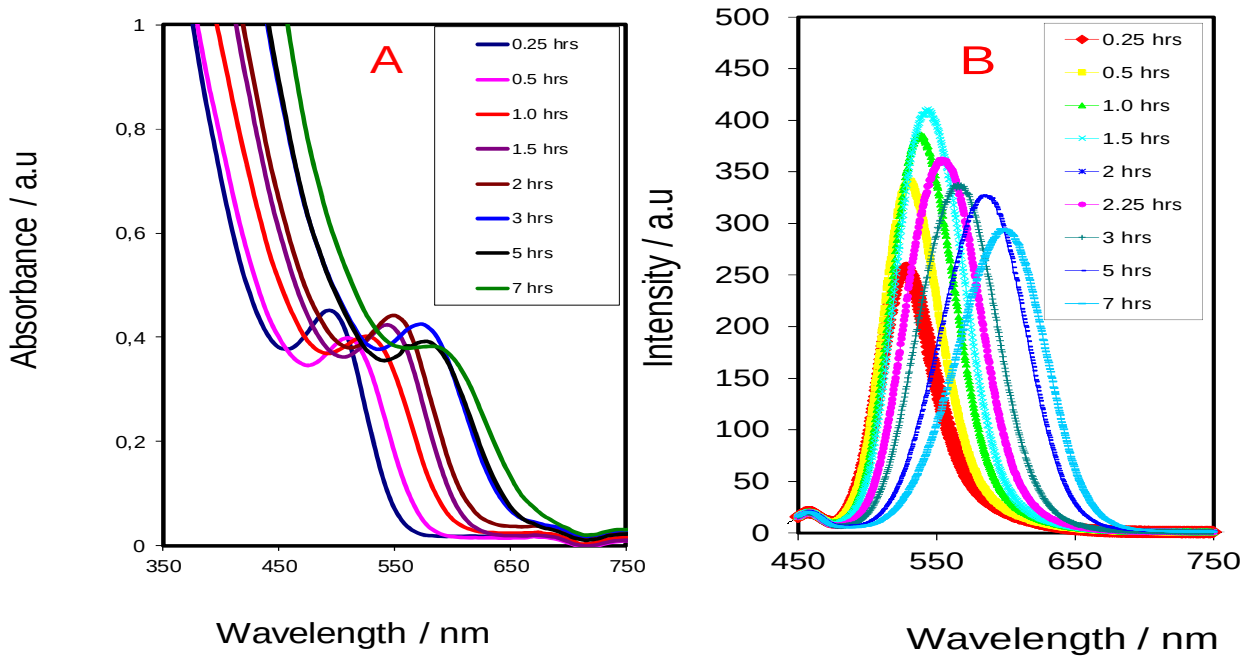

Figure 4.9: A) Absorption and B) Emission spectra of as-synthesised MPA capped CdTe/CdSe/ZnSe NPS at pH 11 with respect to reaction time.

Table 6: optical properties of MPA capped CdTe/CdSe/ZnSe NPs at pH 11.

Reaction time (h)	Absorption Maximum (nm)	Emission Maximum (nm)	Emission intensity (a.u)	FWHM (nm)	Particle Size (nm)	Stoke shift (nm)
0.25	499	522	250	43	2.3	23
0.5	520	529	348	46	2.56	9
1	530	536	382	51	2.7	6
1.5	540	555	408	55	2.9	15
2	549	558	398	56	3	9
2.5	572	581	372	60	3.6	9
3	579	587	335	64	3.8	8
5	580	597	317	70	3.8	17
7	595	602	293	71	4.3	7

The typical absorption and PL spectra of MPA -capped CdTe/CdSe/ZnSe NPs at pH 12 is represented in Fig 4.10 A and B. The absorption spectra (Fig. 4.9A) indicate particles with decreased in energy level (eV) as the reaction time increased from 0.25 h to 7 h. The absorption maxima for the as-synthesised MPA capped CdTe/CdSe/ZnSe NPs ranges from 484 nm to 597 nm within 7 h reaction time. Figure 4.10 (A) shows sharp excitonic peak indicating particles with focussed size distribution throughout the reaction time. This is attributed to the passivation of the surface by MPA at the beginning of the reaction and by the CdSe and ZnSe shell formation as the reaction progressed. This passivation also prevents aggregation from taking place. The photoluminescence spectra presented in Fig. 4.10 indicate band edge luminescence with emission maxima ranging from 513 nm (0.25 h) to 618 nm (7 h). Similar observation from green to red region has been previously reported by Li *et al* (2013) for the synthesis of CdTe/CdS/ZnS NPs. The emission spectra for one pot synthesis of MPA capped CdTe/CdSe/ZnSe NPs without any purification reveal narrow emission peaks with FWHM ranging from 35 nm (0.25 h) to 47 nm (7 h) indicating NPs with good optical properties. The as-synthesised CdTe/CdSe/ZnSe NPs emit in the green to red region under the UV light. The lower fluorescence intensity at the beginning of the reaction might be due to high concentration of unreacted precursors that can act as surface defects. The increase in the luminescent intensity after the addition of the selenium sources and zinc source is attributed to the depletion of monomer concentration and proper passivation of the core by the shell formation. The decrease in the emission intensity at the latter stage (at 7 h) might be attributed to the increase in particle size and formation of excess shell layer on the surface of the NPs which can also act as surface defect.

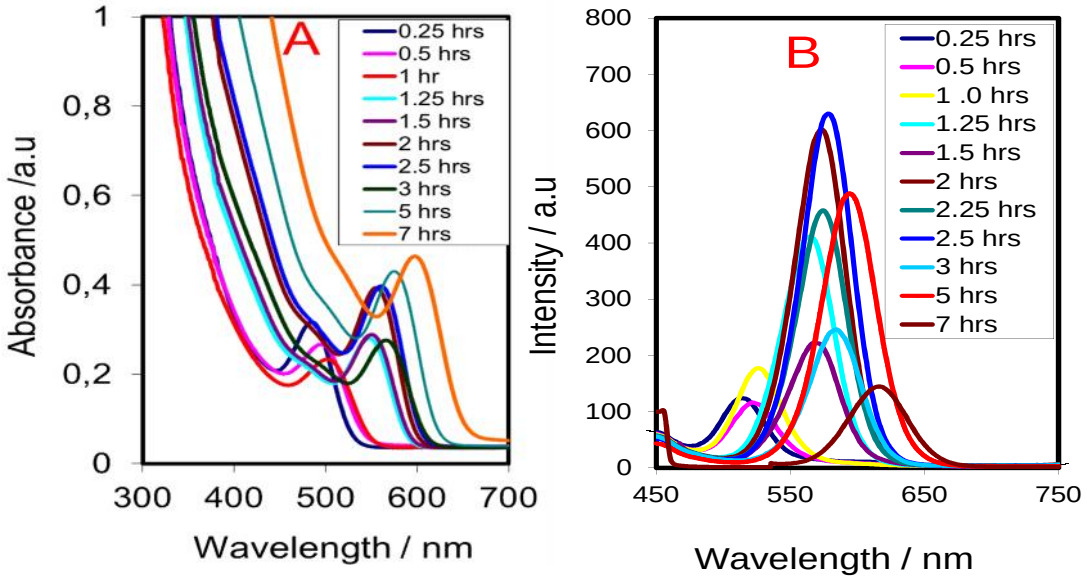

Figure 4.10: A) Absorption and B) Emission spectra of as-synthesised MPA capped CdTe/CdSe/ZnSe NPS at pH 12 as a function time.

Table 7: optical properties of MPA capped CdTe/CdSe/ZnS NPs at pH 12

Reaction time (h)	Absorption Maximum (nm)	Emission Maximum (nm)	Emission intensity (a.u)	FWHM (nm)	Particle Size (nm)	Stoke shift (nm)
0.25	492	511	109	40	2.3	19
0.5	499	522	114	35	2.34	23
1	504	526	176	35	2.4	22
1.5	545	569	410	45	2.9	24
2	560	572	607	43	3.3	12
2.5	570	577	626	44	3.5	7
3	573	580	245	47	3.6	7
5	581	595	485	47	4.8	14
7	606	620	144	47	4.8	

4.1.3.1 pH effect

Figure 4.11 reveals the pH effect on absorption maxima, emission maxima, emission intensity and FWHM. All the as-synthesised CdTe/CdSe/ZnSe NPs at different pH show red shift with prolong reaction time indicating increase in particles size. The absorption positions as indicated in Fig. 4.11(A) reveals an increase of 20 nm, 30 nm and 41 nm for pH 9, pH 11 and pH 12 respectively after the addition of the selenium source indicating the shell formation. The particles synthesised at pH 12 showed the greatest increase in particle size after the addition of the shell on the core. The emission position (Fig 4.11B) for CdTe/CdSe/ZnSe NPs follows the same trend as the absorption position confirming that the largest growth occurred at pH 12. The significant shift in the emission position for CdTe/CdSe/ZnSe is accompanied by a huge increase in the fluorescence intensity (Fig. 4.11C) than that of CdTe NPs immediately after addition of the shell. Thus, addition of the shell enhanced effective passivation of the surface vacancies on the CdTe core. The emission position (Fig 4.11 B) follow the same trend as absorption position with NPs at pH 12 emitting at longer wavelength than those at pH 9 and 11. The full width at half maximum (FWHM) of the as-synthesised CdTe/CdSe/ZnSe NPs as shown in Fig. 4.11 D are 63 nm (pH 9), 71 nm (pH 11) and 48 nm (pH12) for the highest reaction time of 7 h. Thus, CdTe/CdSe/ZnSe NPs with high fluorescence intensity, narrow emission width and larger particles can be obtained at pH 12 than those at lower pH.

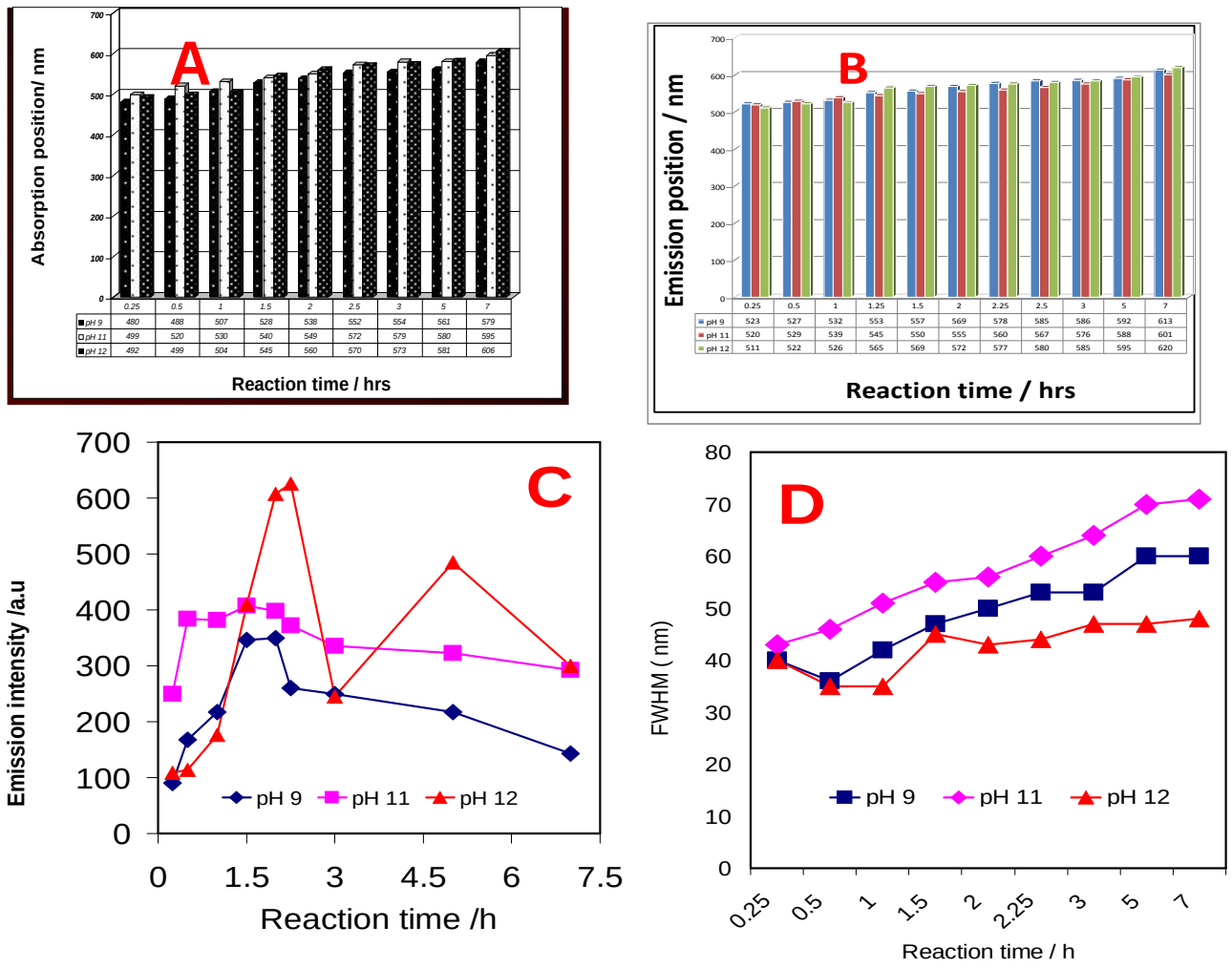

Figure 4.11: Effect of pH on (A) Absorption and (B) Emission ($\lambda_{400\ nm}$) position (C) emission intensity and (D) FWHM of MPA capped CdTe/CdSe/ZnSe NPs as a function of time.

4.1.4 STABILITY TEST

The stability of highly fluorescence MPA capped CdTe synthesised at pH 12 was evaluated by monitoring the emission property. Table 9 shows the emission property for the as-synthesised CdTe NPs at pH 12 after storage in ambient condition for 32 days. The emission position of the as-synthesised CdTe NPs in Fig. 4.12 A indicate no significant change in the emission maxima position for the as-synthesised CdTe NPs up to 4 days and showed slight decrease after 4 days. The

slight decrease in emission position of the as-synthesised CdTe NPs after 4 days as indicated in Fig 4.12 (B-D) was accompanied by an increase in the emission intensity at 0.25 h reaction time which decreases after 0.5 h and increase again at 2 hours and for the rest of the reaction. The decreased in the emission intensity may be attributed to the leaking of cadmium ions that act as surface defects due to instability of as-synthesised CdTe NPs in solution. The full width at half maxima showed no significant change as the material ages from 0 to 32 days indicating focussed size distribution.

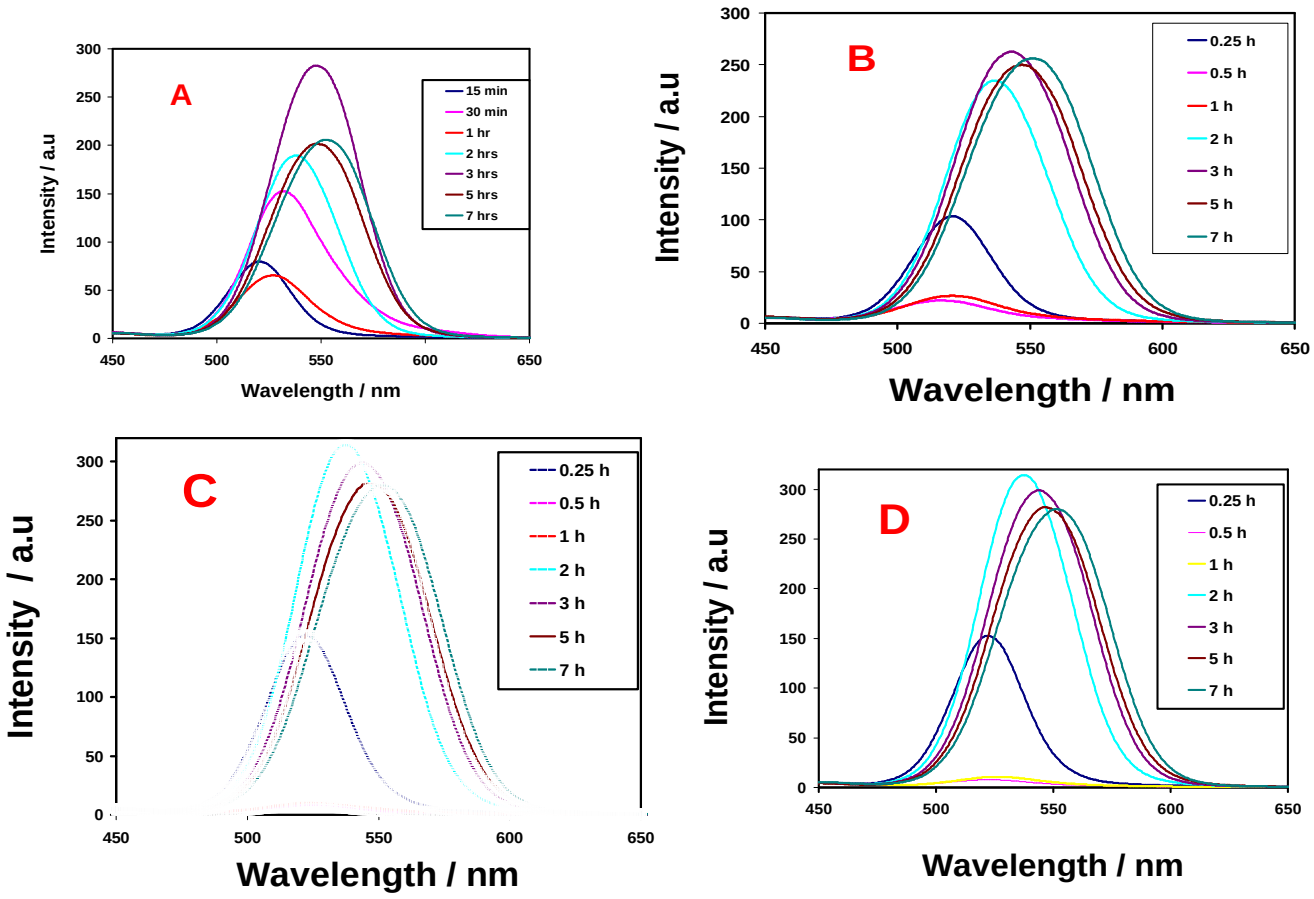

Figure 4.12: stability test of the as-synthesised CdTe NPs at pH 12 after 4 day (A), 8 days (B),16 days(C) and 32 days (D)

Table 8: The stability results of as-synthesised CdTe NPs at pH 12

Reaction time /h	PL intensity at			PL 4 days		PL 8 days		PL 16 days			PL 32 days		
	λmax / nm	**Intensity/ a.u**	**FWHM/ nm**	**λmax / nm**	**Intensity/ a.u**	**λmax / nm**	**Intensity / a.u**	**λmax / nm**	**Intensity/ a.u**	**FWHM/ nm**	**λmax / nm**	**Intensity/ a.u**	**FWHM/ nm**
0.25	524	38	32	522	79	521	103	522	152	35	522	152	35
0.5	530	152	45	533	152	518	22	524	8	41	524	8	41
1	536	164	40	530	65	521	26	528	11	39	528	10.7	39
2	541	256	45	539	189	537	234	538	313	46	538	312	46
3	547	282	48	549	282	544	262	544	299	50	544	297	50
5	550	291	49	549	201	547	252	547	281	53	547	281	53
7	552	293	61	554	204	551	258	552	279	54	553	278	54

The emission spectra's at Fig. 4.13 outline the stability test result for the as-synthesised CdTe/CdSe NPs at pH 12 after 4 day (A), 8 days (B),16 days(C) and 32 days (D). These results in Table (10) are summarised by (E) emission position, (F) FWHM (G) emission intensities for the aging period. The emission maxima position, full width at half maxima and emission intensity were used to measure the stability of the as-synthesised CdTe/CdSe NPs. The emission maximum peak positions remain the same with increase in emission intensity for all the NPs during the aging period. This indicates that the synthesized materials are highly stable against oxidation. This stability (Fig. 4.13 E) with increase in emission intensity has been attributed to the effective passivation of the surface defects by the CdSe shell. The emission intensity of the material increased with increase in storage time (Fig.

4.13 E) for all the aging period. This is a better result when compared with the core CdTe NPs in which the emission intensity decreases with aging time. The increase in intensity with ageing period has been attributed to the reduction in the non-radiative recombination thus confining the wave function of the electron -hole pair inside the nanocrystals. The full width at half maximum (FWHM) remain the same at different reaction times during the ageing period (Fig. 4.13 G) indicating that the size distribution remain constant during the aging period. The stability and the high fluorescence of the materials after aging under ambient condition validate their potential as a fluorescence probes when compared to organic dyes.

Table 9 : The stability results of as-synthesised CdTe/CdSe NPs at pH 12

Reaction time / h	PL at synthesis			4 days			8 days			18 days			32 days		
	ƛ max/ nm	Intensity/ a.u	FWHM / nm	ƛ max/ nm	Intensity/ a.u	FWHM/ nm	ƛ max/ nm	Intensity / a.u	FWHM / nm	ƛ max/ a.u	Intensity / nm	FWHM/ a.u	ƛ max/ nm	Intensit y/ a.u	FWHM/ nm
0.25	522	69	31	521	139	34	521	119	35	521	158	35	521	190	40
0.5	529	111	35	526	187	37	526	182	37	526	199	38	525	283	40
1	536	142	40	533	223	41	531	225	40	531	229	44	532	304	41
1.25	576	202	42	575	353	44	575	386	47	575	428	44	576	447	46
1.5	578	190	41	577	330	44	577	313	45	577	379	45	577	406	45
2	585	156	41	584	224	43	583	224	45	583	180	45	588	166	48
3	590	151	42	589	256	42	589	273	43	590	309	43	590	338	44
4	593	135	42	593	244	42	591	250	42	594	288	43	594	285	44
5	597	127	43	598	225	43	597	229	43	598	244	43	600	249	45
7	601	127	47	601	210	46	601	219	46	601	229	46	602	251	46

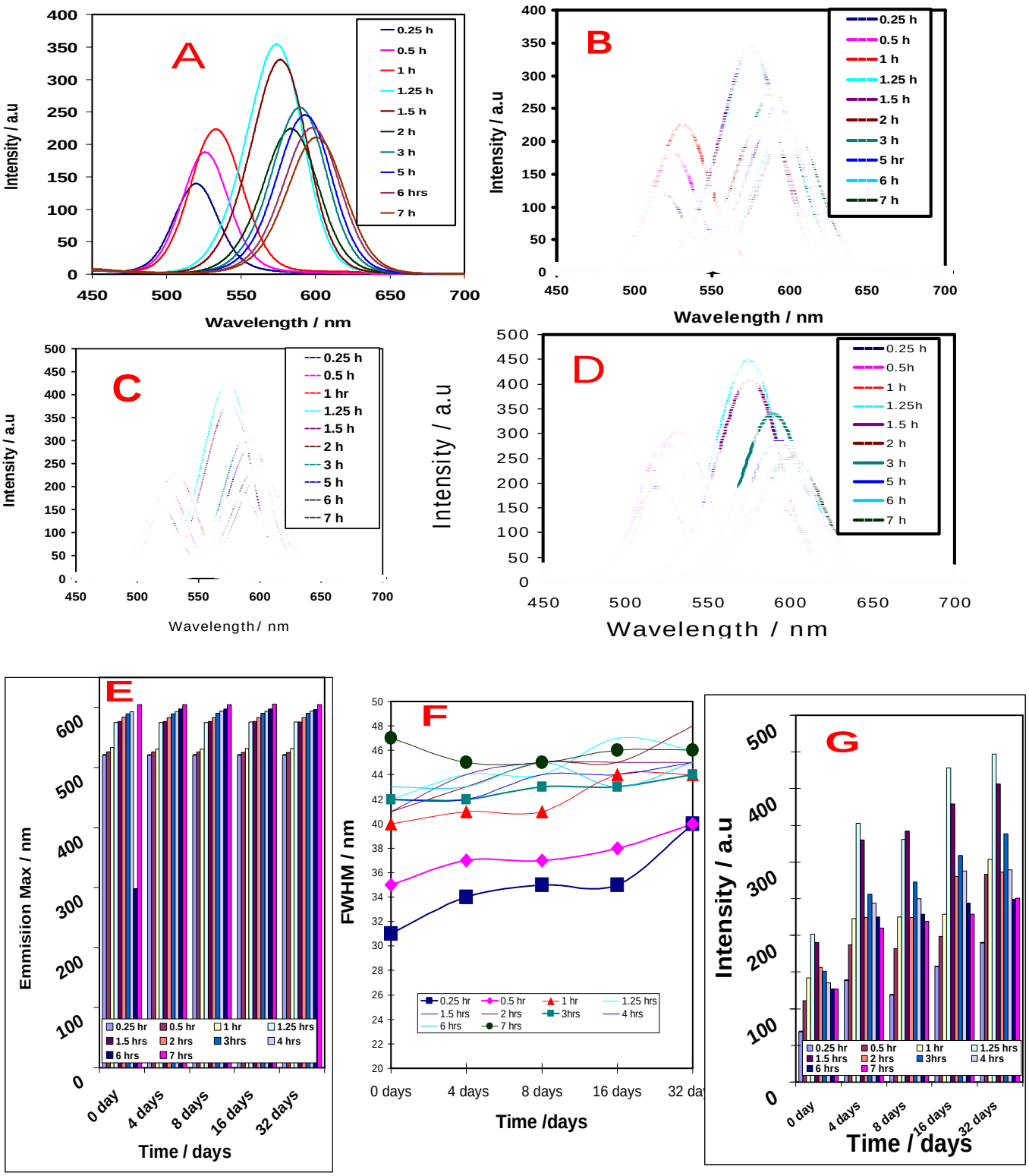

Figure 4.13: The photoluminescence spectra of as-synthesised CdTe/CdSe NPs at different reaction time after aging for (A) 4 days, (B) 8 days , (C) 16 days, (D) 32 days, and summarised optical properties; (E) Emission maxima, (F) FWHM and (G) Intensity.

4.1.5 Functionalisation of CdTe/CdSe and CdTe/CdSe/ZnSe NPs

Amino acids are material with different functional groups. These functional groups contribute to the surface binding effect as well as stabilisation of nanoparticles. Thus, surface properties of the NPs can also be manipulated by using amino acid coating. The amino acid coating results in NPs with high colloidal stability and strong optical properties (*Mao et al 2013*). Figure 4.14 indicates the effect of the amino acid functionalisation on the as-synthesised CdTe/CdSe and CdTe/CdSe/ZnSe NPs. The absorption maximum position for CdTe/CdSe NPs (Fig 4.14 A) is red shifted from 590 nm to 610 nm and remains the same for CdTe/CdSe/ZnSe NPs after functionalisation with arginine. Although there was no shift in the absorption maxima position for CdTe/CdSe/ZnSe NPs, the absorption spectra became broad after the functionalisation as seen with CdTe/CdSe NPs. The emission spectra (Fig 4.14 B) showed narrow emission spectrum for both MPA and arginine capped CdTe/CdSe and CdTe/CdSe/ZnSe NPs and exhibit band edge luminescence at the excitation wavelength of 400 nm. The emission spectra follow the same trend as absorption spectra for CdTe/CdSe NPs with a red shift of about 20 nm after functionalisation. This was accompanied with a significant increase in the emission intensity. The arginine capped CdTe/CdSe/ZnSe NPs showed significant increase in the emission intensity compared to MPA- capped CdTe/CdSe/ZnSe NPs. However, there were no changes in the emission position after functionalisation. The increase in the emission intensity indicates proper passivation of the NPs by arginine which is in line with (Mao *et al.,*; 2007) report that, the functionalisation with amino acids enhances the optical properties of NPs.

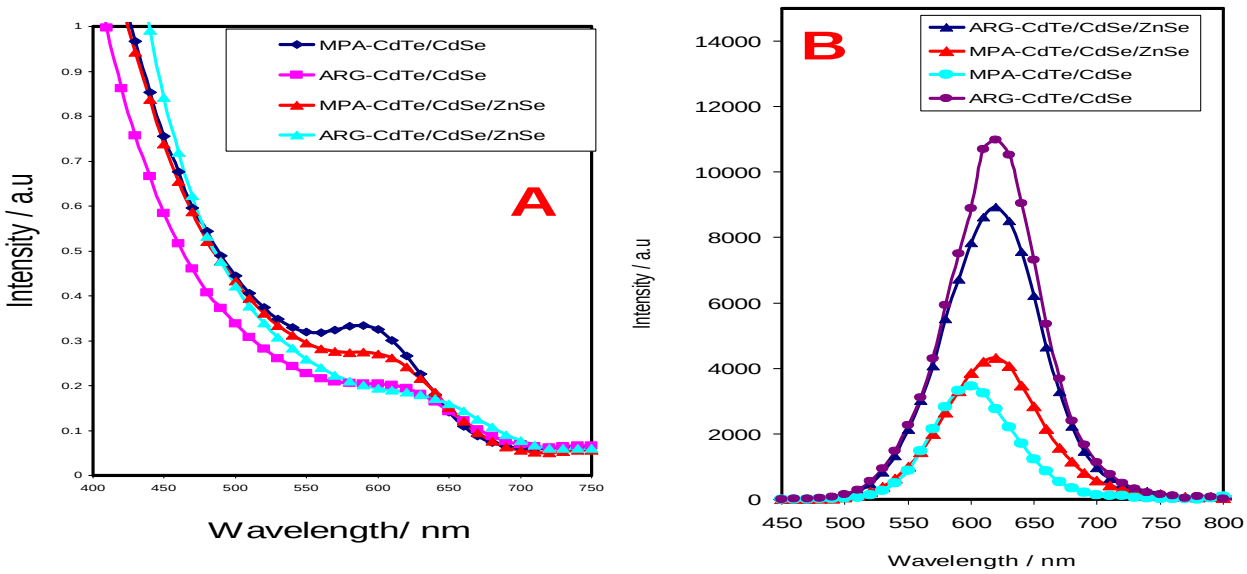

Figure 4.14: (A) absorption (B) emission spectra of MPA and arginine capped CdTe/CdSe and CdTe/CdSe/ZnSe NPs.

4.2. Electron Microscopy

The transmission electron microscope was used to determine the morphology, the particle size as well as the crystallinity of the material. A typical TEM image of as-synthesised CdTe NPs is shown in Fig 4.15 A_1. The micrograms show the presence of small, monodispersed, spherical particles with average particle size of 3.5 ± 0.60 nm. The TEM average particle size is in agreement with the results obtained from optical analysis. The particle size distribution (Fig 4.15A_2) shows that the particles are in the range 1 nm to 5.8 nm. The HRTEM image inserted in Fig 4.15 A_1 shows lattice fringes indicating the crystallinity of the as-synthesised CdTe NPs and this is confirmed in Fig 4.15 A_3 by the circular rings of the selected area electron diffraction.

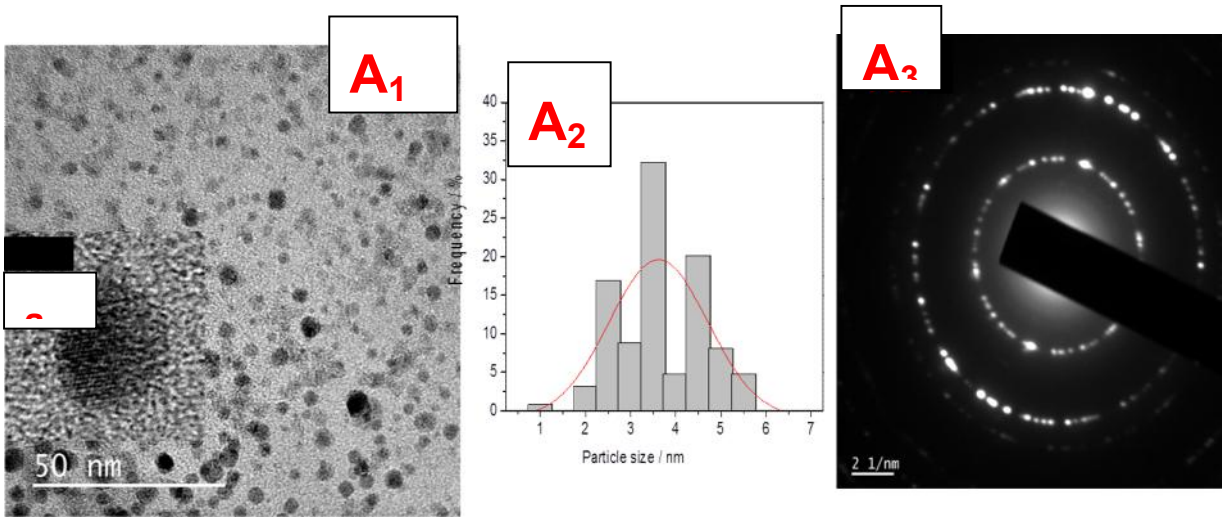

Figure 4.15 A: TEM micrograms (A_1), with particle size distribution (A_2) and SAED (A_3) of the as-synthesised CdTe NPs.

TEM, HRTEM and SAED images of the as-prepared CdTe/CdSe NPs are shown in Fig. 4.15 B_1, B_2 and B_3 respectively. The low magnification image of the as-synthesised CdTe/CdSe (Fig. 4.15 B_1) show good monodispersed spherical particles. The existence of a well-resolved lattice fringe on the HRTEM image (Fig. 4.15 B_2) further confirmed the crystalline structure of the as-synthesised core shell material. Figure 4.15 B_3 illustrates a typical SAED pattern of CdTe/CdSe core/shell NPs which indicates that the as-synthesised materials are of hexagonal (wurtzite) phase confirming the CdSe layer on the CdTe core.

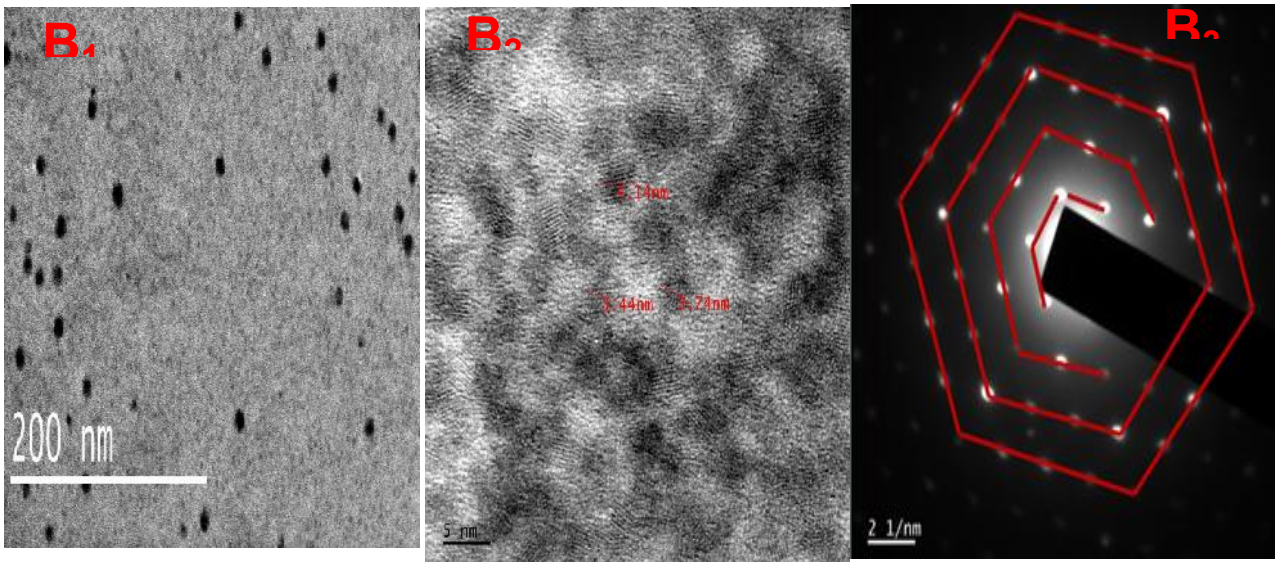

Figure 4.15B: TEM micrograms (B_1), HRTEM (B_2) and SAED (B_3) of the as-synthesised CdTe/CdSe NPs.

The typical representative microscoping images of as-synthesised MPA capped-CdTe/CdSe/ZnSe nanoparticles are shown in figure 4.15 C. The particle size distribution curve shows that the particles are in the range of 2.5 to 6.5 nm with average particle diameter size of 3.7 nm. The TEM image of (Fig 4.15C_2) indicates the presence of NPs. The HRTEM and (Insert) show that the NPs are well order single crystal with clear lattice fringe confirming the crystallinity of the NPs with no observed interfacial layer. The absence of the interfacial layer may be due to the lattice match between the core and the shell, thus the shell grows along the lattice. (Zang *et al.,* 2009; Zare *et al.,* 2015).

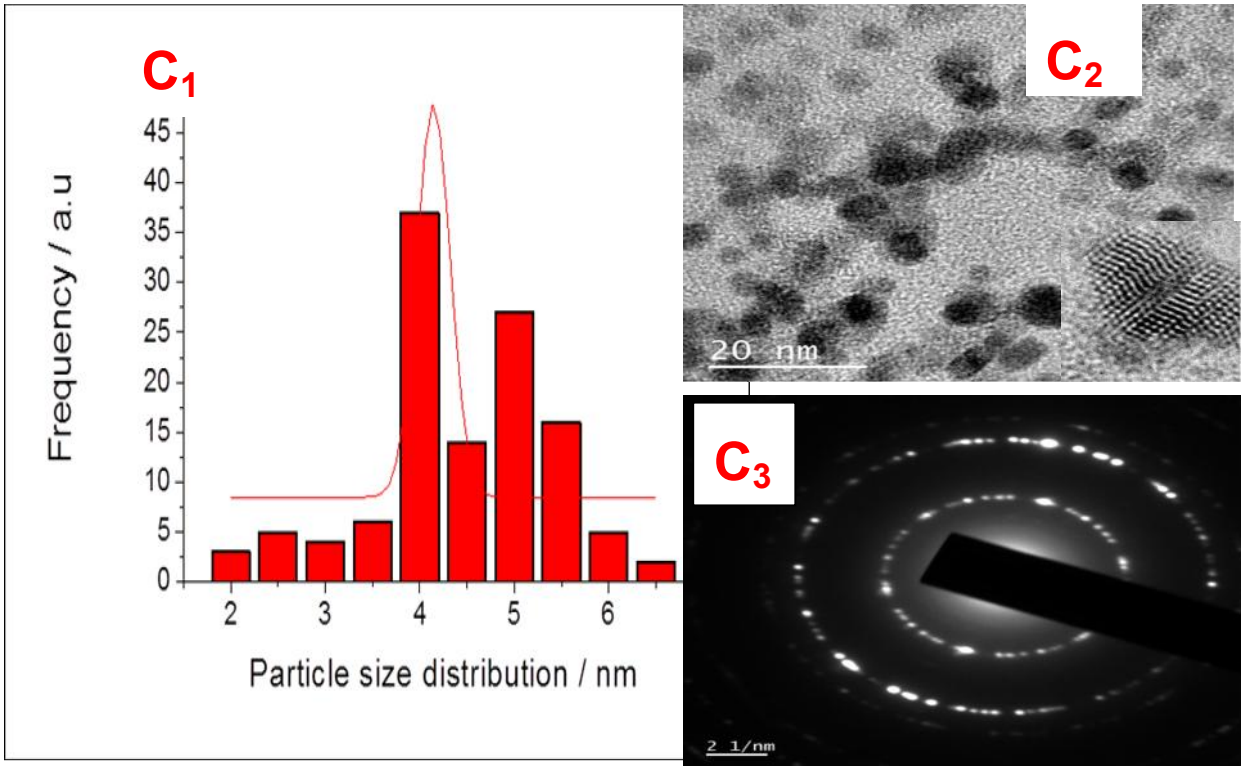

Figure 4.15 C: TEM results of as-synthesised CdTe/CdSe/ZnSe, (C_1) with particle size distribution (C_2) TEM micrograms with HRTEM insert and (C_3) SAED.

In this study, EDS was used to identify the elemental composition, complexation by capping group as well as formation of the core shell (figure 4.16A_1-A_3) on the surface of CdTe NPs. The EDS spectrum for the CdTe/ CdSe NPs (Fig. 4.17A_1) shows the presence of Cd, Te and Se peaks indicating the formation of CdTe/CdSe NPs while the presence of sulphur peak confirmed the capping by MPA. The EDS spectrum for CdTe/CdSe/ZnSe NPs shows the presence of zinc peak in addition to all the other constituent peaks identified with CdTe/CdSe NPs. The presence of zinc peak and increase in the intensity of the selenium peak compared to the CdTe/CdSe EDS spectrum indicate the formation of CdTe/CdSe/ZnSe NPs. The EDS spectrum for the arginine functionalized CdTe/CdSe NPs (Fig.4.16 A_3) shows the presence of nitrogen peak in addition to other constituent peaks present in CdTe/CdSe NPs.

Furthermore, the elemental table (Fig. 4.16 A_3 inset) shows that the nitrogen peak % in the as-synthesized functionalized CdTe/CdSe NPs is greater than the sulphur peak %. This further confirms the functionalisation of CdTe/CdSe NPs with arginine. The highest copper peak % in all the EDS spectra is due to the copper grid used for TEM analysis.

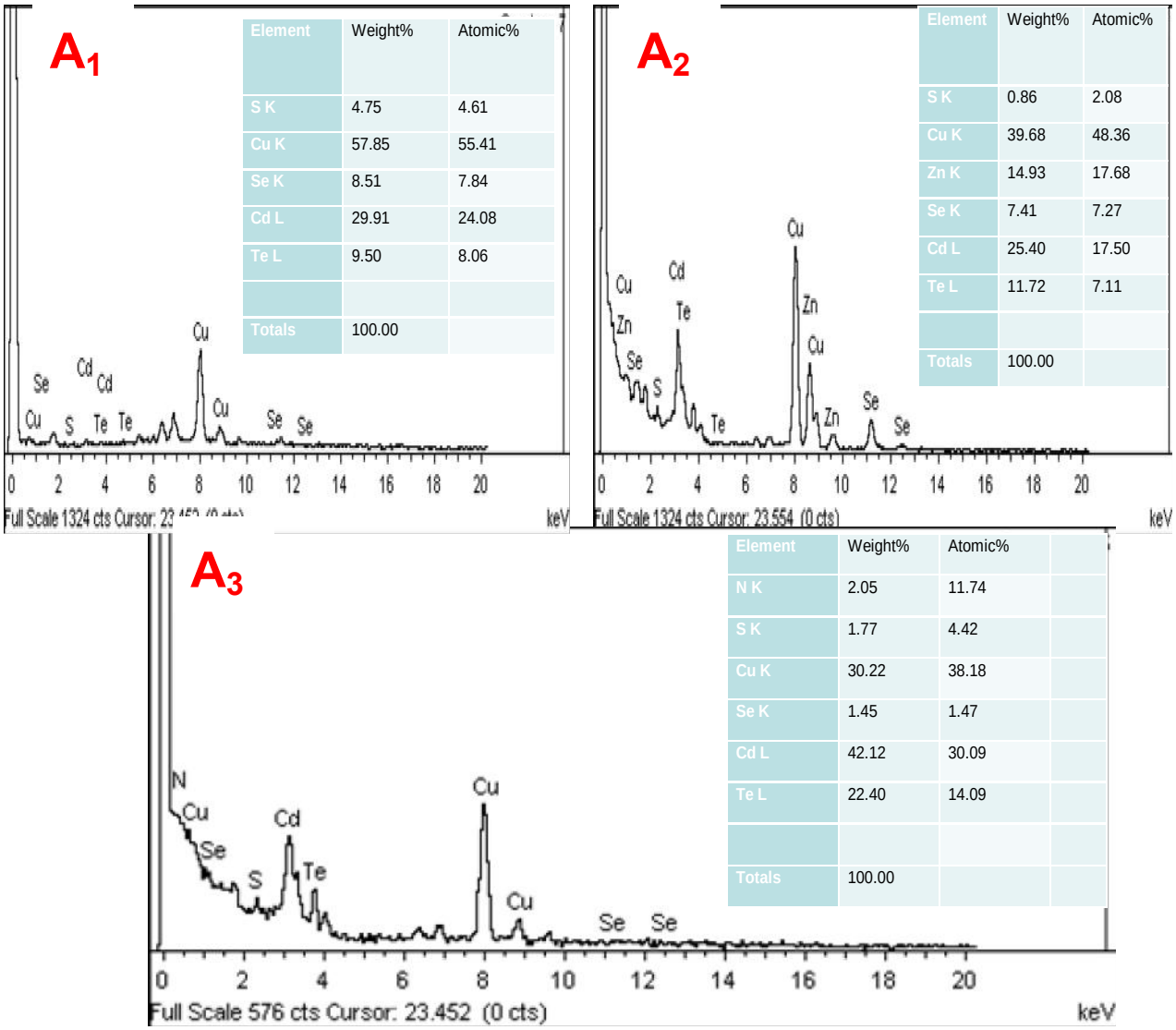

Figure 4.16: EDS of the spectra of MPA capped CdTe/CdSe NPs (A_1); MPA capped CdTe/CdSe/ZnSe (A_2) NPs and Arginine capped CdTe/CdSe NPs (A_3).

4.3 In Vitro study of the as-synthesised NPs

4.3.1 Toxicity study

As quantum dots are said to be ideal candidates for imaging of cancer cells and drug delivery the challenge of their toxicity against human cells and organisms has become a serious concern. The presence of cadmium in most cadmium based NPs led to a belief that they are toxic towards cells. Several studies have shown that the cytotoxic of the quantum dots depends both on Cd^{2+} ions and the surface chemistry of the QDs (Su *et al.,* 2009; Chen *et al.,* 2012; Bradburne *et al.,* 2013). Though the QDs synthesised in this study were produced via a completely green synthetic routes, the study of their cytotoxicity is imperative. This is necessary in order to ascertain if the green synthetic method could lead to the reduction of their cytotoxicity towards living organisms. This will also serve as litmus test for determining the suitability of the as-synthesised QDs for *in vivo* imaging. Determination of the cytotoxicity via an *in vitro* method using MTT assay has been known to be an easy, inexpensive, reproducible ideal route for nanotoxicology research (Hosono *et al.,* 2007; Riss et al., 2013). The MTT assay for cell viability is measured as a function of metabolic activity. The reduction of MTT solution by cells results in formazan a blue solution that is measured by absorbance plate reader to determine the quantity of the live cell in the reaction vessel (the greater the absorbance, the more live cells in the solution). In this study LM 8 and KM-Luc/GFP cell lines were used for the cytotoxicity study. The LM-8 cells used in the study are murine osteosarcoma cell line derived from Dunn osteosarcoma. They have high metastic potential to lungs and known to be tumorigenic when injected internally into syngeneic hosts, consistently forming local tumor masses as well as distant lung

metastases (Hosono *et al.,* 2007; Asia *et al.,* 1998; Sugiyasu *et al.,* 2011). KM-Luc/GFP cells are stable cells expressing a fusion of luciferase (Luc) and green fluorescent protein genes (EGFP). KM-Luc/GFP cell line was prepared by transfection of malignant fibrous histiocytoma-like (MRL/N-1) cells with pEGFPLuc using lipofectin transfection reagent. MRL/N-1 cells which act as a source of origin for KM-Luc/GFP cell line were established from the spleens of MRL/MpTn-gld/gld mice (Kato *et al.,* 2015; Li *et al.,* 2013, Furukawa *et al.,* 2009 and Hasegawa *et al.,* 2003). These important cells are ideally suited for use in the development of imaging modalities to improve the assessment of cancer metastasis.

The pipetting study for accurate MTT assay was done using 200 µL of KM-Luc/GFP cell line with a concentration of 1×10^{4} cell/mL. The absorbance was measured in order to get the value of R^2 closer to 1, the closer the R^2 value to 1 the more accurate the technique. Figure 4.17 A-D show different R^2 values for MTT assay pipetting techniques. The R^2 values are within a range of 0.9961 to 0.9993, indicating a good pipetting technique for MTT assay analysis.

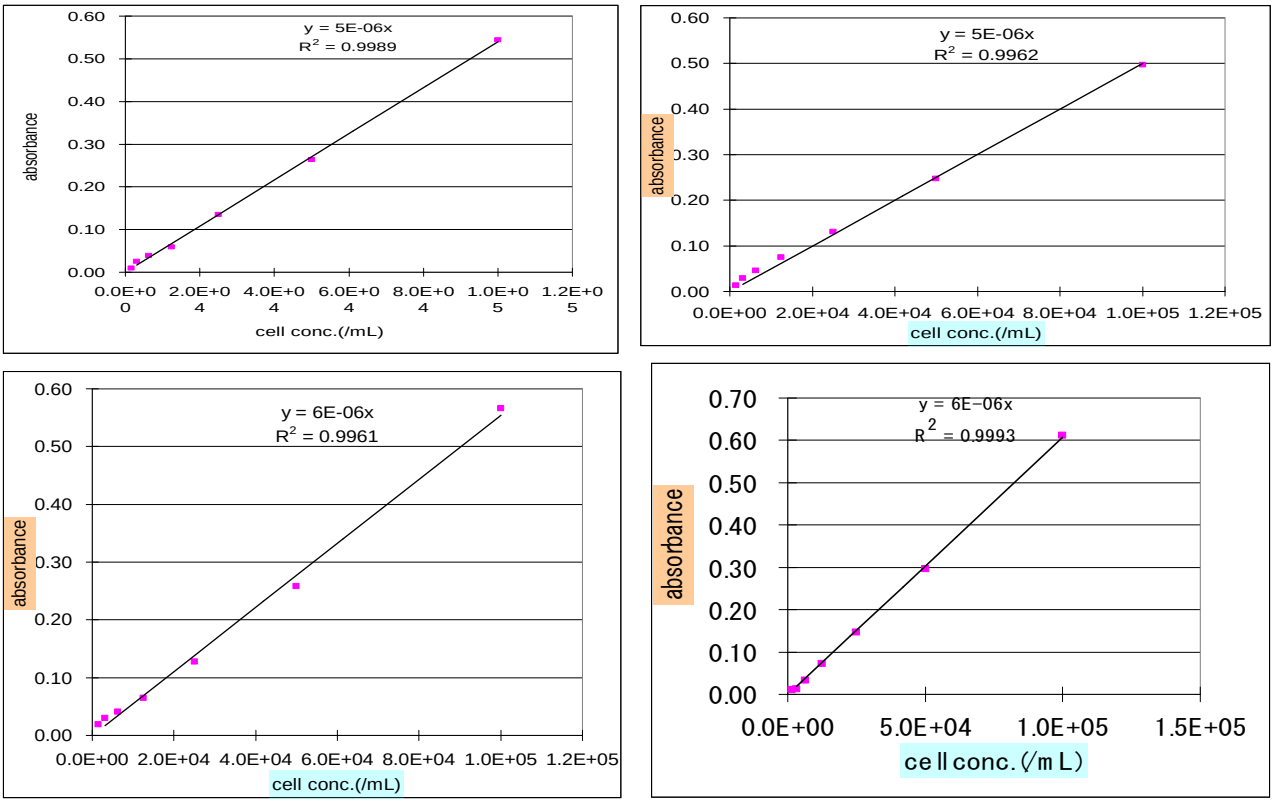

Figure 4.17: the MTT assay results of KM-Luc/GFP cell line at different concentrations (cell / mL) using the medium as dilution solvent.

Figure 4.18 is the cell viability study of the different concentrations of CdTe NPs synthesised at pH 12 at 7 h reaction time on (A) LM 8 and (B) KM-Luc/GFP cell lines. The concentration of the cells was kept at 1.0 x 10^5 cell/mL using phosphate buffer solution as a control. The cell viability study for the LM 8 cell line (Fig. 4.18A) varies from 56 % at the lowest concentration of 0.1 µM to 23 % at the highest concentration of 60 µM. Fig 4.18 B shows the cell viability of CdTe NPs on KM-Luc cell line. The cell viability ranges from 94 % at concentration of 0.1 µM to 20 % at the highest concentration of 60 µM. The two results indicated that, the greater the concentration of CdTe NPs the more toxic the material become on the cell line. The drastic decrease in cell viability with increase in NPs concentration especially for KM-Luc/GFP cell line might be attributed to the rate at which the NPs accumulate in the cell. At higher concentration, more NPs will accumulate in the cell; this will impair the

cell growth and thus increase the mortality rate. The as-synthesised MPA-capped CdTe NPs maintain cell viability greater than 80 % at the concentration of 10 µM which is below the 30µg daily intake that act as the reference point for cadmium consumption in human body (Satarug *et al.,* 2000).

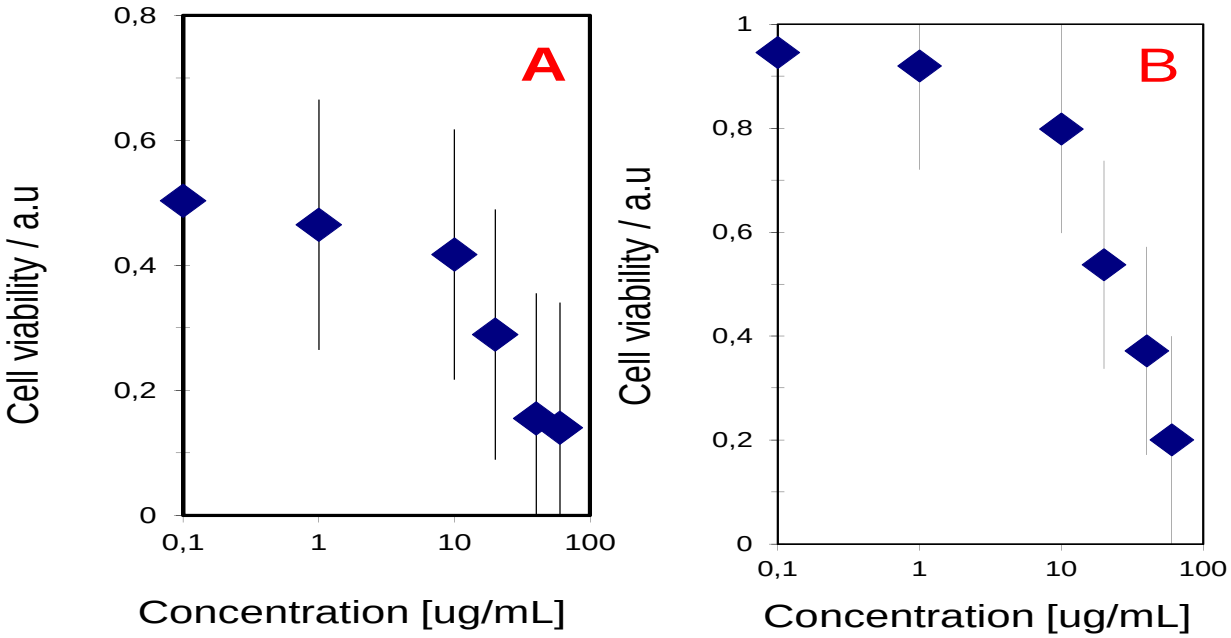

Figure 4.18: Cell viability assay of CdTe NPs synthesised at pH 12 (7 h) at different concentrations on (A) LM8 and (B) KM-Luc/GFP cell line.

The stabilisation of the CdTe NPs by CdSe shell NPs has been previously reported to play a significant role in reducing the toxicity of the material in living cells. The more stable the material is in aqueous solution, the less toxic it becomes. Fig 4.19 shows the cytotoxicity result for the CdTe/CdSe NPs at different concentrations using LM 8 (A) and KM-Luc/GFP (B) cell lines. LM 8 cell line (Fig 4.19 A) indicates a great vulnerability when treated with CdTe/CdSe NPs. This leading to increase in the mortality rate by 30 % from lowest concentration (0.1 µM : 58 %) to the highest (60 µM: 20 %). The results show a tremendous increase in the toxicity of the

CdTe/CdSe NPs with respect to increase in concentrations. The cell viability of CdTe/CdSe on KM-Luc/GFP (Fig 4.19 B) cell line lies within a range of 91 % to 32 % as the concentration increased from 0.1 to 60 µM indicating a decrease of 59 %. The drastic decrease of 50 % from 10 to 60 µM shows the effect of concentration on the toxicity level of CdTe/CdSe NPs against the KM-Luc/GFP cell line.

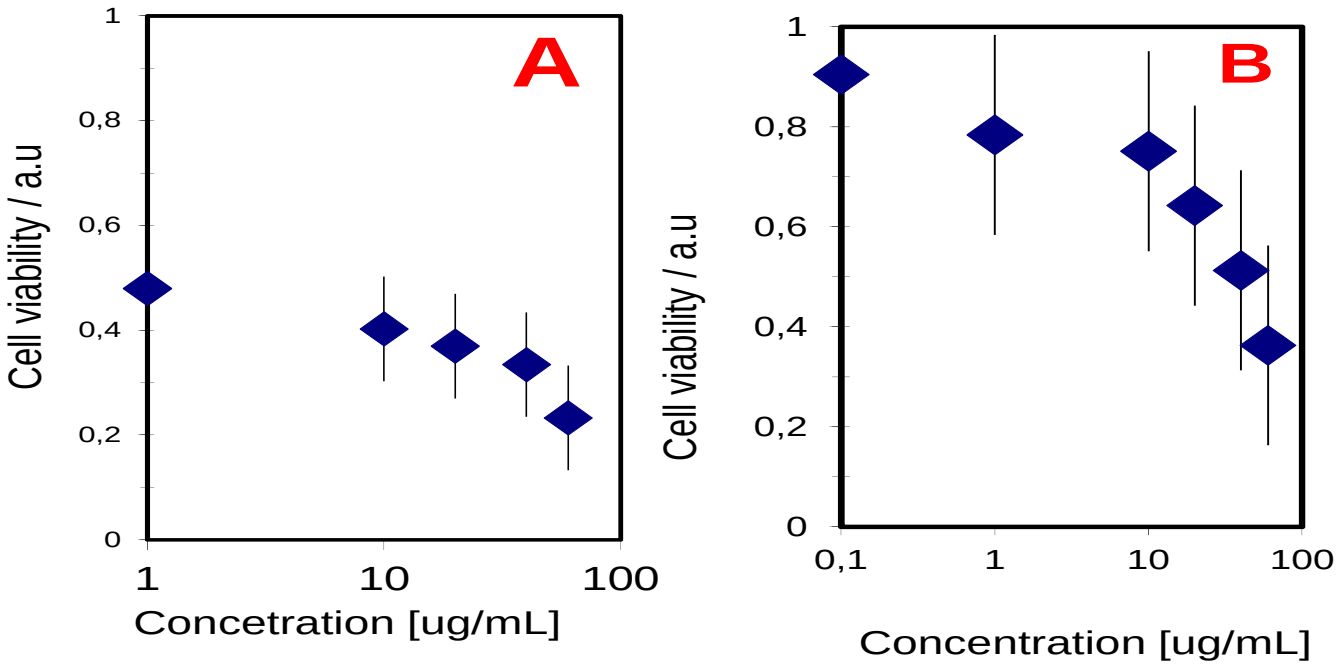

Figure 4.19: Cell viability assay of CdTe/CdSe NPs synthesised at pH 12 (7 h) on (A) LM 8 and (B) KM-Luc/GFP cell line at different concentrations (µg/mL).

It has been reported that certain compounds such as zinc and/or ascorbic acid have the abilities to protect organisms against Cd embryo toxicity (Renata *et al.,* 2015; Dzugan *et al.,*2012; Thompson and Bannigan 2001). In this section, the cytotoxicity of the CdTe/CdSe/ZnSe core multi-shell synthesised by growing a ZnSe shell on the as-synthesised CdTe/CdSe NPs was investigated using both LM 8 and KM-Luc/GFP cell lines. Fig. 4.20 shows the cell viability study for the CdTe/CdSe/ZnSe core multi-

shell NPs at different concentrations. The LM 8 cell line (Fig. 4.20 A) shows that the toxicity of the CdTe/CdSe/ZnSe NPs increase with increase in concentration reaching a maximum of 91 % at lower concentration (0.1 µM) and a minimum of 37 % at higher concentration (60 µM). This gradual decrease in the mortality rate with respect to increase in concentration may be attributed to the proper passivation of the cadmium by the Zinc shell. Fig.4.20 B shows that the toxicity of the CdTe/CdSe/ZnSe NPs on KM-Luc/GFP cell line increase from a maximum of 94 % at lower concentration (0.1 µM) to a minimum of 38 % at higher concentration (60 µM). The cytotoxicity of CdTe/CdSe/ZnSe at KM-Luc/GFP cell line shows a gradual decrease at lower concentration (0.1-10 µM) and fast decrease in the mortality rate at higher concentration (20 to 60 µM).

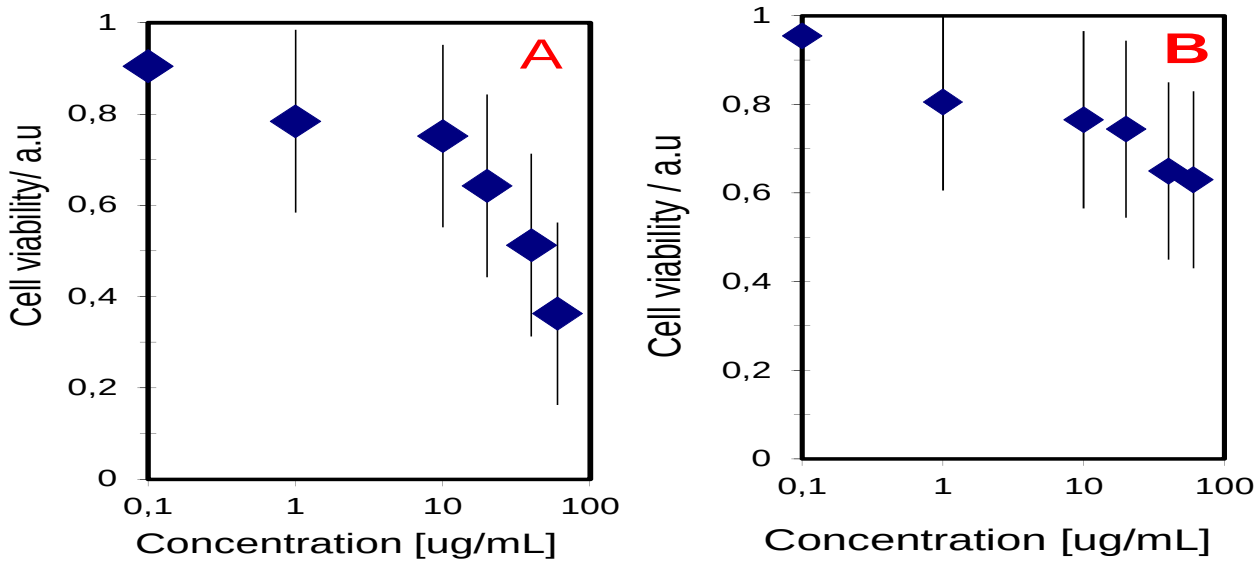

Figure 4.20: Cell viability assay CdTe/CdSe/ZnSe NPs synthesised at pH 12 (7 h) on (A) LM8 and (B) KM-Luc/GFP cells line at different concentrations (µg/mL).

Figure 4.21 shows the effect of the shell growth on the toxicity of core CdTe NPs on (A) LM 8 and (B) KM-Luc/GFP cell lines at different NPs concentrations. The results

show that KM-Luc/GFP cell display less mortality rate than LM 8 cell line for all the as-synthesised NPs at each different concentrations. Fig 4.21 clearly shows that the cytotoxicity of NPs can be modulated through elaborate surface coatings. The cell viability for the LM 8 cell line (Fig.4.21 A) is less than 60 % for all the as-synthesised CdTe, CdTe/CdSe and CdTe/CdSe/ZnSe NPs at all concentrations. The cell viability for the KM-Luc cell line (Fig. 4.21 B) was 95 % at lower concentration of 0.1 µM. This decreases to 70% at 10 µM (tolerable conc. for human being) and finally to 46 % at 60 µM. The KM-Luc/GFP cell line show resistance against quantum dots than LM 8 cell line. For all the as-synthesised NPs, the mortality rates increase with increase in concentration. The order of increase cell viability at different NPs concentrations for the two cell lines is CdTe/CdSe/ZnSe > CdTe/CdSe > CdTe NPs. This indicates that, addition of the shell does not only improve the quantum yield and stability of the core CdTe NPs, it also improves cell viability. The highest cell viability obtained after the addition of the second shell (ZnSe) suggest that, coating the surface with an additional higher band gap material further reduced the surface defects and protect the core CdTe from interacting with the surrounding aqueous medium. This prevents the core CdTe from degradation and aggregation. Several reports have indicated the interaction of the core CdTe NPs with surrounding aqueous medium as the major sources of their degradation, aggregation, poor photo stability and reduced quantum yield (Law *et al.,* 2009; *Li et al.,* 2011; He *et al.,*2008; Chen *et al.,* 2012). These results show that the CdTe/CdSe/ZnSe core–multi–shell structured NPs synthesized directly in aqueous phase are highly promising biological fluorescent probes for cellular imaging as they show the lowest cytotoxicity against both the LM 8 and KM-Luc/GFP cell lines

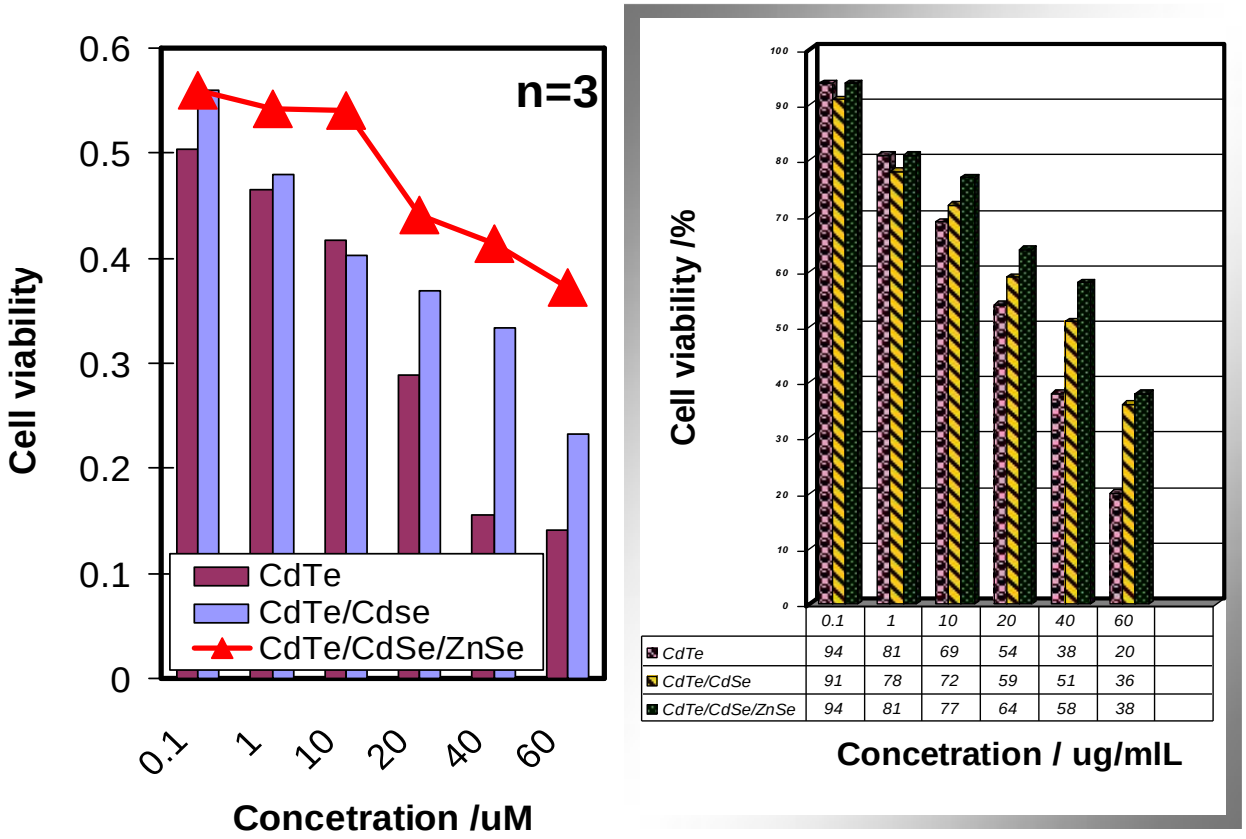

Figure 4.21: The combined cell viability assay for the as-synthesised CdTe, CdTe/CdSe and CdTe/CdSe/ZnSe NPs on (A) Lm 8 and (B) KM-Luc/GFP cells line at different concentrations.

4.3.2 Effect of Functionalization

The amino acid functionalisation renders NPs very soluble and stable in biological fluids with remarkable reduction in cellular toxicity. The cell viability increased from 0.91 for MPA capped CdTe/CdSe NPs (Fig 4.22 A) to 0.95 for arginine capped CdTe/CdSe NPs (Fig 4.22 B) indicating decrease in cell mortality rate by 4 %. The as-synthesised arginine CdTe/CdSe/ZnSe (Fig 4.22 C) NPs showed decreased mortality rate than MPA capped CdTe/CdSe/ZnSe NPs (Fig 4.22 D). The cell viability rate for MPA capped CdTe/CdSe/ZnSe NPs is 94 % at lowest concentration of 0.1 ug/ml and decrease to 32 % at the highest concentration of 60 µg/ml while for the

arginine capped-CdTe/CdSe/ZnSe NPs the cell viability decrease from 94 % (0.1 ug/ml) to 64 % (60 ug/ml). This results show that even at the highest concentration the mortality rate is less than 50 % after functionalisation.

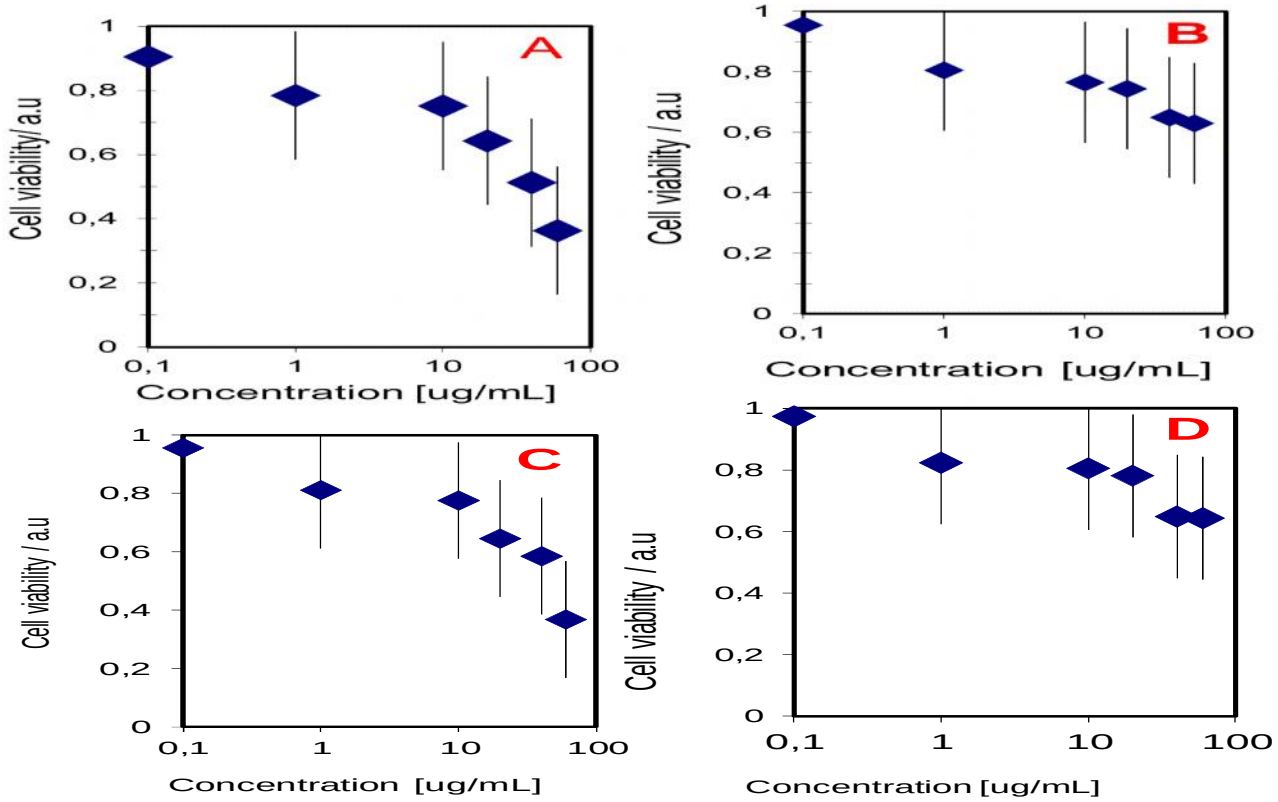

Figure 4.22: The cell viability assay of (A) MPA capped-CdTe/CdSe NPs, (B) Arginine capped-CdTe/CdSe NPs (C) MPA capped-CdTe/CdSe/ZnSe NPs and (D) Arginine capped-CdTe/CdSe/ZnSe NPs at 7 h reaction time on KM-Luc/GFP cell line at different concentrations.

Figure 4.23 indicate the overall chat of the as-synthesised CdTe/CdSe NPs and CdTe/CdSe/ZnSe NPs before and after functionalisation with arginine. The functionalisation decreased the mortality rate of the cell when exposed to CdTe/CdSe NPs and CdTe/CdSe/ZnSe NPs. At lower concentration of 0.1 µg/ml the effect of functionalisation on cell viability is not insignificant. However as the NPs concentration increase, the effect of functionalisation becomes feasible. That is the

mortality rate decrease by almost 50% for both CdTe/CdSe NPs and CdTe/CdSe/ZnSe NPs functionalised with arginine than when capped with MPA. Thus functionalisation of NPs enhances both optical and biological properties of the material.

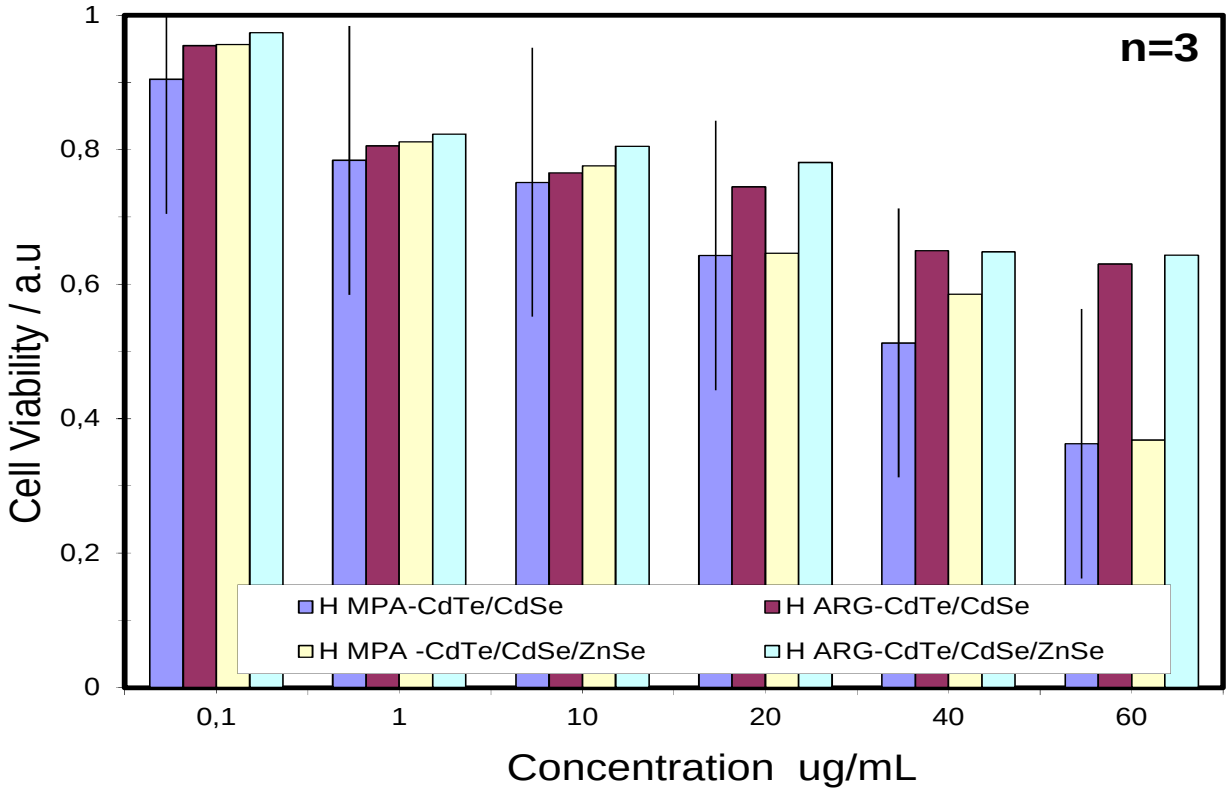

Figure 4.23: The effect of functionalisation on cell viability study of as-synthesised MPA capped-CdTe/CdSe and CdTe/CdSe/ZnSe QDs.

4.3.3. Cell imaging.

Studies have shown that toxicity of NPs does not depend only on the concentration of the free cadmium ions but also on whether the particles are ingested by the cells or not. Therefore the evaluation of the cellular uptake and intracellular localisation of the NPs is crucial for their biological impact. The images of KM-Luc/GFP cell line treated with control, Lipofectamine (cationic liposome to render NPs permeable to

the cells) and NPs-Lipofectamine complex are shown in Fig. 4.24. The images of the cells treated with lipofectamine (Fig.4.24 A) showed no visible fluorescence under the fluorescence light of the confocal microscope. The confocal microscope image shows that NPs complex has entered and accumulated inside the cells as indicated by red fluorescence in Fig. 4.24 (B and C) images under the fluorescence light after incubation for 18 hours. This suggests the efficient transportation across the plasma membrane. Thus, modified NPs can provide bright and stable fluorescence signal for intracellular imaging.

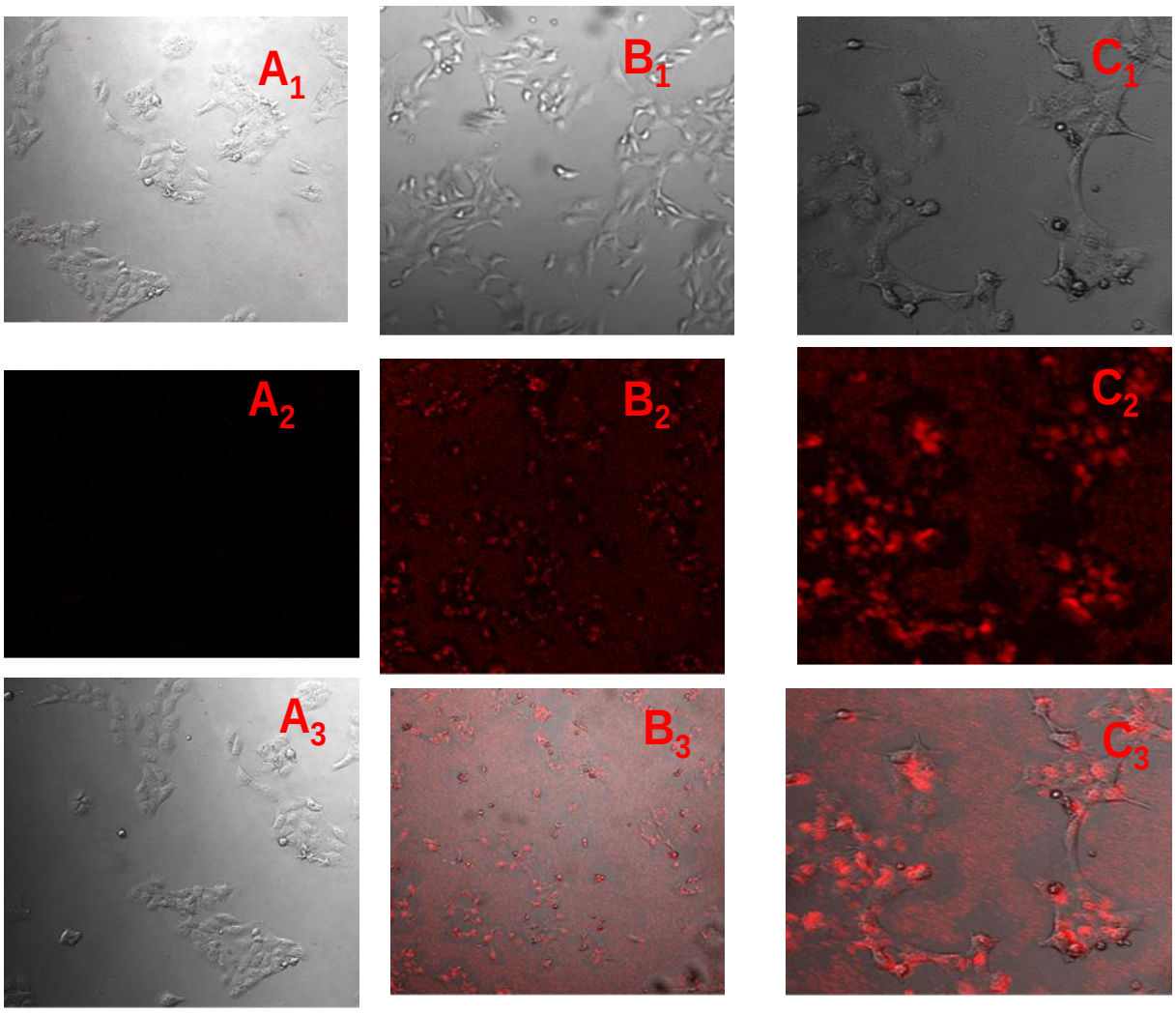

Figure 4.24: The confocal images of KM-Luc/GFP cell line treated with (A) Lipofectamine as the control, (B) Lipofectamine-CdTe/CdSe complex and (C) Lipofectamine-CdTe/CdSe complex at higher concentration. Subscripts 1, 2 and 3 represent image under normal light, fluorescence light and over lay of 1 and 2 respectively

CHAPTER 5

Conclusion and Recommendations

5.1 **Conclusion**

MPA capped CdTe nanoparticles have been successfully synthesised in aqueous phase by varying the pH of the solution while keeping all other parameters constant. The CdTe Nanoparticles synthesised through this route are blue shifted in respect to CdTe bulk indicating quantum confinement. The optical properties revealed a red shift in the band gap of CdTe NPs as the reaction time and pH increased, indicating increase in particle size. The particles emit from green to orange region with narrow emission width indicating focused size distribution. The formation of the CdTe/CdSe core shell NPs was indicated by a significant increase in the emission position accompanied by enhancement in the fluorescence intensity after the addition of the selenium solution. The red shifting increased as the pH increase with pH 12 having the highest emission position. The emission intensity reveal two stages of growth: (i) increase from 0.25 h to 1.5 h and (ii) decrease from 2 h until the end of the reaction with 1.5 h having the highest emission intensity. The addition of the multi shell was also accompanied by significant increase in the emission intensity and emission position towards the red region. The stability of the NPs in biological fluid increase with the addition of the shell, thus addition of the shell protects the nanoparticles from oxidation and therefore retains their properties for a longer time. The functionalizations of the core-shell with amino acid shift the emission position further towards the red region and enhance the emission intensity. The functionalizations of the core multi shell only enhance the fluorescence intensity with no observable change in the emission position. The particle size as calculated using Yu *et al* ., method varies from 2.0 to 3.0 nm for CdTe NPs core as the reaction time increase from 0.25 h to 7 h. This increased from 2.1 to 4.1 nm for CdTe/CdSe core shell NPs

and finally from 2.3 to 4.8 nm for CdTe/CdSe/ZnSe the core multi shell at highest pH (pH 12). The formation of the shells and multi shell as well as functionalisation was confirmed by EDS. The presence of Se and Zn confirmed for the formation of the shell (CdTe/CdSe) and multi shell (CdTe/CdSe/ZnSe) respectively while the presence of S and N confirms the presence of MPA and arginine respectively. The TEM micrographs showed that nanoparticles that are small, spherical, monodispersed and highly crystalline are produced in aqueous phase. The HRTEM confirms that the particles are highly crystalline in the nanosized regime. The FTT confirmed the single crystalline nature for all nanoparticles with no observable lattice mismatch between the core and the shell while the SAED clearly showed that the as-synthesised CdTe/CdSe/ZnSe NPs are of hexagonal phase. Prolonging the reaction time give better interaction with the cell membrane thus increase the cell viability up to 90 %. Functionalization with amino acid changes the ionic strength of the nanoparticles with good response against cell membrane and increased cell viability. The insight gained from this study revealed that the high fluorescence water-soluble synthesised CdTe, CdTe/CdSe and CdTe/CdSe/ZnSe nanoparticles are potential probes for monitoring the long term interaction of multiple-labelled biological molecules as they show bright fluorescence field inside the cells.

5.2 Recommendations

The purpose of this work is to synthesize CdTe NPs via a completely green method in the absence of an inert atmosphere and investigates the effects of reaction time, pH and shell formation on the optical properties of the as-synthesised nanomaterial and their biological assay. Though these have been achieved however, more characterisation still needs to be carried out for better understanding and for application purposes. Thus we recommend that

- XPS analysis should be carried out to understand the surface reaction that took place in the as-synthesised nanomaterials
- XRD analysis of the material should be done to further investigate the crystallinity and the crystalline structure of the as-synthesised nanoparticles.
- The method should also be employed for the synthesis of other semiconductor nanoparticles.
- Based on the cell viability of the nanoparticles more work has to be done in order to understand the mechanism that leads to the toxicity of the as-synthesised nanoparticles.
- Flow cytometry after endocytosis should be carried out to understand the localisation of the NPs inside the cell.
- Finally in *vivo* analysis has to be carried out as the internal ingestion work differently from the *in vitro* analysis.

REFERENCES

Aldana J., Wang Y.A. and Peng X. (2001): Photochemical instability of CdSe nanocrystals coated by hydrophilic thiols. *J Am Chem Soc* 123: 8844–8850.

Algar, W. R. & Krull, U. J. 2007 Luminescence and stability of aqueous thioalkyl acid capped CdSe/ZnS quantum dots correlated to ligand ionization. *Chem. Phys. Chem*. 8, 561–568.

Alivisatos A.P. (1996): Semiconductor clusters, nanocrystals, and quantum dots. *Science* 271:933–937.

Allhoff F., Lin P., & Moore D. (2010): What is nanotechnology and why does it matter? From science to ethics. *Hoboken, NJ: Wiley-Blackwell Publishing*.

Ananthakumar S., Ramkumar J. and Babu S.M. (20014): Effect of ligand exchange in optical and morphological properties of CdTe nanoparticles/P3HT blend. *Sol. Energy* 16, 151–158.

Asai T, Ueda T, Itoh K, et al., (1998): Establishment and characterization of a murine osteosarcoma cell line (LM8) with high metastatic potential to the lung. *Int. J. Cancer* 76: 418-422.

Ayele D.W., Chen H.M., Su W.N., Pan C.J, Chen L.Y., Chou H., Cheng J., Hwang B., and Lee A.(2011). Controlled synthesis of CdSe quantum dots by a microwave-enhanced process: a green approach for mass production. *Chem. Eur. J.* 17, 5737 – 5744.

Bagalkot V., Zhang L., Levy-Nissenbaum E., Jon S., Kantoff P. W., Langer R. & Farokhzad O. C. (2007): Quantum dot-aptamer conjugates for synchronous cancer imaging, therapy, and sensing of drug delivery based on bi-fluorescence resonance energy transfer. *Nanoletters* 7, 3065–3070.

Bailey, R.E. and Nie, S.M. (2003) Alloyed semiconductor quantum dots: tuning the optical properties without changing the particle size. *J. Am. Chem. Soc*. 125, 7100–7106.

Ballou B., Lagerholm B.C., Ernst L.A. Bruchez M.P. and Waggoner A.S. (2004): Non-invasive imaging of quantum dots in mice. *Bioconjugates Chem*. 15, 79–86.

Bangal M., Ashtaputre S.,Marathe S., Ethiraj A., Hebalkar N., Gosavi S.W. Urban J. and Kulkarni S. K. (2005): Semiconductor Nanoparticles. *Hyperfine interactions*; 160, (1), 81-94.

Bao H., Hao N., Yang Y. and Zhao D. (2010): Biosynthesis of Biocompatible Cadmium Telluride Quantum Dots Using Yeast Cells. Nano Res 3: 481–489

Bar-Ilan O., Albrecht R.M., Fako V.E. and Furgeson D.Y. (2009): Toxicity assessments of multisized gold and silver nanoparticles in zebrafish embryos. *Small* 5: 1897–1910.

Bawendi. M.G. (2000): Self-assembly of CdSe-ZnS quantum dot bioconjugates using an engineered recombinant protein. *J. Am. Chem. Soc*. 122, 12142–12150.

Biju V, Mundayoor S, Omkumar RV, Anas A and Ishikawa M. (2010a): Bio conjugated quantum dots for cancer research: present status, prospects and remaining issues*. Biotechnol Adv.*, 28: 199–213.

Biju V, Tamitake Itoh T and Ishikawa M (2010b): Delivering quantum dots to cells: bio conjugated quantum dots for targeted and nonspecific extracellular and intracellular imaging. *Chem Soc Rev* 39: 3031–3056.

Binnig G. and Rohrer H. (1986): "Scanning tunneling microscopy". *IBM Journal of Research and Development* 30: 4-10.

Bohland J. and Smigielski K.(2000): CdTe module manufacturing experience; environmental, health and safety results, Proceedings of the 28th IEEE Photovoltaic Specialists Conference, Anchorage*, First Solar's*.

Bradburne C.E., Delehanty J.B., Gemmill K.B., Mei B.C., Mattoussi H., Susumu K., Blanco-Canosa J.B., Dawson P.E. and. Medintz I.L.(2013): Role of QD Surface Ligand, Delivery Modality, Cell Type, and Direct Comparison to Organic Fluorophores. *Bioconjugate Chem*. 24, 1570−1583.

Bu H-B., Kikunaga H., Shimura K., Takahasi K., Taniguchia T. and Kim D-G. (2013): Influence of pH on optical properties: Hydrothermal synthesis of thiol-capped CdTe nanoparticles and their optical properties. *Chem. Phys.,* 15, 2903-2911.

Bullen C.R. and Paul Mulvaney P. (2004): Nucleation and Growth Kinetics of CdSe Nanocrystals in Octadecene. *Nano Lett.* 4 (12), 2303–2307.

Chan W.C.W. and Nie S.M. (1998): Quantum dot bioconjugates for ultrasensitive nonisotopic detection. *Science* 281, 2016-2018.

Chan W.C.W., Maxwell D.J., Gao X., Bailey R.E., Han M. and Nie S.(2002): Luminescent quantum dots for multiplexed biological detection and imaging. *Current Opinion in Biotechnology* 13, 40–46.

Chen N., He Y., Su Y., Li X., Huang Q., Wang H., Zhang X., Tai R., and Fan C. (2012) The cytotoxicity of cadmium-based quantum dots. *Biomaterials* 33, 1238−1244.

Chen S. and Liu W. (2006): Oleic acid capped PbS nanoparticles: Synthesis, characterisation and tribological properties. *Material Chemistry and physics*. 98, 183-189.

Chen X., Li L., Lai Y., Yan J., Tang Y. And Wang X. (2015): Microwave-Assisted Synthesis of Glutathione-Capped CdTe/CdSe near-infrared quantum dots for cell imaging. *Int. J. Mol. Sci.* 16, 11500-11508.

Chen, H-S.; Lo, B.; Hwang, J. Y.; Chang, G. Y.; Chen, C. M.; Tasi, S. J.; Jassy Wang, S-J.J.(2004): Colloidal ZnSe, ZnSe/ZnS, and ZnSe/ZnSeS Quantum Dots Synthesized from ZnO. *Phys. Chem. B,* 108 (44), 17119–17123.

Cho S. J., Maysinger D., Jain M., Roder B., Hackbarth S. and Winnik F.M. (2007): Long-term exposure to CdTe quantum dots causes functional impairments in live cells, *Langmuir*.23 (4):1974-1980.

Cutler P. J., Malik M. D., Liu S., Byars J. M., Lidke D. S., & Lidke K. A. (2013). Multi-Color Quantum Dot Tracking Using a High-Speed Hyperspectral Line-Scanning Microscope, *PLoS ONE*, 8(5), e64320.

Dabbousi, B.O. et al., (1997) (CdSe) ZnS core-shell quantum dots: synthesis and characterization of a size series of highly luminescent nanocrystallites. *J. Phys. Chem.* 101, 9463–9475.

Davids L.M., and Kleemann, (2011) Combating melanoma: the use of photodynamic therapy as a novel, adjuvant therapeutic tool. *Cancer Treat Rev.* 37(6) 465-475.

Deng, Z., Cao, L., Tang, F. and Zou, B. (2005). A new route to Zinc-Blend CdSe Nanocrystals: Mechanism and synthesis *J. Phys. Chem.* B, 109, 16671-16675.

Dlamini N.N., Rajasekhar V. S. R. P and Revaprasadu N. (2011): Synthesis of triethanolamine (TEA) capped CdSe nanoparticles. *Materials Letters* 65(9):1283-1286.

Dobson P. and Ng T. (2007): A facile route to CdTe nanoparticles and their use in bio-labelling. *J. Mater. Chem.* 17, 1989-1994.

Donega C.M., Hickey S.G., Wuister S.F., Vanmaekelbergh D., Meijerink A. (2003): Singlestep synthesis to control the photoluminescence quantum yield and size dispersion of CdSe nanocrystals. *J Phys Chem B*. 107:489–496.

Dowling A.P. (2004): Development of nanotechnologies. *Materials Today* 7; 12, 30–35.

Ebenstein Y.; Mokari T.; Banin U.(2002): Fluorescence quantum yield of CdSe/ZnS nanocrystals investigated by correlated atomic-force and single-particle fluorescence microscopy. *Appl. Phys. Lett*. 80, 4033–4035.

Ethirajan M., Chen Y., Joshi P., Pandey RK. (2011): The role of porphyrin chemistry in tumor imaging and photodynamic therapy. *Chem. Soc. Rev*. 4.:340–362.

Eychmüller A. and Weller, H. (2002): Thiol-capping of CdTe nanocrystals: An alternative to organometallic synthetic routes. *J. Phys. Chem*. B 106, 7177–7185.

Faraday M. (1957): The bakerian lecture: Experimental relations of gold (and other metals) to light, *Philos. Trans. R. Soc. Lond.,* 147, 145–181.

Furukawa H., Kitazawa H., Kaneko I., Kikuchi K., Tohma S., et al., (2009) Mast cells inhibit CD8+ T cell-mediated rejection of a malignant fibrous histiocytomalike tumor: Involvement of Fas-Fas ligand axis. *Am. J. Immunol.* 5: 89–97.

Gao X.H. and Nie S.M. (2003): Molecular profiling of single cells and tissue specimens with quantum dots. *Trends Biotechnol* 21(9):371–373.

Gaponik N., Talapin D.V., Rogach A.L, Eychmuller A. and Weller H. (2002) Efficient Phase Transfer of Luminescent Thiol-Capped Nanocrystals: From Water to Nonpolar Organic Solvents. *Nano letters* 2, (8) 803-806.

Gaponik N., Talapin D.V., Rogach A.L., Hoppe K., Shevchenko E.V. Kornowski A. and Guilinger J.(1999): Assessment of Critical Thin Film Resources; Cadmium Telluride, *RAF-9-29609*.

Green M, Williamson P., Samalova M., Davis J., Brovelli S., Dobsond P. and Caciallic F. (2009): Synthesis of type II/ type I CdTe/CdS/ZnS quantum dots and their use in cellular imaging. *J. Mater. Chem.* 19, 8341–8346.

Green M., Harwood H., Barrowman C., Rahman P., Eggeman A., Frestry F., Dobson P., Ng T., 2007. A facile route to CdTe nanoparticles and their use in bio-labelling. *J. Mater. Chem.* 17, 1989–1994.

Gui R. and An X. (2014): Layer-by-layer aqueous synthesis, characterization and fluorescence properties of type-II CdTe/CdS core/shell quantum dots with near-infrared emission. *RSC Adv.* 3, 20959–20969.

Guilinger J. 1999 “Assessment of Critical Thin Film Resources,” Contract RAF-9-29609, *World Industrial Minerals, Golden, CO*.

Guo J, Yang W, Wang C. (2005): Systematic study of the photoluminescence dependence of thiol-capped CdTe. *J Phys Chem B*. 109; 37: 17467-17473.

Hasegawa H, Kohno M, Sasaki M, Inoue A, Ito MR, et al., (2003) Antagonist of monocyte chemoattractant protein 1 ameliorates the initiation and progression of lupus nephritis and renal vasculitis in MRL/lpr mice. *Arthritis Rheum* 48: 2555–2566.

He Y., Lu H. T., Sai L. M., Lai W. Y., Fan Q. L., Wang L. H. and Huang, W. (2006): Synthesis of CdTe QDs through program process of microwave irradiation. *J. Phys. Chem. B* 110, 13352-13356.

He Y., Lu H.-T., Sai L.-M., Su Y.-Y., Hu M., Fan C.-H., Huang W. and Wang L.-H. (2008): Microwave synthesis of water-dispersed CdTe/CdS/ZnS core-shell-shell quantum dots with excellent photostability and biocompatibility. *Adv. Mater.* 20, 3416−3419.

He Y., Sai L. M., Lu H. Tu M., Lai W. Y., Fan Q. L., Wang L. H. and Huang W.(2007): Microwave-assisted synthesis of water-dispersed CdTe QDs with high luminescent efficiency and narrow size distribution. *Chem. Mater.* 19, 359 365.

Henglein A. (1989): Small-particle research: physicochemical properties of extremely small colloidal metal and semiconductor particles. *Chem. Rev.* 1861–1873

Hoshino A, Fujioka K, Oku T, Suga M, Sakaki Y.F, Yasuhara M, et al (2004): Physicochemical properties and cellular toxicity of nanocrystal quantum dots depend on their surface modification. *Nano Lett* 4, 2163–2169.

Hosono K., Nishida Y., Knudson W., Knudson C.B., Naruse T., Suzuki Y., and Ishiguro N. (2007): Hyaluronan Oligosaccharides Inhibit Tumorigenicity of Osteosarcoma Cell Lines MG-63 and LM-8 in Vitro and in Vivo via Perturbation of Hyaluronan-Rich Pericellular Matrix of the Cells. Osteosarcoma Hyaluronan Oligosaccharides. *Am. J. Pathol* 171, 274-286.

Hsieh S.C., Wang F.F., Lin C.S., Chen Y.J., Hung S.C., et al., (2006): The inhibition of osteogenesis with human bone marrow mesenchymal stem cells by CdSe/ZnS quantum dot labels. *Biomaterials* 27, (8) 1656–1664.

Jaiswal J.K., Mattoussi H., Mauro J.M. and Simon S.M. (2003): Long-term multiple color imaging of live cells using quantum dot bioconjugates. *Nat Biotechnol.* 21:47–51.

Jiang W., Mardyani S., Fischer H., and Chan W.C.W. (2006): Design and Characterization of Lysine Cross-Linked Mercapto-Acid Biocompatible Quantum Dots. *Chem. Mater*., 18 (4), 872–878.

Jin S., Hu Y., Gu Z., Liu L. and Wu H-C. (2011): Application of Quantum Dots in Biological Imaging. *Journal of Nanomaterials*, Article ID 834139, doi:10.1155/2011/834139.

Kahn J. (2006): "Nanotechnology". *National Geographic* 98-119.

Kanaras, A. G., Kamounah, F. S., Schaumburg, K., Kiely, C. J. & Brust, M. (2002) Thioalkylated tetraethylene glycol: a new ligand for water soluble monolayer protected gold clusters. *Chem. Commun*. 2294–2295.

Kato S., Mori S. and Kodama T. (2015): A Novel Treatment Method for Lymph Node Metastasis Using a Lymphatic Drug Delivery System with Nano/Microbubbles and Ultrasound. *Journal of Cancer* 6(12): 1282-1294.

Kim S., Fisher B., Eisler H-J. and Bawendi M. (2003): Type-II Quantum Dots: CdTe/CdSe(Core/Shell) and CdSe/ZnTe(Core/Shell) Heterostructures. *Journal of the American Chemical Society* 125 (38), 11466-11467.

Kirchner C., Liedl T., Kudera S., Pellegrino T., Munoz Javier A., Gaub H.E., et al (2005): Cytotoxicity of colloidal CdSe and CdSe/ZnS nanoparticles. *Nano Lett.* 5:331–338.

Kobayashi H., Hama Y., Koyama Y., Barrett T., Regino C.A., Urano Y. and Choyke P.L. (2007): Simultaneous multicolor imaging of five different lymphatic basins using quantum dots. *Nano Lett*. 7(6):1711–1716.

Koch C.C. (2003): Top-down synthesis of nanostructures material: mechanical and thermal processing method. *Rev. Adv. Mater. Sci.* 5, 91-99.

Koch, C.C. 1989. Materials synthesis by mechanical alloying. *Annual Review of Mater. Sci*. 191 21-143.

Krinitsyn P. G (2000): Study of the Conditions of CdTe and $Cd_{1-x}Zn_xTe$ Crystal Growth. *Chemistry for Sustainable Development*, 8, 167-170.

La-Mer V.K. and Dinegar R.H. (1950): Theory, Production and Mechanism of Formation of Monodispersed Hydrosols. *J. Am. Chem. Soc*.72, 4847–4854.

Law W.C., Yong K.T., Roy I., Ding H., Hu R., Zhao W.W. and Prasad PN. (2009): Aqueous-phase synthesis of highly luminescent CdTe/ZnTe core/shell quantum dots optimized for targeted bioimaging. *Small* 5 (11):1302–1310.

Li C.L. and Murase N. (2005) Surfactant- dependent photoluminescence of CdTe nanocrystals in aqueous solution. *Chemistry Letters*, 34, 92–93.

Li L., Mori S., Sakamoto M., Takahashi S. and Kodama T. (2013) : Mouse Model of Lymph Node Metastasis via Afferent Lymphatic Vessels for Development of Imaging Modalities. *PLoS ONE* 8(2): e55797.

Li L., Qian H. F., Fang, N. H. and Ren, J. C. (2006): Significant enhancement of the quantum yield of CdTe nanocrystals synthesized in aqueous phase by controlling the pH and concentrations of precursor solutions. *J. Lumin*. 116, 59-66.

Li L., Qian H. F., Ren J. C. (2005): Rapid synthesis of highly luminescent CdTe QDs in the aqueous phase by microwave irradiation with controllable temperature. *Chem. Commun*., 528-530.

Lim S.J., Zahid M.U. , Le P., Ma L., Entenberg D., Harney A.S, Condeelis J. and Smith A. M. (2014): Brightness-equalized quantum dots*. Natural communications*. 6:8210-8216.

Lim Y.T., Kim S., Nakayama A., Stott N.E., Bawendi M.G. and Frangioni JV. (2003): Selection of quantum dot wavelengths for biomedical assays and imaging. *Mol. Imaging* 2(1):50-64.

Liu Y., Chen W., Joly A.G., Wang Y., Pope C., Zhang Y., Bovin J-O., and Sherwood P. (2006): Comparison of Water-Soluble CdTe Nanoparticles Synthesized in Air and in Nitrogen, *J. Phys. Chem. B* ;110, 16992-17000.

Lovric J., Bazzi H.S., Cuie Y., Fortin G.R.A., Winnik F.M., Maysinger D.(2005): Differences in subcellular distribution and toxicity of green and red emitting CdTe quantum dots. *J. Mol. Med.* 83:377–385.

Luan W., Yang H., Fan N. and Tu S-T. (2008): Synthesis of Efficiently Green Luminescent CdSe/ZnS Nanocrystals Via Microfluidic Reaction. *Nanoscale Res*. *Lett.* 3, 134-139.

Manna R. and Bhattacharya S. (2009): Structural, Optical and Electrical Characterization of CdSe nanoparticles. *Chalcogenide Lett*. 6 (11), 611 – 616.

Mansur A.A.P., Mansur H.S., Borsagli F.LG.L.M. and Ramanery F.P. (2015): Bio-functionalized water-soluble ZnS quantum dots using carboxymethylchitosan. 17th International Conference on Solid Films and Surfaces: *Materials Science and Engineering* 76.

Mao W.Y., Guo J., Yang W., Wang C., He J. and Chen J. (2007): Synthesis of high quality near-infrared-emitting CdTeS alloyed quantum dots via the hydrothermal method. *Nanotechnology* 18 (48) 7.

Masoud S, Mehdi B and Majid G., (2015): Facile sonochemical synthesis and characterization of CdTe nanoparticles*. Synthesis and Reactivity in Inorganic, Metal-Organic, and Nano-Metal Chemistry 45*. (10) 1558-1564.

Mathew S., Bhardwaj B. S., Saran A. D., Radhakrishnan P., Nampoori V.P.N., Vallabhan C.P.G., Bellare J. R.(2014): Effect of ZnS shell on optical properties of CdSe–ZnS core–shell quantum dots. *Optical Materials* 39, 46–51.

McElroy N., Page R.C, Espinbarro-Valazquez D., Lewis E., Haigh S. ,O'Brien P., Binks D.J..(2014): Comparison of solar cells sensitised by CdTe/CdSe and CdSe/CdTe core/shell colloidal quantum dots with and without a CdS outer layer. *Thin Solid Films* 560, 65– 70.

Mntungwa N., Rajasekhar P. V.S.R. and Revaprasadu N. (2011): A facile route to shape controlled CdTe nanoparticles. *Materials Chemistry and Physics* 126, 500–506

Moskowitz P., Bernholc N., Fthenakis V.M., Pardi R., Steinberger H. and Thumm W.(1990): Environmental, Health and Safety Issues of Cadmium Telluride Photovoltaic Modules, *Advances in Solar Energy*, Vol. 10, Chapter 4, American Solar Energy Society, Boulder CO.

Murase N., Gaponik N. and Weller H. (2007): Effect of chemical composition on luminescence of thiol-stabilized CdTe nanocrystals. *Nanoscale Res Lett* 2:230–234.

Murray C.B., Norris D.J., Bawendi M.G.(1993): Synthesis and characterization of nearly monodisperse CdE (E = sulfur, selenium, tellurium) semiconductor nanocrystallites. *J. Am. Chem. Soc.* 1993, 115, 8706-8715.

Nazzal A.Y., Wang X.Y., Qu L.H., Yu W., Wang Y.J., Peng X.G. and Xiao M.(2004): Environmental effects on photoluminescence of highly luminescent CdSe and CdSe/ZnS core/shell nanocrystals in polymer thin films. *J. Phys. Chem. B* 108, 5507–5515.

Ncapayi V., Oluwafemi S.O., Songca S.P. and Kodama T. (2015): Optical and cytotoxicity properties of water soluble type II CdTe/CdSe nanoparticles synthesised via a green method. *Mater. Res. Soc. Symp. Proc*. Vol. 1748.

Nemchinov A., Kirsanova M., Hewa-Kasakarage N. N. and Zamkov, M. (2008): "Synthesis and characterization of type II ZnSe/CdS core/shell nanocrystals." *J. Phys. Chem. C* 112, 9301-9307.

Nirmal M., Dabbousi B.O., Bawendi M.G., Macklin J.J., Trautman J.K. Harris T.D. and BrusL.E. (1996): Fluorescence intermittency in single cadmium selenide nanocrystals. *Nature (London)* 383, 802–804.

Oluwafemi O.S. (2009): “A novel "green" synthesis of starch-capped CdSe nanostructures,” *Colloids and Surfaces B: Biointerfaces*, 73, 2, 382–386.

Oluwafemi O.S.; Olamide A. Daramola O.A. and Ncapayi V. (2014): A facile green synthesis of type II water soluble CdTe/CdS core shell nanoparticles. *Materials Letters* 133; 9–13.

Pan D.C., Jiang S.C., An L.J. Jiang B.Z. (2004): Controllable synthesis of highly luminescent and monodisperse CdS nanocrystals by a two-phase approach under mild conditions. Adv. Mater 16:982.

Peng A.Z. and Peng X. (2001): Formation of High-Quality CdTe, CdSe, and CdS Nanocrystals Using CdO as Precursor *J. Am. Chem. Soc.* 123, 183-184.

Peng X. G., Wickham J. and Alivisatos A. P. (1998): Kinetics of II-VI and III-V colloidal semiconductor nanocrystal growth: "Focusing" of size distributions. *J. Am. Chem. Soc.* 120 (21), 5343-5344.

Pitkethly M.J. (2004): Nanomaterial – the driving force. *Nanotoday* 20-29.

Plachy J. Cadmium, Session 17, U.S. *Geological Survey Minerals Yearbook* 2001.

Pradhan N., Reifsnyder D., Xie R, Aldana J. and Peng X. (2007): Surface ligand dynamics in growth of nanocrystals. *J Am Chem Soc* 129:9500–9509.

Qian H. F., Dong, C. Q., Weng J. F., and Ren J. C. (2006): Facile one-pot synthesis of luminescent, water-soluble, and biocompatible glutathione-coated CdTe QDs. *Small*, 2, 747- 751.

Rangarajan S.P and Wang J. (2000): Chemical Synthesis of Nanostructured Metals, Metal Alloys, and Semiconductors. *Handbook of nanostructured materials and nanotechnology Volume* 1, 2000.

Reiss P.; Bleuse J. and Pron A. (2002): Highly luminescent CdSe/ZnSe core/shell nanocrystals of low size dispersion. *Nano Lett*. 2002, 2, 781–784.

Riss T.L., Moravec R.A., Niles A.L., Benink H.A., Worzella J.T. and Minor L.(2013): Cell Viability Assays. *Assay Guidance Manual - NCBI Bookshelf* 14pages.

Robert C. W (1979): Handbook of Chemistry and Physics, 60th edition, *CRC Press,* 1979.

Rogach AL., Katsika L., Kornowski A., Su DS., Eychmueller A., Weller B., Berichte de Bunsen-Gesellschaft (1996): Synthesis and characterisation of thio-stabillised CdTe nanocrystals. *Phys Chem*. 100 (11) 1772-1778.

Rogach L.A. (2000) Nanocrystalline CdTe and CdTe(S) particles: wet chemical preparation, size-dependent optical properties and perspectives of optoelectronic application. *Materials Science and Engineering B* 69 – 70 , 435 – 440.

Samanta A.; Deng Z. and Liu, Y. (2012): Aqueous synthesis of glutathione-capped CdTe/CdS/ZnS and CdTe/CdSe/ZnS core/shell/shell nanocrystals heterostructures. *Langmuir,* 28, 8205–8215.

Sapra S., Rogach A.L. and Feldmann J. (2006): Phosphine-free synthesis of monodispersed CdSe nanocrystals in olive oil. *J. Mater. Chem*. 16- 3391-3395.

Satarug S., Haswell-Elkins MR. and Moore MR. (2000): Safe levels of cadmium intake to prevent renal toxicity in human subjects. *Br. J. Nutr*. 84:791–802.

Saunders BR. and Turner ML. (2008): Nanoparticle–polymer photovoltaic cells. *Advances in Colloid and Interface Science* 138, 1–23.

Seeman C.N. and Belcher A.M. (2002): Emulating biology: Building nanostructures from the bottom up. *Proc Natl Acad Sci U S A*., 99(Suppl 2): 6451–6455.

Shan Y., Xiao, Z., Chuan Y., Li H., Yuan M., Li Z. and Dou S. (2014): One-pot aqueous synthesis of cysteine capped CdTe/CdS core-shell nanowires. *Journal of Nanoparticle Research* 16 (2420), 1-11.

Shavel N. Gaponik A. Eychmuller (2006): Factors governing the quality of aqueous CdTe nanocrystals: calculations and experiment. *J. Phys Chem B*. 110; 39:19280-19284.

Shen Y.; Liu S.; He Y. (2014): Fluorescence quenching investigation on the interaction of glutathione-CdTe/CdS quantum dots with sanguinarine and its analytical application. *Luminescence.* (2):176-82.

Shi F., Liu S., and Su X.2014: Dopamine functionalized–CdTe quantum dots as fluorescence probes for L-histidine detection in biological fluids. *Talanta* 125; 221–226.

Simard J., Briggs C., Boal A. K. and Rotello V. M. (2000): Formation and pH-controlled assembly of amphiphilic gold nanoparticles. *Chem. Commun*. 1943–1944.

Su Y., He H., Lu H., Sai L., Li Q., Li W., Wang L., Shen P., Huang Q., Fan C. The cytotoxicity of cadmium based, aqueous phase – Synthesized, quantum dots and its modulation by surface coating. *Biomaterials* 30 (2009) 19–25.

Su Y., Yao He Y., Lu H., Sai L., Li Q., Li W., Wang L., Shen P., Huang Q. and Fan C., (2009): The cytotoxicity of cadmium based, aqueous phase – Synthesized, quantum dots and its modulation by surface coating. *Biomaterials* 30, 19–25.

Sugiyasu K., Nano K., Tamai N., Hashimoto N., Kishida Y., Yoshikawa H. and Myoui A.(2011): Radio-sensitization of the murine osteosarcoma cell line LM8 with parthenolide, a natural inhibitor of NF-κB. *Oncology letters* 2: 407-412.

Talapin D.V., Haubold S., Rogach A. L. , Kornowski A., Haase M., Weller H. (2001): A Novel Organometallic Synthesis of Highly Luminescent CdTe Nanocrystals. J. Phys. Chem. B, vol. 105, pp. 2260-2263.

Tan B., Liang Y., Wang J, Chen J.,Sun B. and Shao L. (2015) : Facile synthesis of CdTe-based quantum dots promoted by Mercaptosuccinic acid and hydrazine. *New J. Chem*., 2015, 39, 4488—4493.

Tyrrell E. J. and Smith J. M. (2011): Effective mass modelling of excitons in type-II quantum dot heterostructures .*Phys. Rev. B* 84, 165328-40

Vibin M., Vinayakan R., John A., Fernandez B.F. and Abraham A. (2014) : Effective cellular internalization of silica-coated CdSe quantum dots for high contrast cancer imaging and labelling applications. *Cancer Nanotechnology* 5, 1-12.

Wang J. and Han H. (2010): Hydrothermal synthesis of high-quality type-II CdTe/CdSe quantum dots with near-infrared fluorescence. *Journal of Colloid and Interface Science* 351, 83–87.

Wang W., Banerjee S., Jia S., Steigerwald ML. and Herman IP. (2007): Ligand control of growth, morphology, and capping structure of colloidal CdSe nanorods. *Chem Mater* 19(10): 2573–2580.

Wanga C., Yang J., Guohua L., Zhanga B.Z., Jianfeng, Shia and Nan, Lia. (2008): A greener synthetic route to monodispersed CdSe quantum dots with zinc-blende structure. *Journal of Crystal Growth.* 310, 2890–2894.

Wong T S., Brough B., Ho C-M. (2009): Creation of Functional Micro/Nano Systems through Top-down and Bottom-up Approaches. *Molecular & cellular biomechanics : MCB*. 6(1):1-55.

Xia Y. and Zhu C. (2008): Aqueous synthesis of type-II core/shell CdTe/CdSe quantum dots for near-infrared fluorescent sensing of copper (II). *Analyst.* 133(7):928-32.

Xue M., Wang X., Wang H., Tang B. (2011): The preparation of glutathione-capped CdTe quantum dots and their use in imaging of cells. *Talanta* 83, 1680–1686.

Yang H., Holloway P.H., Cunningham G. and Schanze K.S. (2004): CdS: Mn nanocrystals passivated by ZnS: Synthesis and luminescent properties. *J. Chem. Phys*.121, 10233–10240.

Yang T, He Q, Liu Y, Zhu C, Zhao D (2014): Water-Soluble N-Acetyl-L-cysteine-Capped CdTe Quantum Dots Application for Hg(II) Detection. *Journal of Analytical Methods in Chemistry* Volume 2013, Article ID 902951, 6 pages.

Yu G., Tan Y., He X., Qin Y., Liang J. (2014): CLAVATA3 Dodecapeptide Modified CdTe Nanoparticles: A Biocompatible Quantum Dot Probe for In Vivo Labeling of Plant Stem Cells. PLoS ONE 9(2): e89241.

Yu W. W., Wang Y.A. and Peng, X. G (2003). Formation and stability of size, shape, and structural controlled CdTe nanocrystals: ligand effect on monomers and nanocrystals. *Chem. Mater*. 15, 4300-4308

Yu, W. W.; Qu, L. H.; Guo, W. Z. and Peng, X. G. (2003) Experimental determination of the extinction coefficient of CdTe, CdSe, and CdS nanocrystals. *Chem. Mater*. 15, 2854–2860.

Zare H., Marandi M., Fardindoost S., Sharma V.K. Yeltik A., Akhavan O.,Demir H.V. and Taghavinia N. (2015): High-efficiency CdTe/CdS core/shell nanocrystals in water enabled by photo-induced colloidal hetero-epitaxy of CdS shelling at room temperature. *Nano Research* 8, (7) 2317-2328.

Zhang H., Sun P., Liu C., Gao H., Xu L., Fang J., Wang M., Liu L. and Xua S. (2011b): L-Cysteine capped CdTe–CdS core–shell quantum dots: preparation, characterization and immuno-labeling of HeLa cells*. Luminescence* 26: 86–92.

Zhang H., Wang L. P., Xiong H. M., Hu L. H., Yang B. and Li W.(2003): Hydrothermal synthesis for high quality CdTe QDs. *Adv. Mater*. 15, 1712-1715.

Zhang Y. and Clapp A. (2011a): Overview of stabilizing ligands for biocompatible quantum dot nanocrystals. *Sensors* 11(12):11036–11055.

Zhang Y. J., He P.-N., Wang J.-Y., Chen Z.-J., Lu D.-R., Lu J., Guo C.-C., Wang W. and Yang L. (2006): Time-Dependent Photoluminescence Blue Shift of the Quantum Dots in Living Cells: Effect of oxidation by singlet oxygen. *J. Am. Chem. Soc.* 128 (14), 13396- 13401

Zhang Y., Li Y., Yan XP. (2009): Aqueous Layer-by-Layer Epitaxy of Type-II CdTe/CdSe Quantum Dots with Near-Infrared Fluorescence for Bio imaging Applications. *Small* 5 185- 189.

Zhao M.X., Xia Q, Feng X.D., Zhu X.H., Mao Z.W., Ji L.N. and Wang K. (2010): Synthesis, biocompatibility and cell labeling of L-arginine-functional beta-cyclodextrin-modified quantum dot probes*. Biomaterials* 31; 4401–4408.

Zheng Y, Gao S., and Ying J.Y. (2007): Synthesis and Cell-Imaging Applications of Glutathione-Capped CdTe Quantum Dots*. Adv. Mater*., 19, 376–380.

Zrazhevskiy, P. & Gao, X. H. (2013): Quantum dot imaging platform for single-cell molecular profiling. *Nat Commun*. 4, 1619-1631.